January 2021

The Production Of Bio-Based Chemicals And Materials From Renewable Sources

Ian Foerster

THE PRODUCTION OF BIO-BASED CHEMICALS AND MATERIALS FROM RENEWABLE SOURCES

By

Ian Maxwell Foerster
Bachelor of Science, University of North Dakota, 2013

A Dissertation
Submitted to the Graduate Faculty

of the

University of North Dakota

in partial fulfillment of the requirements

for the degree of
Doctor of Philosophy

Grand Forks, North Dakota

May
2021

This dissertation, submitted by Ian Maxwell Foerster in partial fulfillment of the requirements for the Degree of Doctor of Philosophy from the University of North Dakota, has been read by the Faculty Advisory Committee under whom the work has been done and is hereby approved.

DocuSigned by:
Wayne Seames
Dr. Wayne Seames, Chairperson

DocuSigned by:
Brian Tande
Dr. Brian Tande, Committee Member

DocuSigned by:
Yun Ji
Dr. Yun Ji, Committee Member

DocuSigned by:
Surojit Gupta
Dr. Surojit Gupta, Committee Member

DocuSigned by:
Evgenii Kozliak
Dr. Jenya Kozlaik, Committee Member

DocuSigned by:
Dr. Eric Murphy, Committee Member at Large

This document is being submitted by the appointed advisory committee as having met all the requirements of the School of Graduate Studies at the University of North Dakota and is hereby approved.

DocuSigned by:
Chris Nelson
Chris Nelson
Dean of the School of Graduate Studies

5/13/2021
Date

PERMISSION

Title The Production of Bio-Based Chemicals and Materials from Renewable Sources

Department Chemical Engineering

Degree Doctor of Philosophy

In presenting this dissertation in partial fulfillment of the requirements for a graduate degree from the University of North Dakota, I agree that the library of this University shall make it freely available for inspection. I further agree that permission for extensive copying for scholarly purposes may be granted by the professor who supervised my dissertation work or, in his absence, by the Chairperson of the department or the dean of the School of Graduate Studies. It is understood that any copying or publication or other use of this dissertation or part thereof for financial gain shall not be allowed without my written permission. It is also understood that due recognition shall be given to me and to the University of North Dakota in any scholarly use which may be made of any material in my dissertation.

Ian Foerster

30 April 2021

Table of Contents

List of Figures

List of Tables

ACKNOWLEDGMENTS

I would first like to thank my family and friends for all of their support during the years I have spent at UND. I would like to thank my grandfather Connie Ryan who taught me the importance of a hard day's work, your memory continues to inspire me every day. I would especially like to thank my mother Shanna for her constant encouragement and guidance. I would also like to thank all of the fellow graduate students I have had the pleasure to work with during my time in graduate school. I would especially like to thank Michael Linnen, Sara Pourjafar, Clancy Kadrmas, Andrew Kohler, and Jasmine Oleksik for their assistance and guidance in performing laboratory experiments. I would like to thank Dave Hirschmann for his constant guidance and patience as we designed and built reaction systems over the years. I would also like to thank Dr. Alena Kubatova for her patience and willingness in teaching me analytical techniques and graciously allowing me to perform analytical experiments in her laboratory. I would like to thank my committee members for their knowledge and experience. Finally, I need to express my gratitude to my advisor Dr. Wayne Seames for his continuous support and patience as he has guided me through this life changing experience and for all of the opportunities he has provided me.

To My Parents
Matthew and Shanna Foerster

Abstract

Widespread concern with the impacts of global emissions and climate change plays an active role in driving global renewable markets, developing scientific research communities, and setting environmental pollution regulations. Efforts to confront this rise in global emissions are primarily focused on the reduction and replacement of non-renewable fuels and materials. It has become increasingly apparent that reducing global greenhouse gas emissions will require more than just the replacement of fossil fuels, but the development of technologies to convert a diverse set of renewable feedstocks into fuels, chemicals, and materials.

The goal of the work documented herein, was to expand the breadth of knowledge associated with transforming renewable feedstocks into renewable chemicals and materials. This dissertation is organized into three chapters each of which focuses on initial or developmental research for technologies to transform three different renewable feedstocks into fuels, chemicals, and materials. Specifically, this research will focus on soybeans, micro-algae, and forage sorghum as feedstocks to produce carbon fibers, fatty acid-based oils, and chemical intermediates, respectively.

Chapter II, “Production of Mesophase Pitch from Renewable Sources of Tar,” documents initial research efforts for the design, commissioning, and utilization of a novel lab-scale extruder-based reaction system to convert tars generated from the non-catalytic cracking of soybean oil into a mesophase pitch suitable for processing into continuous carbon fibers. This research looks

to replace traditional petroleum-based carbon fiber precursors with renewably sourced materials. Mesophase pitch formation from pyrolysis of soy tars was performed at temperatures of 325, 350, 375, and 390 °C. It was observed that increasing the processing temperature led to increased mesophase pitch formation, with 390 °C providing the only solid pitch products. The preliminary results demonstrate that this approach is technically feasible and recommends additional development towards commercialization.

Chapter III, "The Extraction of Fatty Acids from Algae Oils" details a comparative study evaluating the most viable methods and conditions identified by previous researchers for the extraction of lipids from microalgae biomass in a single, consistent study. The interest in microalgae to produce third generation biofuels has developed entire research fields focused on the recovery of recoverable chemicals and components from their biomass using the most heavily researched, the lipids. The use of microalgae as a renewable feedstock faces several barriers to commercialization including the complexity of lipids extraction from the microalgae biomass. Many researchers have published techniques, with varying success. However, with differing methodologies and analytical methods, it is difficult to determine the relative merits of these techniques or of combinations of these techniques. The goal of this research was to perform a study that investigates all of the primary methods identified by earlier researchers, separately and in certain combinations, in order to provide a consistent comparison of the methods for the efficient extraction of lipids from microalgae.

The lipid extraction techniques investigated were solvent selection coupled with microwave, sonication, or in situ transesterification assisted extraction. Methanol was found to be the best performing solvent for lipid extraction from Chlorella Vulgaris microalgae. Methanol consistently outperformed the other solvents examined, namely: Bligh Dyer, ethanol,

chloroform, acetonitrile, and hexane. Methanol was the top solvent for use with both microwave and sonication assisted extraction, as well as, for in-situ transesterification assisted extraction. Of the techniques investigated, methanol solvent with in situ transesterification followed by ultrasonication provided the highest recovery of lipids from microalgae biomass with 35% of the initial lipids recovered.

Chapter IV includes two distinct studies involving the transformation of the lignocellulosic biomass forage sorghum. Lignocellulosic biomass is one of the most extensively researched and promising renewable feedstocks for fuels, chemicals, and material products traditionally sourced from nonrenewable sources. The work was divided into two efforts, the production of organic acids from the carbohydrates and decomposition of the remaining lignin.

The first section of Chapter IV, "Production of Organic Acids from Sorghum Carbohydrates," documents a study of the catalytic decomposition and transformation of into building block acids, with a focus on lactic acid. Both model sugar solutions plus those derived from forage sorghum carbohydrates were utilized. For the actual samples, the carbohydrates were extracted from the biomass and the cellulose and hemi-cellulose hydrolyzed into glucose and xylose. The glucose and xylose monomers were catalytically transformed into the acids. Experiments were performed to investigate catalyst doping factors and performance, specifically dopant selection and silica-to-alumina ratios. Additional experiments were performed to determine xylose decomposition products and biomass sourced carbohydrate decomposition products.

Batch catalytic decomposition reactions of model glucose in water solutions were performed to determine differences in the impact of using Sn (II) or Sn (IV) as the catalyst dopant, as well as the impact from varying the silica-to-alumina ratio in catalyst scaffold. It was determined that both Sn (II) and Sn (IV) are equally effective at providing Lewis acid sites necessary for the

decomposition of carbohydrates to lactic acid. The silica-to-alumina ratio of the catalyst scaffold was a significant factor in the performance of carbohydrate decomposition reactions. Increasing the alumina content within the catalysts leads to increased Brønsted acid sites causing an increase in levulinic acid formation.

Using a xylose in water solution, it was found that the Sn-Beta catalytic decomposition of xylose leads to increased lactic acid and decreased levulinic acid, when compared to glucose. This is attributed to differences between the proposed reaction pathways for xylose and glucose. It was also found that forage sorghum-derived glucose and xylose mixtures were acceptable feedstocks for Sn-Beta decomposition reactions to form lactic acid. The neutralization step for acid hydrolysis used to generate the mixtures modifies the Sn-Beta catalyst to provide increased lactic acid formation and decreased levulinic acid formation, when compared to model solutions. It was also observed that decreasing sugar-to-catalyst ratios in biomass sourced carbohydrate decomposition reactions leads to increased lactic acid formation, with the highest observed conversion of carbon to lactic acid of 64%.

The second section of Chapter IV, “Base Facilitated Decomposition of Forage Sorghum Lignin” documents experiments with a novel, continuous flow reactor designed to decompose the lignin from forage sorghum. Lignin is one of the most abundant natural polymers, behind cellulose and hemicellulose. Unique amongst renewable biomass, lignin is considered the most promising non-petroleum source of renewable aromatic compounds. Currently, lignin is considered a waste product, with most of its production being burnt for heat and electricity. In order to better exploit the unique phenolic content of lignin, it is necessary to liberate these desirable monomer compounds from the polymer. Given the complex nature of lignin, an efficient method to decompose it into chemical intermediates does not currently exist. A novel non-catalytic

decomposition reactor was utilized and evaluated for the decomposition of softwood kraft lignin and forage sorghum extracted lignin.

Initial experiments using softwood kraft lignin were performed to determine an optimum decomposition temperature. Temperatures of 335, 340, and 350 °C were examined. It was determined that 340 °C provided the highest conversion to monomer and oligomer components. When compared to forage sorghum-derived lignin, Kraft lignin maintains a more complex, recalcitrant nature. Sorghum-derived lignin shows significantly higher oligomer and monomer carbon fractions, when compared to Kraft lignin. The fraction of monomers and oligomers generated in this novel system are higher than those from acid and base catalyzed polymerization methods reported in the literature. This demonstrates that this system has the potential to be used for the decomposition of reactive lignin.

Chapter I. Introduction

It is estimated that pollution from fossil fuel combustion is responsible for 4.2 million deaths a year, or approximately 7.6% of total global deaths.[1] Widespread concern with the impacts of global emissions and climate change plays an active role in driving global renewable markets, developing scientific research communities, and setting environmental pollution regulations. Efforts to confront this rise in global emissions are primarily focused on the reduction and replacement of non-renewable fuels. The International Panel on Climate Change believes that global carbon emissions will need to be a net zero by 2070, with a 25% reduction by 2030, in order to mitigate the worst effects of global climate change.[2] It has become increasingly apparent that reducing global greenhouse gas emissions will require more than just the replacement of fossil fuels, but the development of technologies to convert a diverse set of renewable feedstocks into fuels, chemicals, and materials.

The goal of the work documented herein, was to expand the breadth of knowledge associated with transforming renewable feedstocks into useful chemicals and materials that can replace those currently generated from fossil carbon sources. The dissertation is organized into three chapters each of which focuses on initial or developmental research for technologies to transform different renewable feedstocks into chemicals, and materials. Specifically, this research will focus on soybeans, micro-algae, and forage sorghum as feedstocks to produce carbon fibers, fatty acid-based oils, and chemical intermediates, respectively.

Chapter II, "Production of Mesophase Pitch from Renewable Sources of Tar," Documents initial research efforts for the design, commissioning, and utilization of a novel lab-scale extruder-based reaction system to convert tars generated from the non-catalytic cracking of soybean oil into a mesophase pitch suitable for processing into continuous carbon fibers. This research looks to replace traditional petroleum-based carbon fiber precursors with renewably sourced materials.

The fatty acid based oil from oilseed crops like soybeans have been extensively researched for their application in renewable biofuels.[3] In order to produce a cost effective alternative to traditional fossil fuels, it is necessary to maximize and diversify value added by-products.[4] The decomposition of complex organic substances, such as fatty acids from soybeans, can lead to secondary reactions where-in oligomers form.[5] These materials are typically labeled "tars". Tars are often viewed as low value, waste products. This project examined the isolation and processing of tars, in order to generate a mesophase pitch which can serve as the feedstock for the production of carbon fibers.

Carbon fibers are a structural fiber with a diverse range of applications such as applications for aerospace, military, sporting goods, automotive, industrial, medical, and high-end goods.[6, 7] The global demand for carbon fibers has been experiencing exponential growth for the last decade, driven by the desire for the low density and high strength associated with carbon fibers.[8, 9] Currently, carbon fibers are almost exclusively formed from petroleum precursors.[9, 10] The development of a bio-based carbon fiber will help to transition this market away from fossil fuels and provide an economically desirable by-product to the biofuel industry.

Chapter III, "The Extraction of Fatty Acids from Algae Oils" details a comparative study evaluating the most viable methods and conditions identified by previous researchers for the extraction of lipids from microalgae biomass in a single, consistent study. The use of microalgae as a feedstock for renewable fuels and chemicals has experienced an immense amount of interest as documented in the literature during the last 10 years. This interest is focused on the use of the lipids in microalgae, which are a fatty acid-based oils similar to crop oils, as renewable fuel feedstocks because of algae's ability to produce large amounts of biomass more quickly than traditional oilseed crops.[11] The ability for microalgae to be grown in conditions not viable for

seed oil crops, like arid locations or brackish water, also provide additional benefits when compared to traditional agricultural products.[12] In addition to lipids, microalgae contain a large variety of desirable extractable chemicals and components such as pigments, proteins, carbohydrates, and enzymes.[13-16].

Unfortunately, the use of microalgae as a renewable feedstock faces several barriers to commercialization. One of these barriers is the complexity of lipids extraction from the microalgae biomass, due to its hard cell wall and membrane. Many researchers have published techniques, with varying success, for lipid extraction.[14, 17-19] However, with differing methodologies and analytical methods, it is difficult to determine the relative merits of these techniques or of combinations of these techniques. The goal of this research was to perform a study that investigates all of the most promising primary methods identified by earlier researchers, separately and in certain combinations, in order to provide a consistent comparison of the methods for the efficient extraction of lipids from microalgae.

Chapter IV includes two distinct studies involving the transformation of the lignocellulosic biomass forage sorghum. Lignocellulosic biomass is one of the most extensively researched and promising renewable feedstocks for bio-based fuels and the replacement of chemicals and specialty products traditionally sourced from nonrenewable sources.[20] With over 150 billion tons of lignocellulosic biomass available globally per year, this biomass is considered the most feasible long-term source of renewable carbons and energy.[21, 22] Lignocellulosic biomass is primarily sourced from agricultural wastes like corn stover and wheat straw, but also available from industrial wastes like paper sludge.[23, 24]

The main components of lignocellulosic biomass are cellulose, hemicellulose, and lignin. Each of these lignocellulosic biomass building blocks have the potential to be upgraded into value

added products. Cellulose is composed of highly crystalline linear polymerized D-glucose monomers. Hemicellulose is a highly branched, amorphous polymer consisting of primarily xylose and small amounts of other pentose and hexose monomers, like xylobiose and arabinose.[25] Lignin is a stable, complex polymer consisting of many different phenyl and hydroxyl functional groups.[26] The diversity of compounds found within lignocellulosic biomass provides the potential to be transformed into a large variety of upgraded products.

The first section of Chapter IV, "Production of Organic Acids from Sorghum Carbohydrates," documents a study of the catalytic decomposition of both model sugar solutions and sugar solutions derived from carbohydrates extracted from forage sorghum into building block acids, with a goal of maximizing the production of lactic acid. The majority of forage sorghum biomass is composed of polymeric hexoses and pentoses of glucose and xylose. The recovery from biomass and conversion of these carbohydrates into sugars is a well-documented process, with most of the recent literature focus being placed on optimization of conditions for carbohydrate extraction and expanding into unique biomass sources. [27, 28] Carbohydrates extracted from lignocellulosic biomass are primarily used in biological applications, like fermentation to ethanol or lactic acid.[29] These biological processes experience limitations associated with high costs, when compared to starch and sucrose biorefineries.[23] One major barrier associated with these biomass processes is the formation of compounds which inhibit biological activity.[25, 28] Thus, non-biological applications may be more attractive for utilization of lignocellulosic sourced carbohydrates. This section documents studies with a non-biological option; the glucose and xylose monomers contained within the cellulose and hemi-cellulose of biomass are catalytically transformed into the acids.

The second section of Chapter IV, “Base Facilitated Decomposition of Forage Sorghum Lignin” documents experiments with a novel, continuous flow reactor designed to decompose the lignin from forage sorghum. Lignin is one of the most abundant natural polymers, behind cellulose and hemicellulose. Found within lignocellulosic biomass, lignin is a complex, stable polymer responsible for giving a plant structure and rigidity. This functionality is common amongst all plants, including herbaceous species. Structurally, lignin consists of mainly phenyl and hydroxyl functional groups, like p-coumaryl alcohol, p-hydroxyphenal alcohol, coniferyl alcohol, and sinapyl alcohol.[26, 30] Unique amongst renewable biomass, lignin is considered the most promising non-petroleum source of renewable aromatic compounds.[31] The chemical composition of lignin varies widely, depending on the original source where it was formed.

The largest source of commercial lignin is the pulp and paper industry, with annual production of 50 million tons.[32] Currently, lignin is considered a waste product, with most of its production being burnt for heat and electricity. In order to better exploit the unique phenolic content of lignin, it is necessary to liberate these desirable monomer compounds from the polymer. Given the complex nature of lignin, an efficient method to decompose it into chemical intermediates does not currently exist. Extensive research has been performed around the concept of lignin decomposition, but no significant discoveries have been made in this regard. This section documents studies with a novel non-catalytic decomposition reactor to evaluate the decomposition of softwood kraft lignin and forage sorghum extracted lignin.

Chapter II. Production of Mesophase Pitch from Renewable Sources of Tar

Abstract

Carbon fibers are a structural fiber with a diverse range of applications. Currently, carbon fibers are primarily used in applications for aerospace, military, sporting goods, automotive, industrial, medical, and high-end goods The global demand for carbon fibers has been experiencing exponential growth for the last decade, driven by the desire for the low density and high strength associated with carbon fibers. Currently, carbon fibers are almost exclusively formed from petroleum precursors, more specifically polyacrylonitrile (PAN). The costs associated with manufacturing PAN fibers has been shown to be a barrier to their more widespread use in additional applications. Currently the only replacement feedstocks capable of providing carbon fibers with a similar strength and structure to PAN are coal tar or petroleum tar-derived mesophase pitch-based fibers. The development of a bio-based carbon fiber will help to transition this market away from fossil carbon and provide an economically desirable by-product to the biofuel industry.

In the research presented herein, a novel lab-scale extruder-based reaction system was designed, commissioned, and used in experiments with tars generated from the non-catalytic cracking of soybean oils. The goal was to demonstrate the technical feasibility of this novel pitching method and to identify reaction conditions that are optimum for mesophase pitch production.

A pre-processing and continuous pitch processing system was successfully demonstrated for the production of mesophase pitch from the non-volatile organic compounds generated during the non-catalytic cracking of a triglyceride oil (soybean oil). The crackate from this research provided an overall mass recovery to bio-tar of approximately 17 wt% based on the inlet oil mass feed rate and an overall conversion of 4.3 wt% of the inlet oil into a mesophase pitch product with properties close to those required for carbon fiber production.

After successful technology demonstration, the primary factor optimized was the operating temperature of the pitching reactor. Operating temperatures of 325, 350, 375, and 390 °C were investigated. All of these temperatures experienced additional devolatilization of the tar feed stock, with 390 °C experiencing the highest degree of devolatilization at 25 wt% pitch product recovery. Thus, even if mesophase pitch production is not the target of this work, the recovery of the additional heavy distillates for conversion into other fuel and chemical products would justify adding devolatization processing to a cracking-based biorefinery.

TGA data showed minimal differences between the tars processed at 325, 350, and 375 °C but a significant increase in thermal stability in the 390 °C sample, indicating that there was an increase in complex components formed within the pitch product at the higher operating temperature. From this we conclude that devolatilization alone is not sufficient to generate mesophase pitch. Instead, adequate time after devolatilization is needed for complex component formation and alignment under shear. The 390 °C operating temperature was the only condition tested which produced a solid pitch product. However, the softening point of this pitch product was 122 °C, which is too low for stable continuous carbon fiber formation and indicates that the system still requires improvement either by operation at an even higher temperature, or at longer residence time (or both). Both of these parameter changes require equipment modification within the pitching system.

2.1 Introduction

The first known use of carbon fibers can be traced back to the 1880s, when Thomas Edison was attempting to find filament materials for use in incandescent lightbulbs.[33, 34] A more traditional

commercial carbon fiber used for structural/reinforcement applications was not seen until the 1960s when the Union Carbide Corporation developed rayon based fibers (1959), polyacrylonitrile (PAN) based fibers (1962), and pitch based fibers (1963).[33, 35] These fibers were found to be desirable for their low density and high strength, with approximately four times the strength of steel.[8]

Since these early developments, the carbon fiber industry has been growing steadily with the demand between 1999 and 2010 doubling to 34,200 tons per year of carbon fiber consumption globally.[36] The global demand for carbon fibers nearly doubled again between 2010 and 2015 growing to 58,000 tons per year, with market reports expecting this demand to increase to 120,000 tons by 2022.[9] A graph of this growth can be seen in figure 2.1-1. This graph shows an exponential growth trend in the demand for carbon fibers, highlighting the potential in this market.

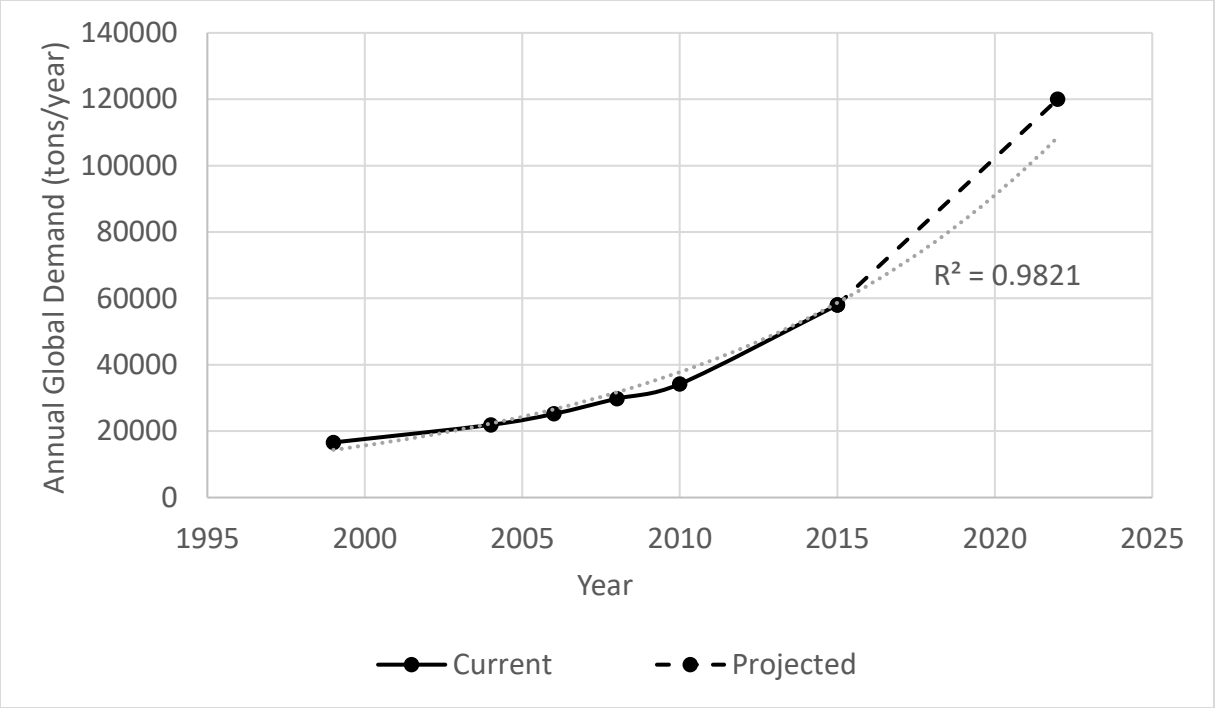

Figure 2.1- 1: Annual Global Demand for carbon fibers in tons per year, with exponential trendline[7, 9]

This growth is driven by the fact that uses for carbon fibers are diverse and expanding into new applications. Currently, carbon fibers are primarily used in applications for aerospace, military, sporting goods, automotive, industrial, medical, and high-end goods.[6, 7] In 2010, the highest global use application for carbon fibers was industrial with 17,500 tons annually and aerospace as the next highest, consuming 9,800 tons annually.[7] Unfortunately, the use and growth of the carbon fibers market is impeded by the high costs associated with production, limiting its use to specialty products and applications.[6, 7] There is significant effort to remove this barrier through the use of lower cost precursors and/or processing methods.[6]

Carbon fibers are distinguished by their high carbon content, comprising at least 92% carbon by weight with graphite fibers comprising at least 99 wt% carbon. These fibers are generally composed of stacked graphene layers. These graphene layers can be arranged in an orderly

parallel pattern, known as graphitic crystals, or in random arrangements, known as turbostatic crystals.[36, 37] The crystalline structure, tensile strength, and modulus of the final fiber are determined by the precursor, spinning method, and stabilization temperatures used to produce the fiber.[38] The research presented here focused on precursor preparation.

Ideal carbon fiber precursors are those capable of forming stable strands of carbon when spinning. This is often attributed to a high degree of intermolecular interactions, complex molecular structures, aromaticity, and low ash content.[34, 35, 37] Precursor candidates that have previously been demonstrated include polymers like PAN, aromatic industrial wastes like coal or petroleum tar/pitch, bio-based polymers like lignin, and polymer/biomass blended feedstocks.[8, 10, 36] Each of these precursors use different processing conditions to develop a stable final fiber and result in different final fiber properties. In 2005, greater than 95% of carbon fiber capacity was formed from PAN precursors, with the remainder of production coming from coal/petroleum pitch precursors.[36] Recent literature shows that PAN remains the dominant carbon fiber precursor.[9, 10]

Table 2.1-1 shows the tensile strength and modulus of carbon fibers using various precursors for fiber formation.[8, 10, 34, 35, 37, 39] A wide variety of modulus and tensile strength combinations can be obtained by changing the precursor used for carbon fiber production. Traditional PAN fibers exhibit the highest tensile strength and high modulus, providing them superior strength and desirable flexibility for high performance applications. [37] The next highest strength and modulus belongs to mesophase pitch. The modulus reaches higher levels than PAN fibers, because mesophase pitch forms a more graphitic structure than PAN fibers.[35] The next highest strength and modulus is found in the blended PAN and lignin fibers. This represents a considerable decrease in performance when compared to pure PAN fibers. Increasing the content of lignin

causes a decrease in performance due to the introduction of defects in the final carbon fiber.[8] This makes the use of PAN blended fibers less desirable, due to the high associated costs of the initial PAN feedstock and the negative impact these additives have on the final fiber properties. The next highest tensile strength is from Rayon fibers. These fibers were one of the original precursors for carbon fiber, but are no longer commercially produced in favor of PAN fibers.[34] The modified lignin precursors have potential for improved performance, but require extensive improvements to the defects associated with the final fibers formed.[8] Considering these precursors, the present study focused on the production of a mesophase pitch precursor.

Table 2.1- 1: Tensile strength and Modulus of carbon fibers from various precursors [8, 10, 34, 35, 37, 39]

Carbon Fiber Precursor	Modulus (GPa)	Tensile Strength (MPa)
PAN	100-500	3000-7000
Mesophase Pitch	200-800	1000-3000
Isotropic Pitch	33	700-800
PAN and Lignin (25%) Blend	217	2250
PAN and Lignin (30%) Blend	230	1720
Softwood Kraft Lignin	32	645
Hardwood Kraft Lignin	29	520
Rayon	70	1500

Pitch is typically defined as a heavy molecular weight, viscous, residue by-product formed during destructive distillation of petroleum or coal. These pitches are often comprised of polycyclic hydrocarbons, polycyclic aromatics, asphaltenes, and low molecular weight aliphatics.[35, 40, 41] The carbon content of pitch is generally >80%, providing the potential to be used as a cheap feedstock for carbon fiber production.[7] Additional sources of pitch are pyrolyzed polymers, like PVC.[7, 36]

Mesophase pitch is an organized liquid nematic crystalline phase, known as the anisotropic or carbonaceous mesophase, that forms when the feedstock tars are exposed to temperatures between 300 °C and 500 °C.[42] The formation of mesophase pitch was first documented by

Brooks and Taylor in the 1960s.[43] The reaction pathway to form mesophase pitch has been theorized in literature with four steps:

1. Low molecular weight volatile components are removed through extended heating while simultaneous condensation and/or de-alkylation reactions occur.[38]
2. Small spherical clusters of ordered aromatic/cyclic layers are formed.[44] This is the mesophase within the un-ordered isotropic bulk fluid.
3. The spherules continue to grow and coalesce as more of the bulk phase transitions into the mesophase.
4. A bulk mesophase is formed having a molecular weight between 200 and 1600 amu.[44]

Mesophase pitch is commonly produced through two different methods: pyrolysis or solvent treatment.[35, 38] Pyrolysis is performed by exposing the pitch to extended heating under inert atmospheres, facilitating the formation steps previously discussed. Solvent treatment first washes the pitch with targeted solvents to concentrate the high molecular weight fraction before heat treatment. Generally, pyrolysis requires reaction times up to 40 hours while solvent treatment, although utilizing additional chemicals, requires as little as 10 minutes of reaction time.[35] No structural difference between these two methods is noted in the literature. When comparing the methods for forming mesophase pitch, it is important to consider the costs associated with long processing times versus the costs associated with increased solvent use and requirements.[35] In the present study, a pyrolysis method for mesophase pitch formation was developed with a significantly reduced residence time. The method also avoids added processing steps/solvents.

There are several key properties desired for mesophase pitch as a feedstock in carbon fiber production. A suitable pitch should contain a high mesophase content (generally 60-90%), a high softening point temperature (250 – 280 °C), a high degree of orientation within mesophase, and

low ash content.[42, 45-47] The mesophase content and the softening point are largely controlled by the starting material complexity and pitch processing time and temperature.[35, 44] Increasing the degree of orientation and crystallinity within the precursor pitch leads to increased modulus and performance of the final fibers.[45] Ash content within the precursor pitch leads to defects within the final pitch product, forming a non-continuous fiber, significantly reducing performance.[7, 8] Generally speaking, coal based pitches have higher ash content and experience higher fiber defects than petroleum pitches. For this reason petroleum pitch is preferred for use in mesophase pitch production.[36] Even with the use of petroleum sourced pitches, the variability of carbonization rates for different molecules during pyrolysis leads to char formation and low quality mesophase pitch.[40] In the present study tars from a renewable source are used to bypass the issues experienced from coal and petroleum tars due to their ash and impurity content. The University of North Dakota has developed processes to form drop-in compatible fuels through non-catalytic crop oil cracking. This process utilizes a refined crop oil feed stock and produces a heavy tar waste stream, which does not experience ash impurities seen in coal and petroleum.[5]

2.2 Methods/Materials

2.2.1 Reactor Design

The experimental tar pitching work in this research was performed using a novel reactor system designed and built at the University of North Dakota. This experimental apparatus has two distinct operational modes: tar devolatilization and tar pitching. Both of these configurations utilize a shared multi-stage condensation and vacuum system.

The multi-stage condensation and vacuum system was made of 4 functional units: a heavy distillate condenser, a medium distillate condenser, a light distillate condenser, and a vacuum pump. This apparatus, shown in Figure 2.2.1-1, contained the following components:

1. The heavy distillate condenser consisted of a jacketed vertical condensing vessel with a height of 38 cm and a diameter of 12 cm containing an internal stainless steel tubing coil having an internal diameter of 4.6 mm and a length of 122 cm. All pieces of the condensing vessel and cooling coil were made from 316 stainless steel. On the bottom of the condenser was a 15 cm high 316 stainless collection vessel with a diameter of 7 cm and a 2.5 cm diameter 316 stainless steel ball type isolation valve. The heat exchange fluid used in the jacket of the heavy distillate condenser was liquid water at its boiling point, with no phase change within the jacket and coils. The heat exchange fluid was provided by a hot water generator consisting of a 304 stainless steel 63.5 cm high water reservoir with diameter of a 11.4 cm, a 1500 watt/120 volt heating element, and a a Cole-Parmer Masterflex peristaltic circulation pump with pump head 70-16-21 (Cole-Parmer, Chicago, IL, USA). The sample tar devolatilization or tar pitching apparatus was connected to the heavy distillate condenser via an 8-bolt 11.4 cm diameter 304 stainless steel flange.
2. The medium distillate condenser consisted of an unjacketed vertical condensing vessel with a height of 38 cm and a diameter of 12 cm containing an internal stainless steel tubing coil having an internal diameter of 4.6 mm and a length of 122 cm. On the bottom of the condenser was a 15 cm high 316 stainless collection vessel with diameter of 7 cm and a 2.5 cm diameter 316 stainless steel ball type isolation valve. The heat exchange fluid in the medium distillate condenser was cold tap water which had a typical temperature of 10 ^{o}C.

3. The light distillate receiver consisted of a 316 stainless steel vertical condensing vessel with a height of 30cm and diameter of 7.6 cm packed with 17 grams of 316 stainless steel wool from McMaster-Carr (Aurora, OH, USA). This vessel was set in a reservoir of anti-freeze 25 cm high and 12.7 cm in diameter chilled to -40 ^{o}C by a Thermo Neslab CC 100 Immersion Cooler (Thermo Fisher Scientific, Waltham, MA, UAS). The bottom of the light distillate receiver was fitted with a drain line and 316 stainless steel SS-41S2 ball valve from Swagelok (Chaska, MN, USA), to drain and collect any accumulated sample.
4. Finally, the vacuum, if required, was generated by an Edwards RV8 vacuum pump (Edwards Vacuum LLC, Sanborn, NY, USA).

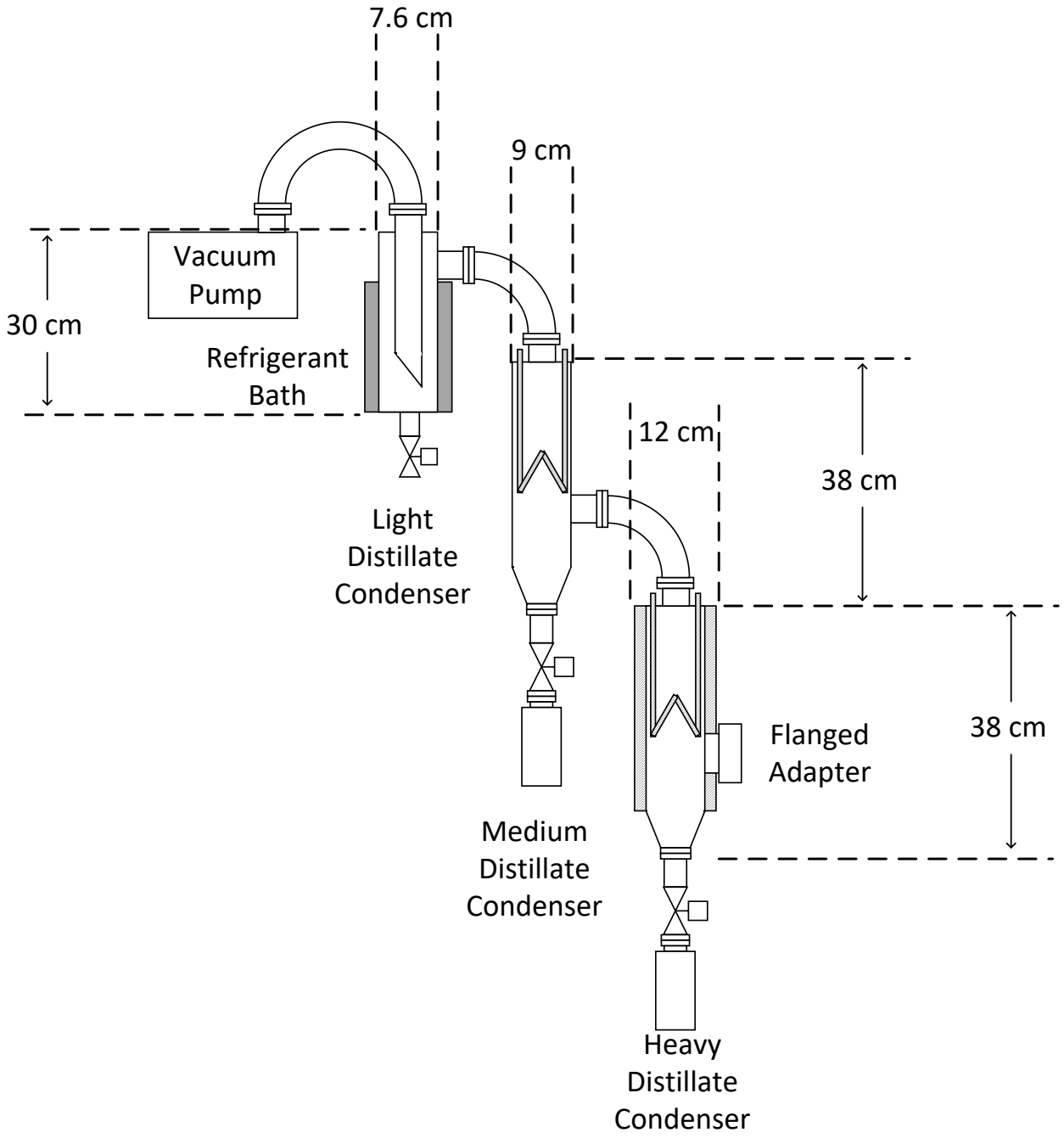

Figure 2.2.1- 1: Diagram of the multi-component distillation unit used including heavy distillate condenser, medium distillate condenser, light distillate condenser, and vacuum pump

The tar devolatilization unit was designed with an 8-bolt 11.4 cm diameter 304 stainless steel flanged modular head with a height of 28 cm and width of 18 cm constructed from 316 stainless

steel. This head was attached to the heavy distillate condenser described previously. The body of the unit consisted of a 316 stainless steel size 35/25 ball joint connector, a 304 stainless steel spiral wound wire brush with overall length of 28 cm from McMaster-Carr (Aurora, OH, USA) with a diameter of 2.5 cm. The brush was used as an internal spinning band for improved separation. The unit also contains a controllable 183 cm 624W/120 volt heat tracing cable from McMaster-Carr (Aurora, OH, USA) to maintain boiling flask temperatures within the distillation head unit. In addition to the devolatilization unit, a 2 L glass round bottom boiling flask with 665 watt heating mantle was loaded with the desired distillation feed and attached to the ball joint connector of the distillation head unit during experimentation. A schematic of the tar devolatilization apparatus can be seen in Figure 2.2.1-2. This apparatus connects to the distillation apparatus shown in Figure 2.2.1-1.

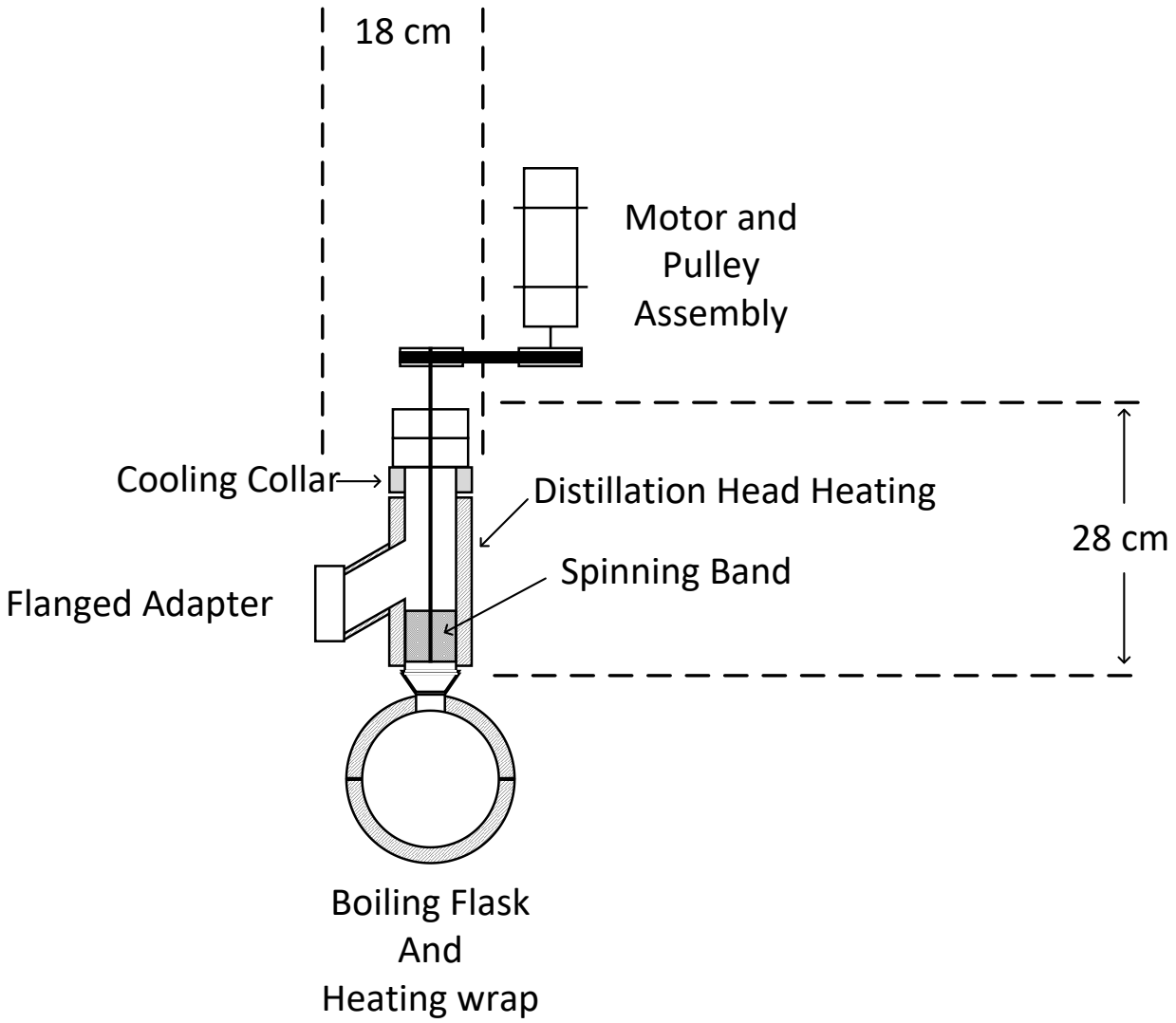

Figure 2.2.1- 2: The tar devolatilization apparatus

The tar pitching reactor was designed as a continuous reaction system to produce a mesophase pitch from a devolatilized soy tar feedstock. To generate the pitch several key goals had to be achieved. The first was operation under an inert atmosphere to avoid combustion of the tar. This was accomplished by using vacuum rated fittings and motor feed throughs to maintain low levels of vacuum generated by the vacuum pump. The second was to maintain reaction temperatures within the reactor at a constant, target temperature. This was accomplished using a coaxial

heating coil installed on the outside of the reactor vessel. The third goal was to maintain a low volume to surface area ratio inside the reactor. This allows for more efficient devolatilization of the tar feedstock and for more of the reactor to be utilized in condensing polymerization reactions as the mesophase is formed and sheared into alignment. This was achieved by high RPM spinning of a helical spiral wound wire brush inserted inside of the reactor. This brush provided a thin film of reacting tar on the inside surface of the reactor wall through high centrifugal forces. The last goal was to accommodate the temperature-dependent viscosity of the tar and forming mesophase pitch. Since the tar experiences very high viscosities and resistance to flow at room temperature, the feedstock storage vessel, transfer line, metering valves and on/off control valves were all heated. Similarly, the pitch product is a hard, glassy solid at room temperature. This meant the product stream coming off the reactor could not be allowed to cool until it had flowed into the final pitch collection vessel. This was accomplished by installing a drip cone at the bottom of the spinning brush portion of the reactor. The hot liquid pitch product exiting the reactor was allowed to collect on the point of the cone and fall into the cooled collection vessel.

A schematic of the pitching reactor can be seen in figure 2.2.1-3. The reactor was vertically mounted on a Unistrut framework and attached to the multi-stage condensation system via an 8-bolt 11.4 cm diameter 304 stainless steel flange and an 11.4 cm diameter copper gasket. The reactor consisted of a 4.5 cm outside diameter schedule 40 by 94 cm long 316 stainless steel pipe. The top of the reactor includes a cross fitting which provides a vacuum rated seal through an elastomer sealed rotary motion feedthrough for the spinning brush motor, an inlet 32 mm Swagelok tube fitting (Chaska, MN, USA) for the feed tar, a k-type thermocouple through a 32 mm Swagelok tube fitting (Chaska, MN, USA), and an 8-bolt 11.4 cm diameter 304 stainless

steel flange for vapor outlet. The bottom of the reactor reduces to a 3.8 cm outside diameter schedule 40 by 71 cm long 316 stainless steel pipe which includes sight glasses to visually confirm product flow and the pitch product collection vessel. The middle section of the reactor was heated with Thermocoax Extreme Heavy Duty Rigid Heating Cable (Thermocoax Inc., Alpharetta, GA, USA). The top and bottom of the reactor required cooling collars with tap water as a heat exchange fluid to avoid damage to the elastomer gaskets providing vacuum rated seals at the motor and the drip cone. The overall height of the reactor was 165 cm with 69 cm of the length containing a 316 stainless steel spiral wound brush with a diameter of 3.8 cm purchased from the Gordon Brush Manufacturing Company (City of Industry, CA, USA) providing reactor agitation and acting as the thin film reactor. It was also noted that an unused 32 mm Swagelok tube fitting (Chaska, MN, USA) gas port is installed 8.9 cm above the bottom 8-bolt 11.4 cm diameter 304 stainless steel flange on the spinning band portion of the reactor. This port is currently covered by insulation and was included for potential future work involving the addition of a gas into the reactor, like hydrogen for deoxygenation reactions. The reactor heating was controlled using Labview (National Instruments Corporation, Austin, TX, USA), additionally the reactor temperatures, pressure, and spinning brush rpm were recorded with Labview data logging.

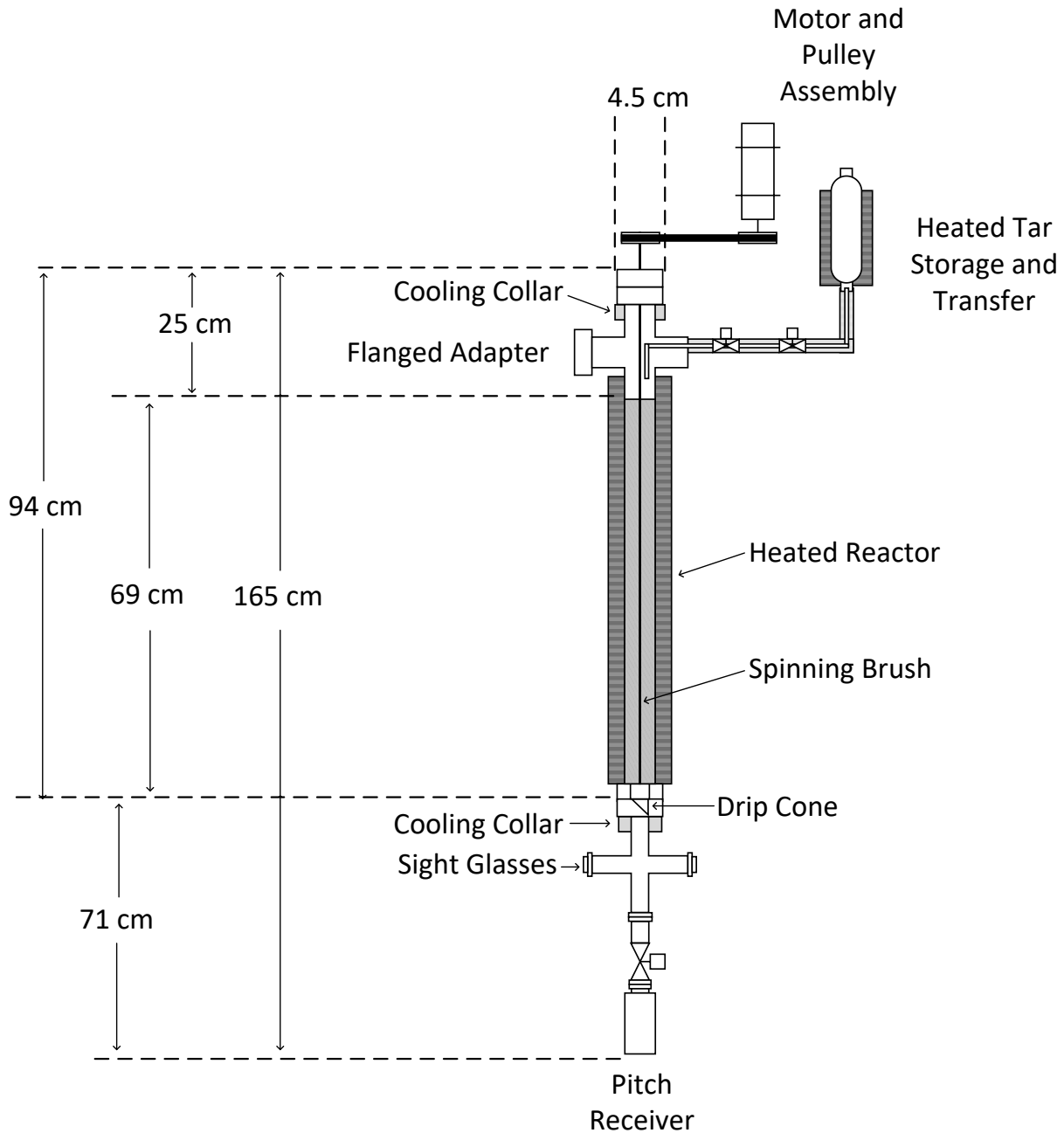

Figure 2.2.1- 3: A schematic of the pitching reactor

2.2.2 Experimental Materials

The only experimental material required for this experimentation was soybean oil acquired from Ag Processing Inc (Dawson, MN, USA).

2.2.3 Tar Feedstock Preparation and Pitching Reactor Operation

Several steps were required to transform feed soybean oil into a bio-tar suitable for use as a feedstock for the tar pitching reactor. A generalized summary of these steps can be seen in Figure 2.2.3-1.

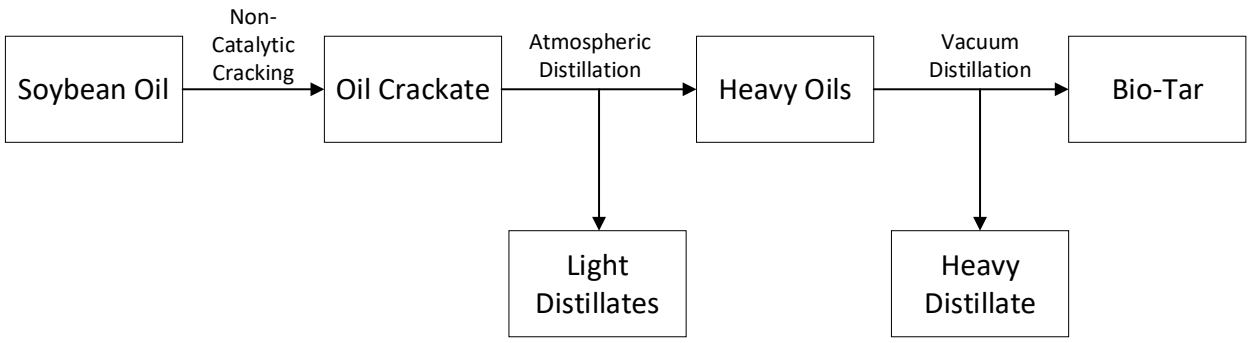

Figure 2.2.3- 1: Generalized processing steps for bio-tar generation

First, soybean oil was non-catalytically cracked using a continuous tubular reactor, designed and built at the University of North Dakota. Soybean oil was cracked by controlling pressure, temperature, and flow rate inside the reactor. In general, soybean oil was cracked using a temperature of 420 °C, a pressure of 2.9 MPa and a flowrate of 2 L/hr. Cooled, collected soybean oil crackate was stored for further processing. The experimental system used was designed and built by M. Linnen and described in his dissertation.[5]

Next, the oil crackate was distilled at atmospheric pressure to remove light-end volatile components. This was performed through a bulk flashing process. This flash used a modified 5 liter Parr Series 4580 High Temperature Reactor (Serial number #4580-0908-12536) purchased from Parr Instrument Company (Moline, IL, USA) as a boiling pot with condenser coil. The crackate from the non-catalytic cracking step was loaded into the reactor vessel of the Parr. The

vessel was then heated from room temperature to 300 °C, while allowing any evolved gases to exit the reactor and condense in the cooling coil. Once at 300 °C, the vessel was allowed to soak for 5 minutes, before cooling the reactor vessel using the internal cooling coils. The heavy oils remaining in the Parr reactor vessel were saved for future use.

The heavy oils from atmospheric distillation were then processed through vacuum distillation to remove heavier-end less volatile compounds. This was performed using the tar devolatilization apparatus and multi-stage condensation system described in section 2.2.1. The heavy oils from the atmospheric distillation step were loaded into the glass boiling flask of the tar devolatilization apparatus. The flask was attached to the distillation head and vacuum was applied. The boiling flask was then heated from room temperature to 350 °C. Once the desired distillation temperature was reached, the heating was stopped and the flask allowed to cool to room temperature, before removing and storing the residual tars within the distillation flask. These residual tars are the bio-tar feedstock used in the pitching reactor.

The remaining non-volatile compounds like asphaltenes, oligomers, and poly-cyclic aromatics, were considered bio-tars. A more detailed description of the bio-tar production process can be seen in Appendix 1.1 Production of Soy Based Tars.

A description of the pitching reactor and multi-stage condenser system used in this experimentation can be found in section 2.2.1 of this document. Operation of the pitching reactor was as follows:

1. The bio-tar feedstock from the vacuum distillation step was filtered and loaded into the tar feedstock vessel on the pitching reactor.

2. The feed preheater was turned on with a setting of 100 °C and an inert atmosphere applied inside the vessel by purging with compressed nitrogen.
3. The vacuum pump was started and used to evacuate the reactor and distillation system to a pressure of 200-400 millitorr. Leak testing was used prior to the actual experiments to insure that vacuum could be maintained
4. The cooling and hot water required for the multi-stage distillation apparatus was turned on and the reactor heating coil was energized.
5. Once the reactor had reached the desired operating temperature, the internal spinning brush was turned on to 900 RPM.
6. The on/off control valve on the tar feed line was opened and the metering valve opened and adjusted to meet the desired tar flowrate.
7. The pitching reactor was allowed to run until the desired amount of product was formed and collected.
8. The tar feed was stopped and the reactor system allowed to cool.

A more detailed description of the pitching reactor operation can be seen in Appendix 1.2 Pitching Reactor Operation.

2.2.4 Analytical Methods

Two primary methods were used to assess the functionality of the tar pitching reactor: gravimetric and thermogravimetric analysis (TGA). Gravimetric analysis allows for the closure of mass balances around the reactor to determine overall recovery. TGA was performed using a Q-Series TGA-DSC SDT-Q600 (TA Instruments, New Castle, DE, USA). TGA allows for the

assessment of thermal stability and can provide insight into the complexity of the formed pitch product exiting the reactor. This was performed with the following temperature profile: ramp at 10 °C/minute to 110 °C, hold isothermal for 5 minutes, ramp at 10 °C/minute to 900 °C, and hold isothermal for 15 minutes. The first ramp in this procedure ensures the sample is dry, the second ramp provides insight into thermal stability of the sample.

2.3 Results and Discussion

The goal of this research was to design and build a reactor system to process bio-based tars into a hard, glassy mesophase pitch product. This reactor was commissioned, and initial trial data evaluated for the production of pitch products from soy-based bio-tars.

Atmospheric and vacuum distillation steps were employed in preparing the bio-tar feedstock from the initial crop oil crackate. Gravimetric analysis was used to evaluate the mass recovery on each of these distillation steps.

Figure 2.3-1 shows the fraction of the inlet mass that ends up in the light distillate and heavy oil fractions after separation via the atmospheric distillation step. The mass distributions from atmospheric distillation were approximately even, with both the light distillates and the heavy oils having a mass recovery of roughly 46%. The overall recovery was approximately 92%, leaving 8% unaccounted for in the overall mass balance. This was assumed to be a combination of a non-condensable gas phase, which was vented, and residual crackate within the reactor vessel, cooling coil, and light distillates receiver.

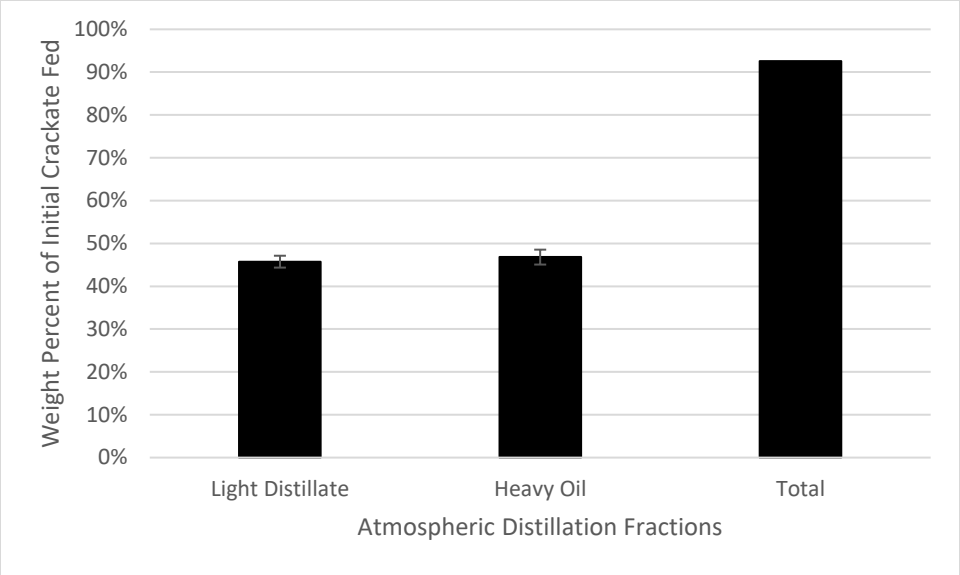

Figure 2.3- 1: Mass fraction of light distillate and heavy oils from the atmospheric distillation step, in wt% of original crackate, with 95% confidence based on 8 replicates.

Gravimetric analysis of the vacuum distillation step can be seen in Figure 2.3-2. This figure shows the mass fraction of the initial heavy oils that were recovered as bio-tar, heavy distillate, and medium distillate. It can be noted that there was no mass collected in the light distillates condenser and the medium distillates condenser received less than 1% mass recovery. This indicates that the initial atmospheric distillation removed all of the light end components, leaving primarily heavy end distillates. The overall mass recovery from the vacuum distillation was 95%. The unaccounted-for mass was assumed to be caused by residual mass left in the heavy distillate condenser and distillation head. It was assumed that no gas was formed during this step given the previous atmospheric distillation step. It was observed that more heavy distillates than bio-tar was recovered. Coupled with the results from previous steps, atmospheric distillation and the vacuum distillation , the overall mass recovery of initial crop oil crackate as bio-tar feedstock was approximately 17 wt%. This shows that, in the crop oil crackate, an appreciable portion is recoverable as bio-tar and justifies attempts to process this waste stream into usable products.

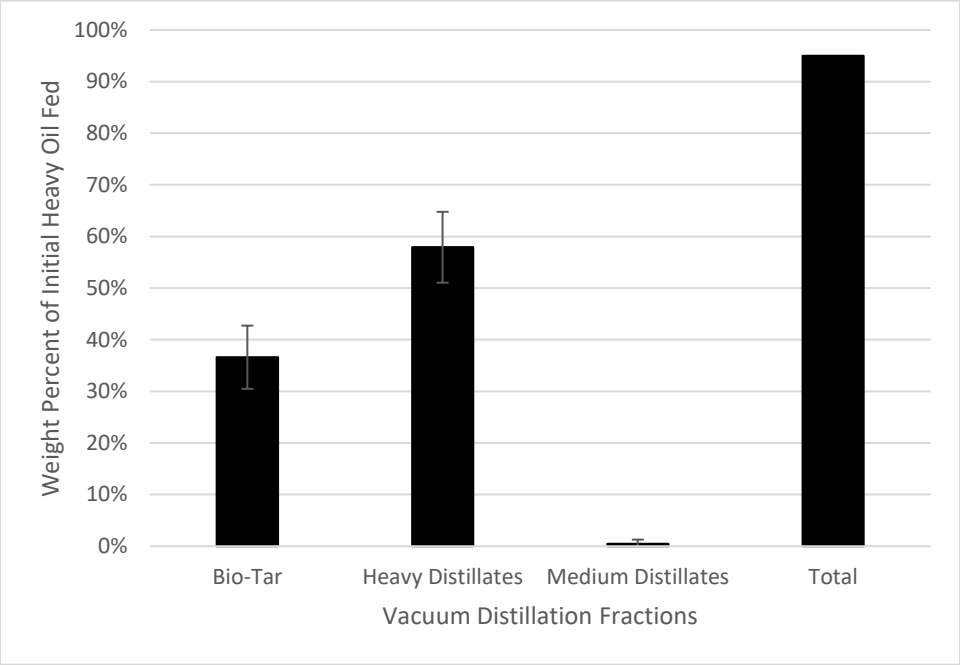

Figure 2.3- 2: Mass Fraction of initial heavy oils recovered as bio-tar, heavy distillate, and medium distillate in wt% with a 90% confidence from 3 replicates.

The pitching reactor was used to perform several different experiments with increasing temperatures. The temperatures examined in this work were 325, 350, 375, and 390 °C. The gravimetric results from these trials can be seen in Figure 2.3-3. This figure shows the fraction of inlet biotar mass collected as pitch product or heavy distillates at each operating temperature. It can be seen that increasing the processing temperature leads to an increase in the mass collected as heavy distillates and a decrease in pitch production. This is attributed to the reactor more effectively volatilizing any remaining heavy end components with higher operating temperatures.

The pitch products from these runs were first evaluated on a visual basis. A mesophase pitch product will transform the sticky tar feedstock into a glassy, hard solid. In this set of temperature trials, the only condition that generated a solid, glassy product was 390 °C. This is attributed to the reactor more rapidly removing residual heavy distillates, allowing for a larger portion of the

reactor residence time to be utilized in mesophase formation reactions. Unfortunately, an approximate upper temperature limit of 400 °C was provided by the manufacturer of the spinning brush utilized in the pitching reactor. This did not allow for higher temperature trials to be performed with the pitching reactor. It is theorized that running a more aggressive vacuum distillation will help to remove additional heavy distillates from the tar feedstock. This would, in turn, improve the effect seen at the 390 °C temperature fraction. Given the weight recovery of 25% pitch product at 390 °C, an overall mass of crop oil crackate to solid pitch product can be calculated using the information seen in Figures 2.3-1,2. This recovery is approximately 4.3 wt%.

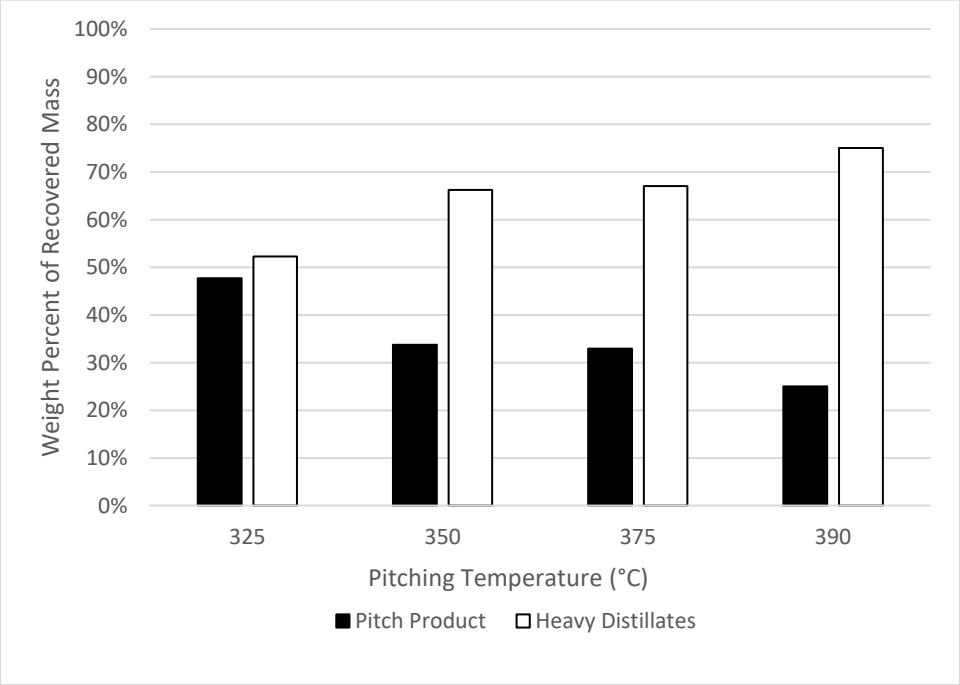

Figure 2.3- 3: The fraction of inlet bio-tar mass collected as pitch product or heavy distillate in wt%.

The results from all distillation and pitching steps are summarized in Table 2.3-1. This table shows the overall mass recovery in wt% of the crop oil crackate fed into the distillation process.

It can be seen that the highest recovery was in the light distillates mass fraction. This is to be expected, considering the crop oil cracking process was designed to optimize fuel production.[5] The next highest recovery was the heavy distillates fraction, followed by mesophase pitch and medium distillates. This process does not provide high production rates of mesophase pitch but does offer a potential use for this waste tar stream. In a companion study, Amsley-Benzie shows that almost 50% of the revenues from a non-catalytic cracking process can be obtained from this low production rate due to the current high value of continuous carbon fibers.[48] Even if mesophase pitch production is not the target of this work, the recovery of the additional heavy distillates for conversion into other fuel and chemical products would justify adding devolatilization processing to a cracking-based biorefinery.

Table 2.3- 1: Overall mass recovery in wt% of crop oil crackate feed from distillation and pitching steps.

Processing Step	Light and Medium Distillates (wt%)	Heavy Distillates (wt%)	Pitch Product (wt%)
Atmospheric Distillation	46%	----	----
Vacuum Distillation	0.2%	27%	----
325 °C Pitching	----	9.0%	8.2%
350 °C Pitching	----	11%	5.8%
375 °C Pitching	----	11%	5.6%
390 °C Pitching	**----**	**13%**	**4.3%**

Sample mass loss as measured by TGA of the initial bio-tar feed and pitch products at 325, 350, 375, and 390 °C can be seen in figure 2.3-4. The mass loss up to 500 °C is considered volatile carbons, while the mass loss after 500 °C is considered fixed carbon. It can be seen that the initial bio-tar feed consists primarily of volatile carbons. The pitch products for 325, 350, and 375 °C all experience similar ratios of fixed and volatile carbons, with increasing fixed carbons over the initial feed. This indicates the pitching reactor acted to remove more volatile species and form more thermally stable components within the pitch product at the entire temperature range.

No specific temperature from the 325, 350, and 375 °C grouping experiences drastically improved performance, being within 1 wt% of each other. This suggests that processing at temperatures below 375 °C was primarily removing volatile components, rather than forming larger, thermally stable components. This supports the conclusion that the formation of a glassy solid mesophase pitch requires both effective devolitization and residence time under shear.

The 390 °C pitch product shows significantly increased thermal stability and fixed carbon content compared to the results from the lower temperatures. This shows drastic improvement when compared to the initial bio-tar feed. It can be seen that higher reaction temperatures produce higher quality pitch products, when examining volatile carbon removal and fixed carbon formation. This 390 °C pitch was sent to the Center for Advanced Engineering Fibers and Films (CAEFF) at Clemson University, SC to evaluate its potential for use in carbon fiber formation. It was found the softening point associated with this sample was 122 °C. Although this shows a large improvement over the sub-ambient softening point experience by the 325, 350, and 375 °C pitch products, this softening point is too low for carbon fiber formation and indicates the molecules within the pitch are too small to be drawn into fibers and stabilized. From these results, a more heavily devolatilized tar feed stock, higher pitching reactor temperature, and/or longer reactor residence time is recommended to form higher quality pitch products.

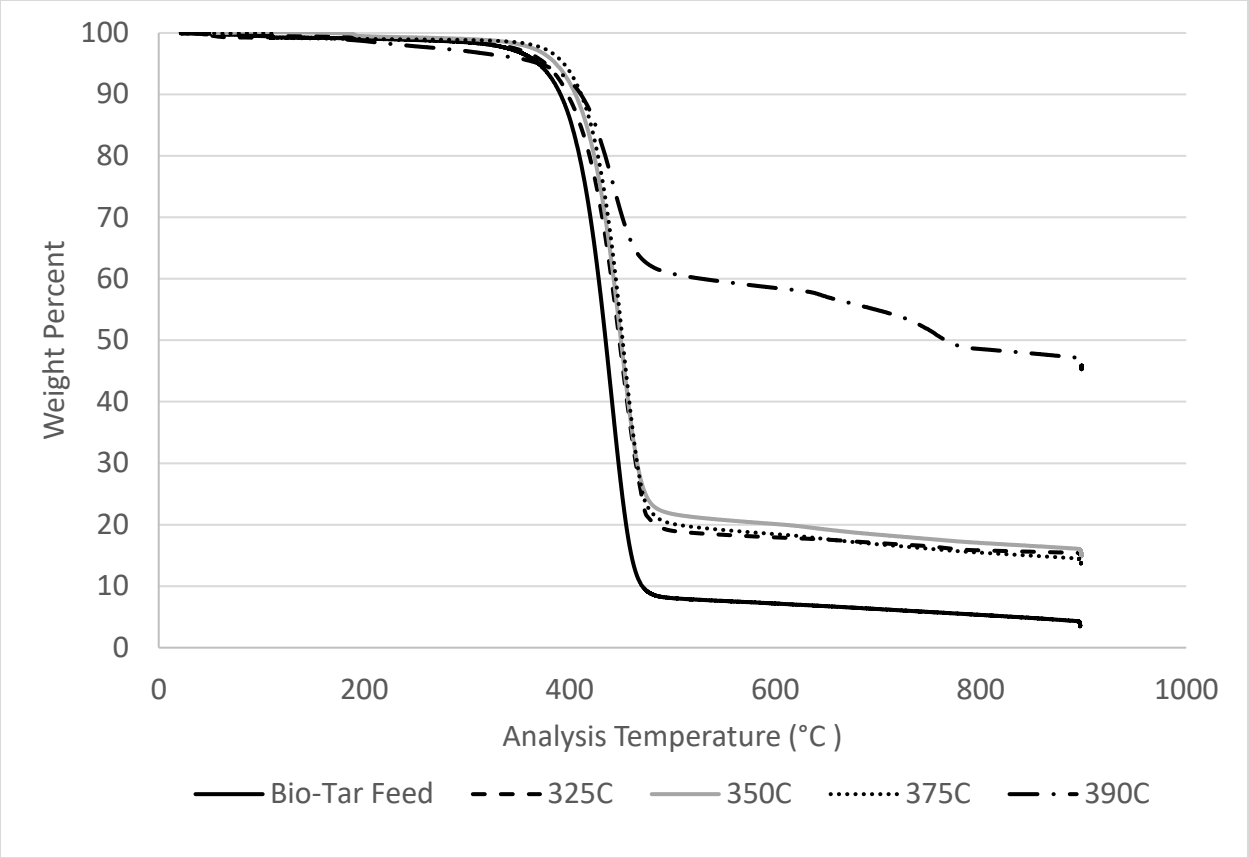

Figure 2.3- 4: Sample mass loss for bio-tar and pitch products generated in the pitching reactor at various pitching temperatures as determined by TGA analysis as wt% of total sample feed.

2.4 Conclusions and Recommendations

- This work successfully demonstrated a pre-processing and continuous pitch processing system for the production of mesophase pitch from the non-volatile organic compounds generated during the non-catalytic cracking of a triglyceride oil (soybean oil).
- The crop oil crackate used in this research provided an overall mass recovery to bio-tar of approximately 17 wt% and an overall conversion of 4.3 wt% into mesophase pitch. The remaining heavy distillates could be processed into asphalt or cracked using visbreaking

technology into additional middle distillate molecules. Another possibility is to generate carbon black, which would make a high value by-product.

- Operating temperatures of 325, 350, 375, and 390 °C were investigated in the pitching reactor. All of these temperatures experienced additional devolatilization of the tar feed stock, with 390 °C experiencing the highest degree of devolatilization at 25 wt% pitch product recovery. Thus, even if mesophase pitch production is not the target of this work, the recovery of the additional heavy distillates for conversion into other fuel and chemical products would justify adding devolatilization processing to a cracking-based biorefinery.
- The 390 °C operating temperature was the only condition tested which produced a solid pitch product, indicating increased shearing time after tar devolatilization leads to improved pitch products.
- The overall mass recovery of crop oil crackate as mesophase pitch products at 390 °C operating temperatures was approximately 4.3 wt%.
- TGA data showed minimal differences between the tars processed at 325, 350, and 375 °C with a significant increase in thermal stability of the 390 °C sample, indicating that there was an increase in complex components formed within the pitch product at the higher operating temperature. This supports the conclusion that devolatilization alone is not sufficient to generate mesophase pitch. Instead, adequate time after devolatilization is needed for complex component formation and alignment under shear.
- The softening point of the 390 °C pitch product was 122 °C. Although this shows a large improvement over the sub-ambient softening point experience by the 325, 350, and 375 °C pitch products, this softening point is too low for carbon fiber formation and indicates the molecules within the pitch are too small to be drawn into fibers and stabilized.

- It is recommended the tar feed stock be more heavily devolatilized in the vacuum distillation step, before being used in the pitching reactor to test if longer post-devolatilization in the pitching reactor will improve the softening point. This would either be done through longer dwell times at the 350 °C temperature used previously or by increasing the maximum devolatilization temperature. It is important to avoid coking of the tar feed stock, as the 350 °C operating temperature is the beginning of the coking region for tars. A tar feedstock with reduced volatility should experience increased reactor efficiency, as seen in initial pitching reactor trials.
- Other options that could be explored are: 1) increase the length of the pitching reactor to increase the time available for complex component formation and 2) replace the existing spinning brush with a material that can withstand higher temperatures so that the pitching reactor can be operated above 390 ^{o}C.
- It is recommended additional analytical steps be performed on the pitch products formed. The components within the tar and pitch product experience boiling points >350 °C, making them difficult to analyze in traditional GC/MS systems. Py-GC/MS can be employed on both tar feedstocks and pitch products to better understand the changes within the tar before and after processing into pitch products, without the likelihood of damaging GC injectors and columns. Additionally, the molecular weight distribution of feed tars and pitch products could be examined using a GPC system, assuming an appropriate solvent was determined for sample preparation. Softening point analysis through the drop formation method was performed on pitch samples by CAEFF and is recommended when measuring the softening point of pitch products. The rheological properties of pitch products should be examined, to determine expected behavior when

melt spinning the samples. This would require a rheometer with heating capabilities, like the TA Instruments AR 2000 in the chemical engineering department at UND.

Chapter III. The Extraction of Fatty Acids from Algae Biomass

Abstract

This chapter details a comparative study evaluating the most viable methods and conditions identified by previous researchers for the extraction of lipids from microalgae biomass in a single, consistent study. The use of microalgae as a feedstock for renewable fuels and chemicals has experienced an immense amount of interest as documented in the literature during the last 10 years. This interest is focused on the use of the lipids in microalgae, which are a fatty acid-based oils similar to crop oils, as renewable fuel feedstocks because of algae's ability to produce large amounts of biomass more quickly than traditional oilseed crops. The ability for microalgae to be grown in conditions not viable for seed oil crops, like arid locations or brackish water, also provide additional benefits when compared to traditional agricultural products. In addition to lipids, microalgae contain a large variety of desirable extractable chemicals and components such as pigments, proteins, carbohydrates, and enzymes.

Unfortunately, the use of microalgae as a renewable feedstock faces several barriers to commercialization. One of these barriers is the complexity of extraction lipids from the microalgae biomass, due to its hard cell wall and membrane. Many researchers have published techniques, with varying success, for lipid extraction. However, with differing methodologies and analytical methods, it is difficult to determine the relative merits of these techniques or of combinations of these techniques. The goal of this research was to perform a study that investigates all of the most promising primary methods identified by earlier researchers, separately and in certain combinations, in order to provide a consistent comparison of the methods for the efficient extraction of lipids from microalgae.

In this research, a series of solvent screening studies were performed using the attractive solvents as found in the literature. Methanol, ethanol, chloroform, acetonitrile, hexane, and Bligh-Dyer

were identified as the most promising candidate solvent to leach lipids out of algae and/or to extract triacylglyceride oils out of crop oil. Also considered in this research was the use of microwave, sonication, and insitu-transesterification as methods to increasing extraction efficiency.

It was determined that methanol was the best performing solvent for lipid extraction from *Chlorella Vulgaris* microalgae. Methanol consistently outperformed the other solvents examined. It was also the top solvent for use with microwave and sonication assisted extraction, as well as, for in-situ transesterification. The highest lipid recovery was found to be 37 wt% of the initial lipids which was achieve using methanol as the solvent with sonication and in situ-transesterification.

In the comparison between microwave and sonication-assisted extraction, it was found that both methods improved extraction, but the microwave provided higher extraction efficiency. This is believed to be due to a higher fraction of additional cell wall rupture provided by the microwave heating, which heats internally, compared to sonication, which heats externally.

The use of in-situ transesterification was found to increase the extraction efficiency of lipids with a methanol solvent. This is believed to be due to increased cell rupture from the transesterification making it more effective at breaking the cell wall-membrane layer.

Additional factors found to have a potential impact on extraction efficiency that warrant further investigation include: pretreatment ball mill grinding speed, extraction temperature, and lipids-to-solvent ratio.

3.1 Introduction

The use of microalgae as a feedstock for renewable fuels and chemicals has experienced an immense amount of interest as documented in the literature during the last 10 years. This interest is focused on the use of the lipids in microalgae, which are a fatty acid-based oils similar to crop oils, as renewable fuel feedstocks because of algae's ability to produce large amounts of biomass more quickly than traditional oilseed crops.[11] The ability for microalgae to be grown in conditions not viable for seed oil crops, like arid locations or brackish water, also provide additional benefits when compared to traditional agricultural products.[12] In addition to lipids, microalgae contain a large variety of desirable extractable chemicals and components such as pigments, proteins, carbohydrates, and enzymes.[13-16].

The research presented herein focused on the extraction of lipids from microalgae. On average, microalgae have a 30% higher lipid content when compared to the triacylglycerides contained in traditional oil producing crops, like soybeans.[11] Regardless of source, these lipids and triacylglycerides are essentially fatty acid (FA) oils. Table 3.1-1 shows a comparison of FA oil production per year in liters per square kilometer and FA oil content for various sources.[49-53] In this table, microalgae has been divided into three separate categories based on lipid content: low, medium, and high. It can be seen that even the highest producing terrestrial crop has an order of magnitude less FA oil production per square kilometer than the low lipid microalgae. This significant difference is attributed to the high growth rate associated with microalgae production allowing for harvesting of biomass in days to weeks instead of months, as seen with traditional oil producing crops.[49, 54] The wide range of lipid content seen within microalgae is attributed to the large number of microalgae strains and the impact of growing conditions on lipid content within the algae cell.[49, 53, 55]

Table 3.1- 1: A comparison of FA oil production per year in liters per square kilometer and FA oil content for various sources. [49-53]

Source	FA Oil Production (L/km^2)	FA Oil Concentration in Source (wt%)
Oil Palm	5.7E+05	35.3
Coconut	2.6E+05	35.3
Jojoba	1.7E+05	48 - 56
Rapeseed (canola)	1.1E+05	30
Peanut	1.0E+05	53 - 71
Sunflower	9.2E+04	47.3
Linseed	4.6E+04	34
Soybean	4.3E+04	17.7
Corn	1.7E+04	4
Low Lipid Microalgae	5.9E+06	30
Medium Lipid Microalgae	9.8E+06	50
High Lipid Microalgae	1.4E+07	70

It is estimated that approximately 40,000 different varieties of microalgae have been identified, providing an immense biodiversity within the research field. Each of these varieties provide a biomass with unique chemical and macromolecular content. Table 3.1-2 shows the average lipid content in weight percent of algae biomass and FA profile of select microalgae strains as the mass fraction of the total FA content.[53] This table highlights the variation of lipid content and distributions seen between microalgae strains. It is important to note that not only are the overall

lipid contents species dependent, the form of lipids within the microalgae cell experience wide distributions as well. This places emphasizes on the necessity of choosing the most appropriate strain of microalgae for the desired application.

Table 3.1- 2: Average lipid content mass fraction of algae biomass and FA profile of select microalgae strains as the mass fraction of total FA content.[53]

Microalgae Strain	Total Lipids (wt%)	Saturated Fatty Acids (wt%)	Monounsaturated Fatty Acids (wt%)	Polyunsaturated Fatty Acids (wt%)
Botryococcus Terribilis	49	43.15	44.29	12.56
Heterosigma sp.	39.9	45.4	31	23.7
Chlorella Vulgaris	**28.07**	**52.15**	**37.51**	**10.33**
Scenedesmus sp.	16	18.59	26.86	30
Chlorella Salina	11	29.34	18.52	40.63

The research presented herein focused on the *chlorella vulgaris* (*CV*) strain of microalgae. This choice was made for several reasons. First, *CV* is well studied within the literature.[12, 15, 18, 52, 56-64] Second, the fatty acid profile for *CV* primarily includes saturated and monounsaturated fatty acids, making it suitable for conversion into renewable fuels and chemicals.[65] The average fatty acid composition of *CV* is as follows - C12:0 (0.7%), C14:0 (1.91%), C14:1 (1.58%), C15:0 (0.9%), C15:1 (1.8%), C16:0 (15.3%), C16:1 (2.63%), C16:2 (6.3%), C16:3 (4.9%), C17:1 (6.47%), C18:0 (3.37%), C18:1 (16.7%), C18:2 (13.8%), C18:3 (12.9%), C20:0 (3.12%), C20:1 (1.85%), C20:2 (1.05%), C20:4 (1.06%), and C20:5 (0.47%).[49] Third, *CV* is a robust strain,

capable of growing in a variety of conditions.[65] This was necessary for the application of this research in the masters work of Jasmine Oleksik (Kreft), who was utilizing the results from current research to both autotrophic and heterotrophic adaptations of this microalgae.[54] Lastly, the work performed in this research was a collaborative effort between Dr. Andrew Ross at the University of Leeds in Leeds, UK and the University of North Dakota. Chlorella vulgaris was the preferred microalgae strain in those collaborative labs.[66, 67]

It is well accepted in the literature that the multiple benefits associated with microalgae discussed previously are not currently feasible for implementation on an industrial scale. One factor is the difficulty associated with extraction the lipids out of the microalgae. Lipids in microalgae are stored as globules within the cell and/or contained within a phospholipid bi-layer membrane. [49] The cell is protected by a rigid cell wall, with estimated tensile strength of 9.5 MPa, making removal of materials from within the cell slow and inefficient. This requires that both the cell wall be disrupted and an appropriate solvent be chosen to maximize lipid recovery.

Two primary categories of cell disruption have been reported previously: mechanical and non-mechanical. Mechanical methods physically destroy the cell wall, often by applying large compressive or shearing forces. Traditional mechanical FA oil extraction techniques seen in seed oil processing, like expeller and oil press, are incapable of accommodating the small size associated with the microalgae cells, typically 3 to 10 μm.[13] Cell disruption methods demonstrated to work with microalgae include ball milling, microwave, and ultrasonication. The use of ball milling/grinding has been shown to increase lipid extraction recovery by approximately 120%, when compared to extraction without cell pretreatment.[62] The use of microwaves has results in lipid recovery improvements of 38 to 610%.[55, 68] Ultrasonication has been shown to increase lipid extraction by 30 to 400%.[14, 68] The actual effectiveness of each of

these methods is largely dependent on the initial microalgae being treated. Microalgae with weaker cell walls see less improvement from mechanical cell disruption, while microalgae with stronger cell walls benefit more significantly from mechanical cell disruption.[15] All of these methods are effective, but energy intensive and often require additional biomass processing.[13]

Non-mechanical cell disruption methods do not rely on physical energy to destroy the cell wall. Instead, they rely on chemical cell lysis and increased penetration and permeability of solvents to effectively remove lipids. Examples of these methods include enzymatic digestion, supercritical fluid extraction, in-situ transesterification, and solvent extraction. Enzymatic digestion has proven to be effective in certain cases, but the long processing time required and general resistance of the cell wall to enzymatic attack make this method less desirable for commercial applications.[68] Supercritical fluid extraction has proven to be effective, but requires high temperatures and very high pressures. These conditions are generally expensive to maintain and less favorable for commercial applications.[13] In-situ transesterification combines lipid recovery and biodiesel production into a one-step process. The transesterification catalyst and presence of esters within the cell facilitate cell rupture. In-situ transesterification has seen total lipid recoveries of up to 98%.[13] The use of non-polar solvents, like hexane, are prevalent in seed oil FA oil extraction, but are not effective in the extraction of microalgae lipids.[64] This is attributed to the inability of non-polar solvents to break the cell wall and membrane, given the strong hydrogen bonding associated with this layer. The most commonly seen solvent extraction methods in literature use two-part solvent extraction. A polar solvent is used to break the cell wall and a non-polar solvent to extract the desired lipids. Common solvents from literature include methanol, chloroform, hexane, and ethanol.[68, 69] The most common solvent combination is 2:1 methanol and chloroform, known as the Bligh-Dyer solvent.[69]

Many researchers have published techniques, with varying success, for lipid extraction. However, with differing methodologies and analytical methods, it is difficult to determine the relative merits of these techniques or of combinations of these techniques. The goal of this research was to perform a study that investigates all of the primary methods identified by earlier researchers, separately and in certain combinations, in order to provide a consistent comparison of the methods for the efficient extraction of lipids from microalgae. The conclusions from this work were then used in subsequent work by others, Kreft [54]and Hamman[70] to optimize the recovery step.

3.2 Methods and Materials

3.2.1 Materials

The *Chlorella Vulgaris* microalgae used for these extraction experiments was provided by the University of Leeds (Leeds, England). This algae was purchased as 80-120 mesh, freeze-dried microalgae manufactured by Qingdao Sunrise Trading Co., Ltd. (Qingdao, China). Mechanical cell rupture on the microalgae was performed using a Retsch MP100 Planetary Ball Mill (Retsch, Haan, Germany). This was done to promote increased extraction efficiency.

This research used the following solvents for lipid extraction experiments: methanol, ethanol, chloroform, acetonitrile, and hexane. The methanol (histological grade, A433S20), Ethanol (>99.5%, BP2818-4), Hexane (>98.5%, H2924), and chloroform (>99%, AC232090010) were purchased from Fisher Scientific (Waltham, MA, USA). The acetonitrile (>99.5%, 36423) was purchased from Alfa Aesar (Haverhill, MA, USA). For transesterification experiments, hydrochloric acid (technical grade, A142212) was purchased from Fisher Scientific (Waltham, MA, USA).

3.2.2 Experimental Methods

This study examines the impact of solvent choice on algae lipid extraction and recovery. This was performed using six different solvents in combination with either microwave or sonication assistance for cell rupture. The solvents investigated in this study are methanol, ethanol, hexane, acetonitrile, chloroform, and Bligh Dyer (2:1 methanol to chloroform). Bligh Dyer was identified and chosen as the most common solvent used in literature solvent extraction. Methanol and chloroform were chosen because of their common use in solvent extraction and to determine if individual contributions to the Bligh Dyer solvent could be observed. Ethanol was chosen as a renewable alternative to methanol and would also be used for in-situ transesterification testing along with methanol. Finally, hexane was chosen as a common oilseed extraction solvent. Generalized experimental methods, described below, were used with each of these solvents.

A summary of the experiments performed can be seen in table 3.2.2-1. Factors considered in this experimental set-up were: solvent type, extraction temperature, ball milling speed, algae-to-solvent ratio, microwave assistance, sonication assistance, and transesterification assistance. These experiments were performed to screen initial conditions to determine what additional experimentation on lipid extraction from microalgae biomass should be pursued. It should be noted that experiments were performed in two separate locations, University of Leeds in Leeds, UK (UoL) and the University of North Dakota in Grand Forks, ND (UND).

Table 3.2.2- 1: Summary of the experimental test plan associated with algae extraction experiments.

Experimental Set	Solvent Type Screening I	Ball Milling Study	Algae-to-Solvent Ratio Study	Extraction Temperature Study	Solvent Type Screening II	Solvent Type Screening III
Number of experiments	18	6	6	12	18	18
Location	UoL	UoL	UoL	UoL	UND	UND
Solvent Type*	M E H C AC BD	M	M	M	M E H C AC BD	M E H C AC BD
Extraction Temperature (°C)	50	50	50	50 60 80 100	50	50
Ball Milling Speed (RPM)	250	250 400	250	250	250	250
Algae to Solvent Ratio (gram biomass:ml)	1:10	1:10	1:10 1:20	1:10	1:10	1:10
Microwave Assisted	+	+	+	-	-	-
Sonication Assisted	-	-	-	+	+	+
Transesterification Assisted	-	-	-	-	-	+

* Solvents: Methanol (M), Ethanol (E), Hexane (H), Chloroform (C), Acetonitrile (AC), and Bligh-Dyer (BD)

3.2.2.1 Microwave Assisted Extraction

Microwave assisted solvent extraction was performed to determine the impact of microwave heating and cell rupture on solvent extraction efficiency. The microwave-assisted extraction experiments were performed using a Milestone Start Synth™ laboratory microwave with an

installed Q20 quartz rotor and Terminal 640 controller (Milestone, Sorisole, Italy). The experimental method was as follows:

1. An appropriate mass of algae was weighed using a balance with a resolution of at least 0.1 mg.
2. The weighed algae was added to the quartz microwave tube.
3. The solvent to be tested was measured by volume in a graduated cylinder
4. The solvent was added to the quartz microwave tube with the microalgae
5. The solvent and algae were agitated to ensure proper wetting of the algae and to avoid any clumps forming.
6. The microwave tube was capped and inserted into the microwave
7. A heating program, as desired for the various experimental procedures described in the test plan seen in table 3.2.2-1 , was then used to facilitate the extraction process.
8. Upon completion of the heating program, the sample was allowed to cool, then the microwave vessel was opened, and the sample removed
9. Samples from the cooled microwave tubes were filtered and both the solid residues and liquid products were collected separately.
10. Both solid and liquid product samples were allowed to dry.

A more detailed description of the microwave assisted extraction method can be found in Appendix 2.1 Microwave Assisted Extraction.

3.2.2.2 Sonication Assisted Extraction

Sonication assisted solvent extraction was performed to determine the impact of sonication cell rupture on solvent extraction efficiency. A Fisher Scientific 5.7-liter MH Series Ultrasonic Bath

(Fisher Scientific, Denver, USA) with non-programmable heating was used for all sonication-assisted extraction experiments. The experimental method was as follows:

1. An appropriate mass of algae was weighed using a balance with a resolution of at least 0.1 mg.
2. The weighed algae was added to a borosilicate glass test tube.
3. The solvent to be tested was measured by volume in a graduated cylinder.
4. The solvent was added to the test tube with the microalgae.
5. The solvent and algae were vortexed to ensure proper wetting of the algae and to avoid any clumps forming.
6. The test tube was capped and placed in a preheated ultrasonic bath
7. The sample was allowed to process for the conditions determined by the experimental procedure described in the test plan seen in table 3.2.2-1
8. Upon completion of the experiment, the sample was removed from the ultrasonic bath and cooled.
9. Samples from the cooled test tubes were filtered and both the solid residues and liquid products were collected separately.
10. Both solids and liquids were allowed to dry.

A more detailed description of the sonication assisted extraction method can be found in Appendix 2.2 Sonication Assisted Extraction.

3.2.2.3 In-Situ Transesterification-Assisted Extraction

The process of reacting the microalgae lipids in-situ with an alcohol to form fatty acid methyl esters (FAMEs) was investigated as a method to increase the removal of the lipids from the microalgae biomass. It has been postulated that the act of transesterification will accelerate algae cell disruption and may make it easier to extract the oil, now in the form of FAMEs, from the algae cells. Further, the same alcohol participating in the reaction can also serve as the solvent for FAMEs extraction. This reaction requires that a catalyst be added to the reacting alcohol. Literature indicates that acid catalysts provide increased FAME formation over alkaline catalysts.[57] For this experimentation, the chosen catalyst was 50 µL of HCl added to 10 ml of the solvent being investigated.

In-situ transesterification was performed in combination with the sonication microalgae extraction procedures discussed in section 3.2.2.2. This was done by following the experimental methods for ultrasonication assisted extraction with the modification of 50 µL of HCl added to 10 ml of the solvent determined in the test plan seen in table 3.2.2-1.

3.2.2.4 Exhaustive Soxhlet Extraction

Exhaustive Soxhlet extraction was performed in order to verify the maximum unassisted lipid extraction that could be achieved from this study's microalgae biomass. A 250 ml Soxhlet extraction apparatus, with heating mantle and total reflux condenser from Fisher Scientific (Waltham, MA, USA) was employed for this experimentation. The experimental method was as follows:

1. 12 grams of algae was weighed using a balance with a resolution of at least 0.1 mg.

2. The weighed microalgae was added to a Soxhlet filter thimble.
3. 125 milliliters of the solvent to be tested was measured by volume in a graduated cylinder.
4. The solvent was added to the Soxhlet boiling flask in the boiling mantle.
5. The glass Soxhlet holder was installed onto the boiling flask.
6. The Soxhlet thimble containing the microalgae was placed into the glass thimble holder.
7. The refluxing condenser was installed above the thimble containing the microalgae.
8. Cooling water was allowed to flow through the condenser.
9. The boiling flask heater mantle was energized and the solvent brought to a boil.
10. The mantle heat delivery was adjusted to slow the flow of condensate from the condenser into the microalgae filter thimble to a rate of approximately 1 drop every 5 seconds.
11. The sample was allowed to process for 24 hours.
12. Upon completion of the experiment, the Soxhlet apparatus was allowed to cool.
13. The solid residue samples were removed from the Soxhlet thimble holder and allowed to dry.
14. The lipid rich solvent was collected from the boiling flask and allowed to dry.

3.2.3 Analytical Methods

Two primary analytical methods were used to assess the extraction efficiency of the solvents being investigated: gravimetric and thermal carbon analysis (TCA).

In gravimetric analysis, the mass of extractable material removed was determined by comparing the mass of the original algae used to the mass recovered in the liquid filtrate after extraction. The mass of the solids residue was also weighed to close the mass balance. In each experiment,

the final solids/liquid mixture was filtered to separate the solid residues from the lipid-rich liquid filtrate. Both liquid and solid samples were allowed to fully dry in a fume hood and the mass of non-volatile components in each was determined.

TCA is used to evaluate the total carbon pyrolyzed from a sample as it is exposed to a series of increasingly aggressive temperature steps.[71] The temperature fraction at which carbon is evolved gives an indication of the complexity/stability of the original sample and its constituents. The TCA analysis was performed using a thermal optical analyzer from Sunset Laboratory Inc. (Portland, OR). Samples were prepared by dissolving the dried filtrate residues in methanol solvent. The solubilized sample was placed on a 2500QAT-UP tissue quartz filter pad (Pall Corp. East Hills, NY) and dried. The filter pad was placed in the TCA oven and analysis was run. Results were calculated as a carbon percentage of total carbon evolved from the sample.

The TCA analysis method used the following temperature steps: 200°C, 300°C, 400°C, 500°C, 890°C, and char (oxidation). Preliminary testing identified a correlation between two of the programmed temperature fractions, 300^{o}C and 400^{o}C and lipids concentration. Thus, the total recovered in these two fractions was assumed to be 100% lipids (or FAMEs). The 200°C fraction was assumed to represent the carbohydrates in the microalgae and the higher temperature fractions were assumed to represent the proteins in the microalgae.[54] The TCA combined carbon results from the 300°C and 400°C temperature fractions were used to calculate what fraction of the inlet biomass carbon and the fraction of the total lipids were recovered. This method, while indirect, was much more time efficient than performing GC or LC analysis of the samples and was considered adequate for the screening level experiments performed.

A more detailed description of the TCA analysis can be found in Appendix 2.3 TCA Analysis

3.3 Results and Discussion

The main objectives for this study were:

1) perform a comprehensive survey of candidate solvent types to identify the most attractive potential solvent(s) for lipid extraction from microalgae,
2) determine which, if any, of the most commonly proposed pretreatment methods (microwave-assist, sonication-assist, grinding, in-situ transesterification) were worthwhile, and
3) identify the near-optimum conditions for lipids extraction from microalgae.

3.3.1 Microwave Assisted Extraction Results and Discussion

Microwave assisted extraction experiments were performed per the experimental test plan provided in section 3.2.2, above. These results also include in-situ transesterification and initial data for additional optimization factors to increase microalgae lipid extraction recovery for future work. All the data presented in this section is based on gravimetric analysis. The gravimetric results are reported in dry wt% of mass extracted in the solvent phase from the initial algae biomass. Microwave assisted extraction samples were not available for TCA analysis due to sample storage equipment malfunctions at the University of Leeds.

The results from the initial solvent screening study are shown in Figure 3.3.1-1. These experiments were performed using ball milled microalgae at 250 rpm for 5 minutes. The samples were processed for 10 minutes at 50°C. From the data, it can be observed that the use of methanol or the Bligh Dyer solution led to the highest mass recovery, with 14.4 wt% and 14.3

wt% of the initial algae biomass, respectively. The next best performing solvents were ethanol and chloroform, with 8.5 wt% and 6.3 wt%, respectively. The worst performing solvents were acetonitrile and hexane, with 1.7 wt% and 1.9 wt%, respectively.

Comparing the methanol only to the Bligh Dyer results it appears that the extraction into the Bligh Dyer solution is mainly due to its methanol portion since the results are almost identical whereas extraction into only chloroform resulted in an 8 wt% lower extraction efficiency. It should also be noted that hexane performed worse than expected, given its common use in oilseed crop oil extraction. The poor performance seen with hexane as a solvent for *Chlorella Vulgaris* lipid extraction agrees with literature.[64, 68] The mass transfer ability of hexane is believed to be inhibited by polarity differences between the polar phospholipid bilayer of the algae cell membrane and the non-polar nature of the hexane.

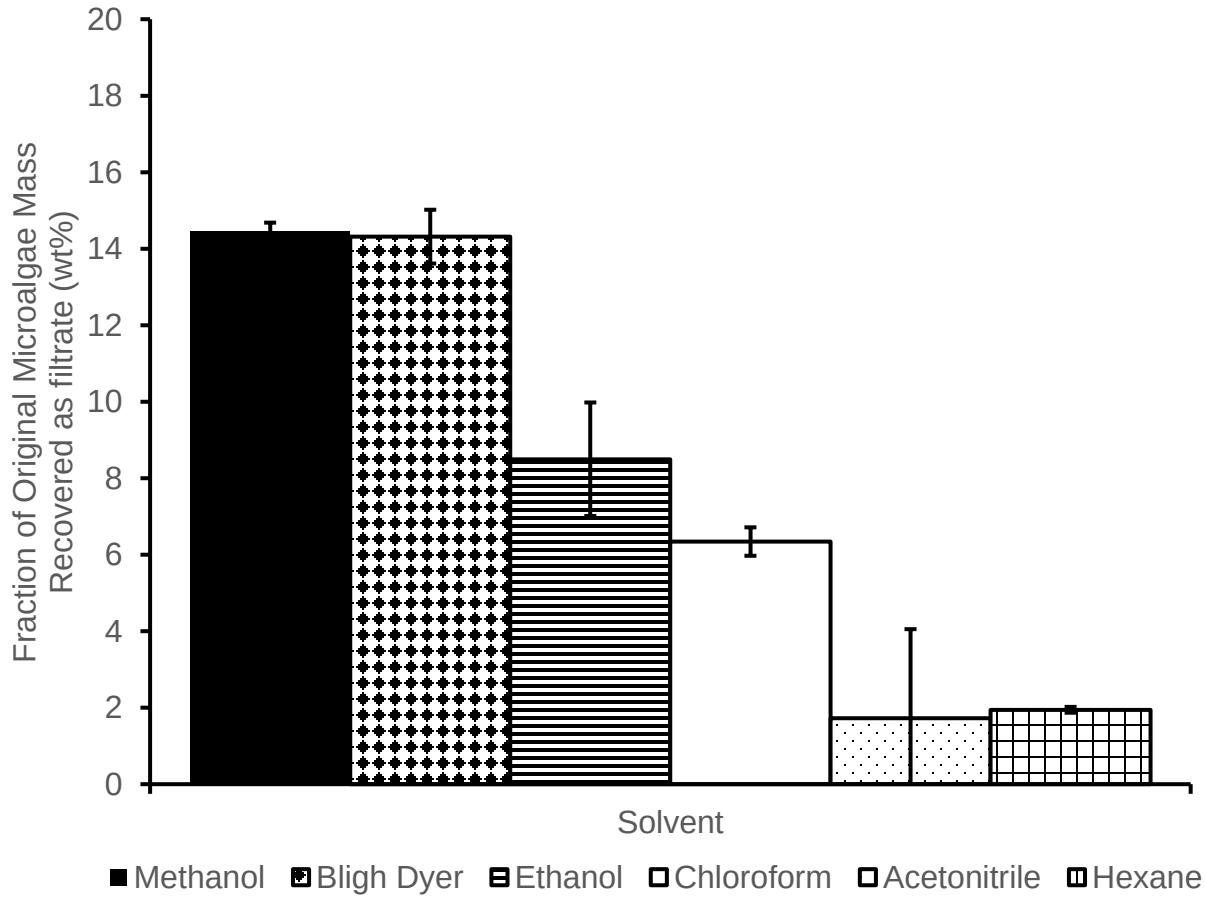

Figure3.3.1- 1 Gravimetric results from microwave assisted solvent screening study. Shown with 90% confidence intervals.

Based on the results seen in Figure 3.3.1-1, methanol was chosen for use in additional experiments to examine the reaction space and determine potential factors for additional investigation. Additional factors were investigated following the test plan shown in Table 3.2.2-1, and included ball mill grinding speed, microalgae to solvent ratio, and temperature. These factors are highlighted in the literature as impacting the amount of lipids extracted from microalgae biomass. [57, 63]

To help understand the impact of ball milling on extraction, experiments were performed using a ball mill grinding speed of 400 rpm to determine the effect of increased grinding speed. In

theory, increased energy input into algae grinding should lead to increased cell wall rupture and availability of lipids. Figure 3.3.1-2 compares extraction efficiency into methanol for microalgae pretreated by ball milling at 250 and 400 rpm grinding speeds. The data shows increased recovery with increasing ball mill grinding speed. This leads to the conclusion that the original cell rupture speed of 250 rpm is insufficient to completely rupture the algae cell walls. The potential for ball mill grinding speed to increase algae extraction efficiency makes this a factor recommended for future research. This factor was examined further by Jasmine Oleksik (Kreft) in subsequent experiments as documented in her thesis.[54]

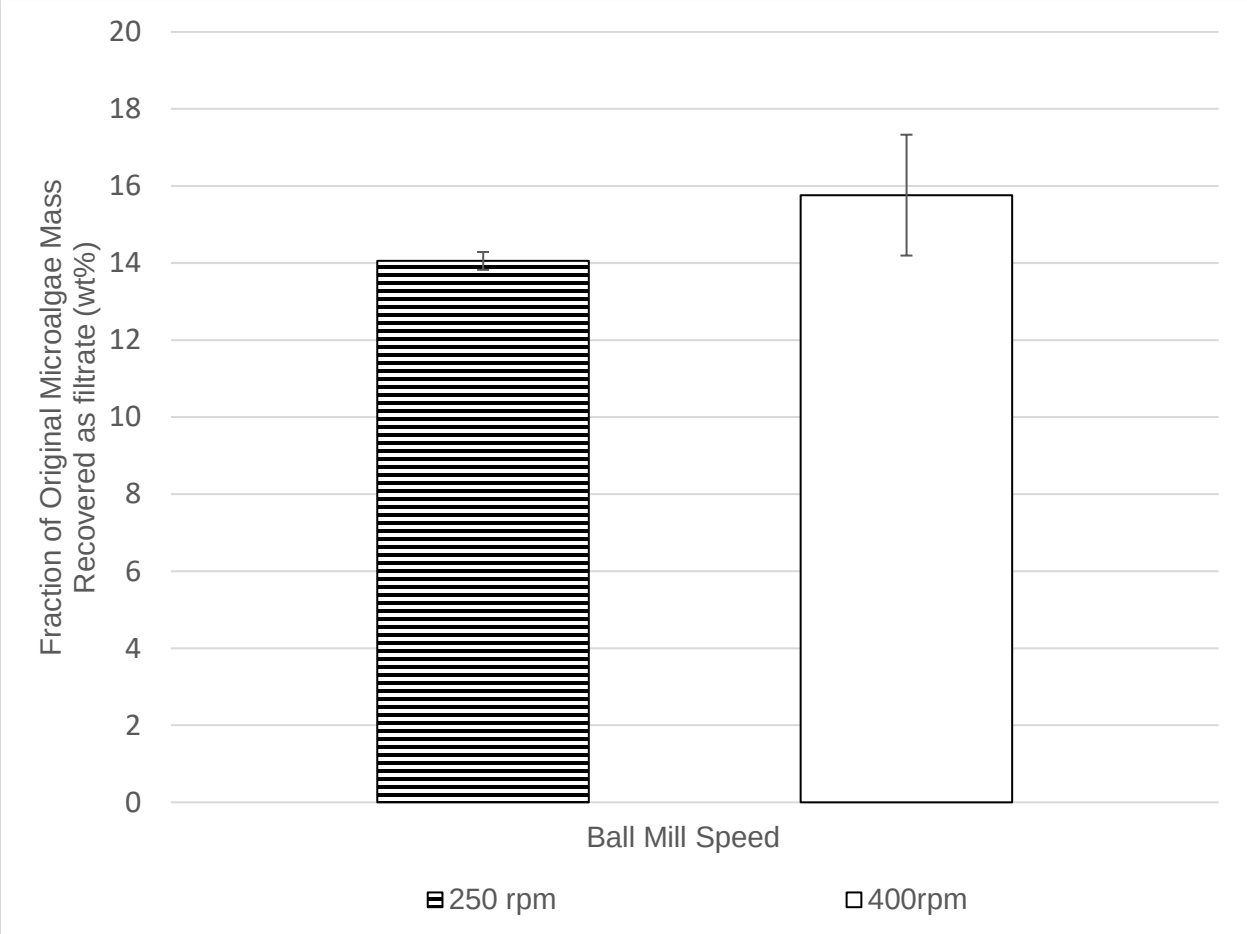

Figure3.3.1- 2 Gravimetric results from microwave assisted extraction varying ball mill grinding speed with a methanol solvent. Shown with 90% confidence intervals.

Turning to the impact of using microwaves for cell disruption, baseline tests were performed first to give an idea of upper and lower extraction limits for methanol solvent extraction. To test the expected lower limit of extraction, all normal microwave extraction procedures were followed, except the microwave was not allowed to heat the sample. This was done to ensure the sample went through the same steps as the other samples, but did not have the benefit of microwave assistance. The results from this experimentation showed an unassisted extraction lower limit of 9.2 wt%. This agrees with Bligh Dyer solvent extraction results documented in previous literature, which found extraction using only ground algae of approximately 8.5 wt%.[62] The unassisted extraction value is approximately 5.2 wt% less than the extraction efficiency determined using ground, microwave assisted extraction (figure 3.3.1-1), indicating that microwave assisted extraction improves methanol extraction efficiency by approximately 58%. This agrees with efficiencies previously reported in the literature which found an increase of 61 wt% when using microwave assistance compared to no treatment with Bligh Dyer solvents.[18]

To determine the upper unassisted extraction limit, an exhaustive 24 hour Soxhlet extraction was performed with methanol. The exhaustive Soxhlet extraction tests gave an upper unassisted extraction lipid recovery of 15.1 wt%. This is approximately 0.7% higher than the microwave assisted extraction of cracked microalgae. This indicates the microwave assisted extraction for 10 minutes at 50°C provides similar extraction to 24 hours of exhaustive methanol extraction. Using these baseline conditions, examined factors can be more readily assessed on performance improvement.

The next factor examined was microalgae to solvent ratio. In these experiments, the solvent ratio was doubled. This was done to determine how, if at all, the solvent loading would impact the extraction products. These experiments gave results of 15 wt% and 14.5 wt% for experiments

performed with 20 ml methanol and 10 ml methanol to 1 gram algae, respectively. Given the error associated with each of these data sets, it was decided that the difference between the two conditions was insignificant. This work did not examine the effect of decreasing the solvent to algae ratio further. This factor was considered more fully in subsequent work by Jasmine Oleksik (Kreft) because of the overall importance of being able to minimize solvent use when trying to scale-up extraction processes to industrial levels.[54]

The last factor examined was the temperature. A parametric series of experiments were performed at 50, 60, 80, and 100 °C. These temperatures were chosen across what was considered the safe operating range for the microwave. The results from this experimentation are shown in Figure 3.3.1-3. The mass extraction efficiencies increased at each temperature step from 50 to 100 °C with the maximum value of 19.1 wt % achieved at 100°C. Using microwave-assisted methanol extraction at temperatures of 60°C or greater provided a extraction efficiency greater than the exhaustive soxhlet extraction performed at 50°C. The most likely explanation is that the increased temperature leads to increased cell rupture from the microwave heating of the sample, since microwaves heat from the center of the sample outwards. Increased cell rupture increased lipid-methanol contact, thus increasing extraction efficiency. It should be noted that the optimum is currently unbounded and increasing temperature above 100°C can potentially lead to an increase in extraction. For this reason, the extraction temperature was further investigated in subsequent work by Jasmine Oleksik (Kreft).[54]

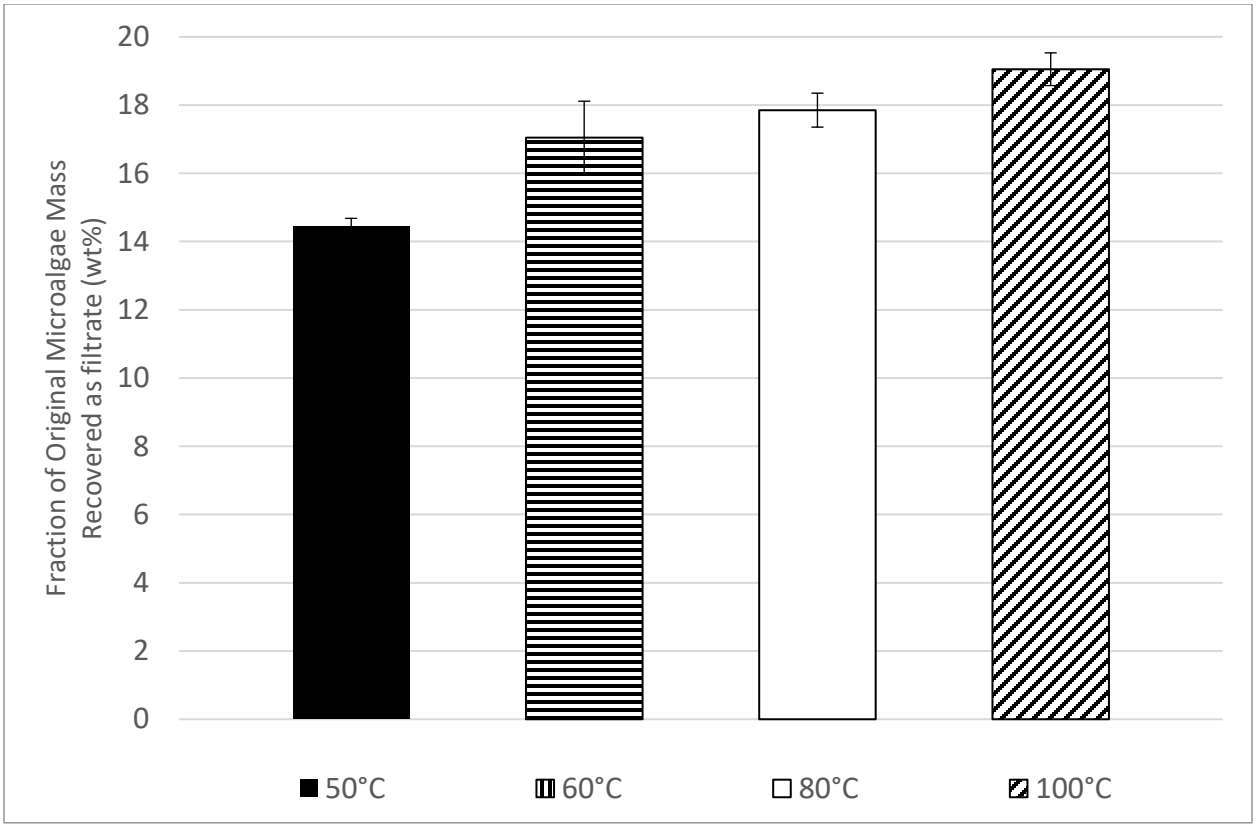

Figure3.3.1- 3 Gravimetric results from microwave assisted extraction varying temperature with a methanol solvent. Shown with 90% confidence intervals.

3.3.2 Sonication Assisted Extraction Results and Discussion

The sonication assisted solvent screening study was performed per the experimental test plan shown in table 3.2.2-1. The results are presented and discussed in this section. For these experiments both gravimetric and TCA analytical methods were employed. All of the following experiments were performed using ball milled microalgae (250 rpm for 5 minutes) at 50°C with 10 minutes of sonication assistance. All solvents were investigated using both pure and transesterification versions to determine if there is an advantage between the two.

The gravimetric results from the sonication-assisted solvent screening study are shown in table 3.3.2-1. Also found in this table are the results from the in-situ transesterification with sonication experiments. The order of extraction efficiency is consistent with the order shown in figure

3.3.1-1 for microwave-assisted extraction. It was observed, as with the microwave extraction, that the methanol and Bligh Dyer solvent had similar extraction recoveries and represented the solvent with the highest extraction yield. Sonication-assisted methanol extraction resulted in an extraction efficiency increase of approximately 40% over the unassisted extraction. This agrees with literature values which saw an increase of 35% between unassisted and sonication assisted extraction with Bligh Dyer solvents.[18]

Table 3.3.2- 1: Gravimetric results from sonication assisted extraction of microalgae, with and without in-situ transesterification, with 95% confidence intervals.

Solvent	Fraction of Original Microalgae Mass Recovered as Filtrate (wt%)	
	Sonication	Sonication with In-situ Transesterification
Methanol	12.8 ± 0.1	16 ± 3
Bligh-Dyer	12.4 ± 0.4	14 ± 1
Ethanol	8.0 ± 0.7	8.0 ± 0.3
Chloroform	5.1 ± 0.1	6.8 ± 1.0
Acetonitrile	3.04 ± 0.04	2.6 ± 0.2
Hexane	1.26 ± 0.01	2.3 ±0.7

The differences in extraction efficiency using microwave- versus sonication-assisted extraction at the same conditions (grinding, temperature, microalgae to solvent loading) are shown in figure 3.3.2-2. For all of the solvents tested except acetonitrile, the extraction efficiency was higher when assisted by microwave rather than by sonication. The acetonitrile results are questionable due to the large uncertainty associated with the microwave assisted acetonitrile results. The largest difference is with the Bligh Dyer solvent at 1.9 wt%. This implies the additional cell rupture and solvent contact from the use of microwave-assisted extraction is more substantial than the cell rupture provided by sonication-assisted extraction.

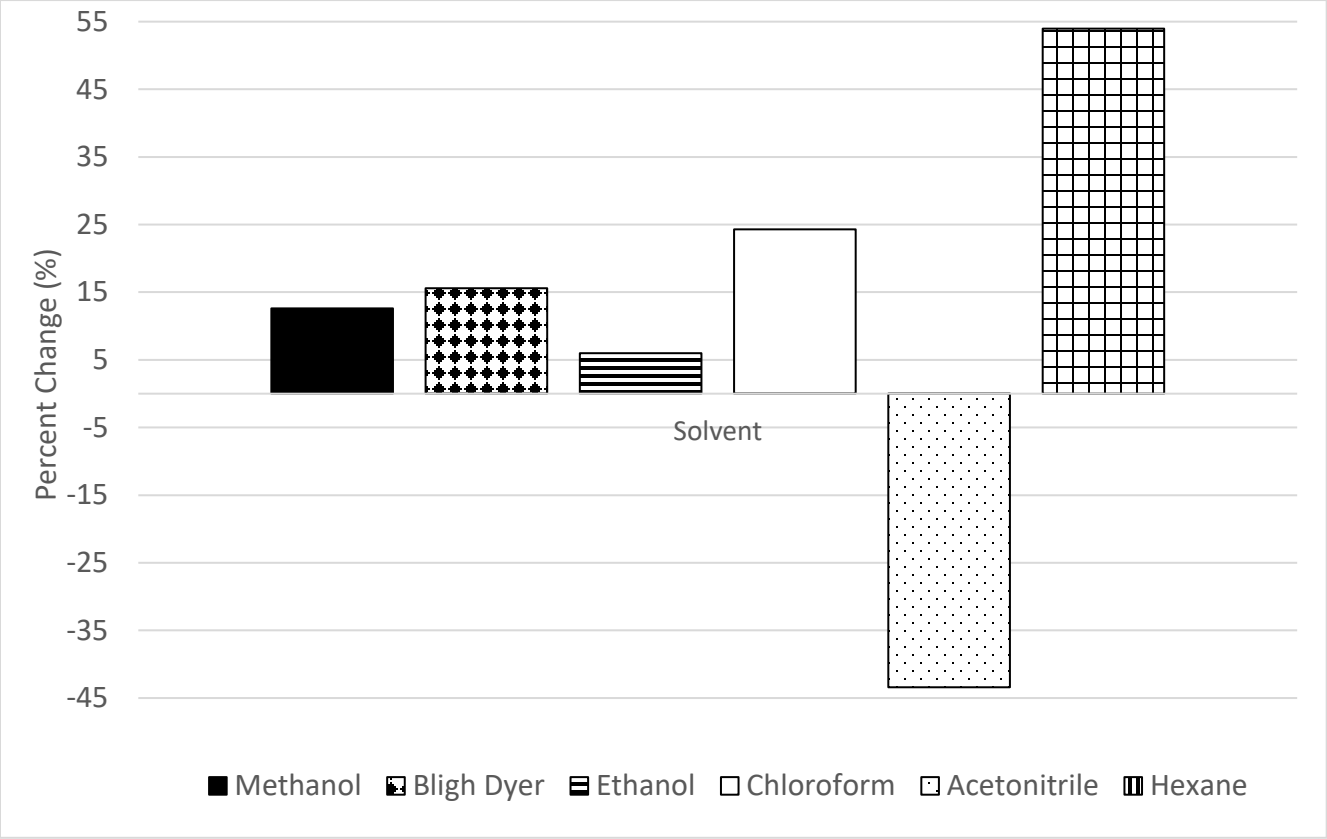

Figure 3.3.2- 1 Lipids Recovery Increase from Microwave Assisted Solvent Extraction Compared to Sonication Assisted Solvent Extraction (% of Inlet Biomass Basis).

The gravimetric results from the experiments using in-situ transesterification followed by sonication-assisted extraction are shown in table 3.3.2-1. The extraction efficiency increased from the methanol-based solvents, methanol and Bligh Dyer, but surprisingly not for ethanol. When comparing these results to literature values, very few instances can be found which do not use methanol as the transesterification solvent. Literature data for in-situ transesterification followed by sonication assisted methanol extraction resulted in an overall extraction of 12.8 wt% lipids, with little change between ultrasonication without insitu-transesterification.[72] This agrees with our results. Additional literature results utilizing temperatures in excess of 100 °C saw 14 – 18 wt% overall lipids extraction from the use of in-situ transesterification with ultrasonic assisted extraction.[12, 69]

TCA analysis results for the initial sonication solvent study can be seen in figure 3.3.2-2. The highest lipid extraction efficiency was obtained using methanol, at approximately 30 wt% of initial lipids in the microalgae feedstock. This agrees with the gravimetric data seen in table 3.3.2-1, where methanol was found to provide the highest recovery. The extraction recoveries using Bligh Dyer, ethanol, chloroform, acetonitrile, and hexanes follow the same relative extraction performance order as seen from the gravimetric results in table 3.3.2-1. This agrees with literature data, which saw approximately 31 wt% lipid recovery from microalgae using ultrasonic extraction with chlorella *vulgaris* in Bligh-Dyer solvents.[68]

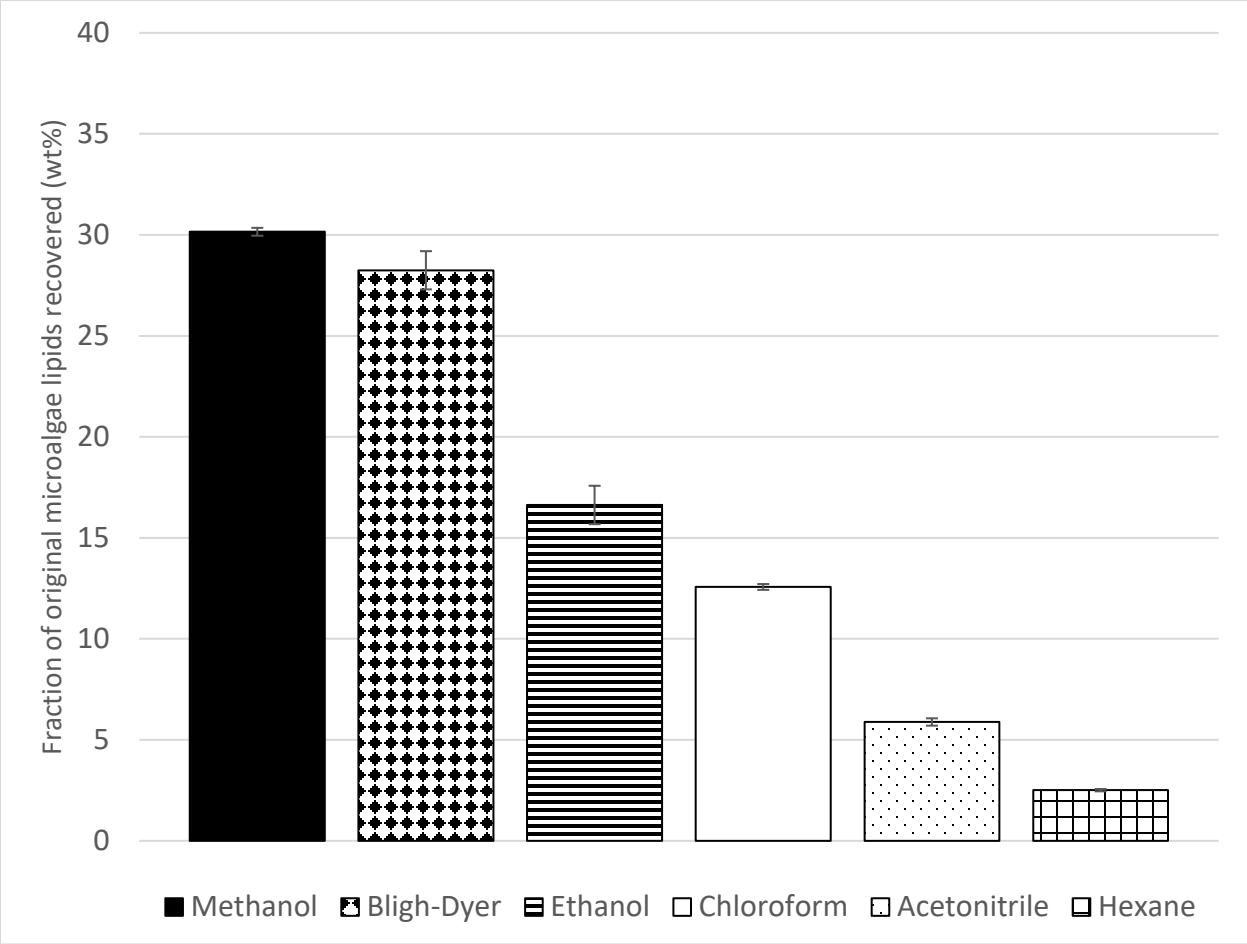

Figure 3.3.2-2 TCA results from sonication assisted solvent screening study for the 300C and 400C temperature fractions with 95% confidence intervals.

TCA analysis results for the experiments using in-situ transesterification followed by sonication-assisted extraction are shown in figure 3.3.2-3. The highest oil recovery efficiency was from methanol, at approximately 35% of the inlet lipids. This agrees with the gravimetric data seen in table 3.3.2-1, where methanol was found to provide the highest mass extraction. Table 3.3.2-1 shows methanol benefited the most from in-situ transesterification with an increase of approximately 6.7 wt% compared to direct extraction, more than double the change any other solvent experienced.

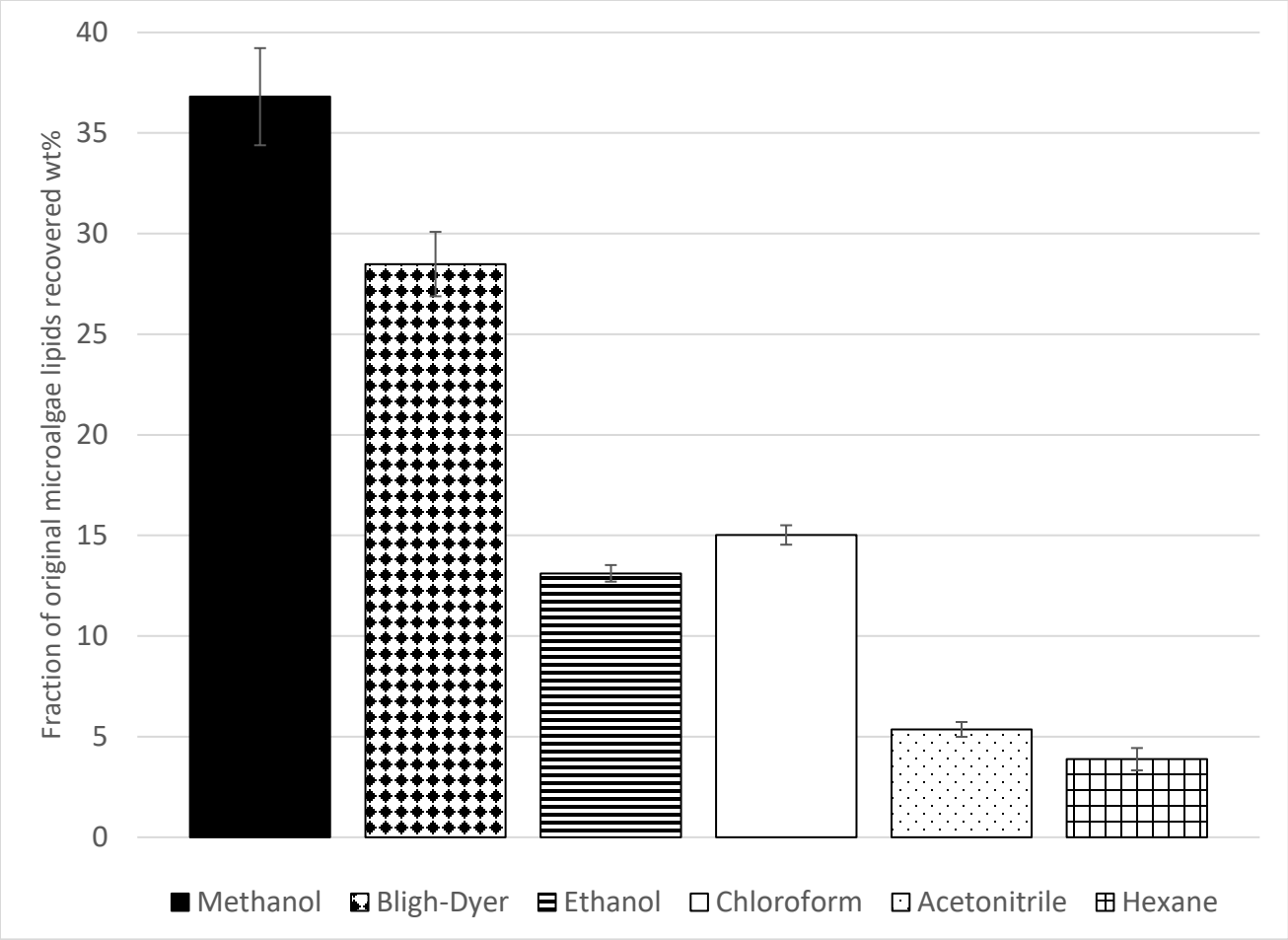

Figure 3.3.2-3 TCA results from sonication assisted in-situ transesterification solvent screening study for the 300C and 400C temperature fractions with 95% confidence intervals.

3.4 Conclusions and Recommendations

1. This study determined methanol was the best performing solvent for lipid extraction from Chlorella Vulgaris microalgae. Methanol consistently outperformed the other solvents examined, namely: Bligh Dyer, ethanol, chloroform, acetonitrile, and hexane. Methanol was the top solvent for use with both microwave and sonication assisted extraction, as well as, for in-situ transesterification assisted extraction.

2. In the comparison between microwave and sonication assisted extraction, it was found that both methods improved extraction, but the microwave provided a higher extraction recovery efficiency. This is believed to be due to a higher fraction of additional cell wall rupture provided by the microwave heating, which heats internally, compared to sonication, which heats externally.

3. The use of in-situ transesterification was found to increase the extraction of lipids for methanol as a solvent. This is believed to be attributed to increased cell rupture from the transesterification of lipids in the cell wall membranes and the polarity of methanol which is effective at breaking the cell wall-membrane layer.[68]

4. Additional factors found to have a potential impact on extraction efficiency that warrant further investigation include: pretreatment ball mill grinding speed, extraction temperature, and algae-to-solvent ratio. These factors were further investigated in subsequent work by Jasmine Oleksik (Kreft) and documented in her thesis.[54]

5. The use of TCA and gravimetric analysis provides a reasonable quantitative analysis of the lipids extracted from microalgae. However, this should be verified using more rigorous analytical methods, like GC/MS, to provide a quantitative lipid analysis. Using GC/MS would help to highlight additional differences seen between the solvents being investigated and whether they impact the quality of lipids being leached. Additional analytical techniques to consider are high temp GC/MS and APCI-MSTOF.

Chapter IV. Decomposition of Forage Sorghum Sourced Carbohydrates and Lignin

4.1 Introduction

Concerns for increasing global carbon emissions have drastically increased the desire to replace traditional fossil fuels-based energy. Substantial research has been focused on the production of bio-based fuels and, increasingly, the replacement of chemicals and specialty products traditionally sourced from nonrenewable sources. One of the most extensively researched renewable feedstocks in this subject area is lignocellulosic biomass.[20] With over 150 billion tons of lignocellulosic biomass available globally per year, this feedstock is considered the most feasible long-term source of renewable carbons and energy.[21, 22] Lignocellulosic biomass is primarily sourced from agricultural wastes like corn stover and wheat straw, but is also available from industrial wastes like black liquor from the pulp and paper industry.[23, 24] The main components of lignocellulosic biomass are cellulose, hemicellulose, and lignin.

Each of these lignocellulosic biomass building blocks have the potential to be upgraded into value added products. Cellulose is composed of highly crystalline linear polymerized D-glucose monomers. Hemicellulose is a highly branched, amorphous polymer consisting of primarily xylose and small amounts of other pentose and hexose monomers, like xylobiose and arabinose.[25] Lignin is a stable, complex polymer consisting of many different phenyl and hydroxyl functional groups, like p-coumaryl, coniferyl, and sinapyl alcohol.[26] The diversity of compounds found within lignocellulosic biomass provides the potential for transformation into a large variety of upgraded products. The two studies documented herein further the development of technologies to maximize the fraction of forage sorghum ligno-cellulosic biomass that is converted into useful renewable fuel, chemicals, and materials.

Forage sorghum is a warm-season grass crop grown in cold climates where grain sorghum will not thrive. It is used primarily as a silage feed or hay. It has been identified as a potential energy

feedstock, desirable for the ability to be grown under cold arid conditions where other crops, like corn, would not thrive.[23] Forage sorghum is composed of approximately 34 wt% cellulose, 22 wt% hemicellulose, 15 wt% lignin, 25 wt% extractives, and 4 wt% ash.[28] This provides approximately 71 wt% of the biomass in the form of compounds that are the focus of this research. This research was performed in two steps. The first is the recovery and utilization of cellulose and hemicellulose. This is found in section 4.2 of this document. The second part of this research is the recovery and decomposition of lignin. This is seen in section 4.3 of this document.

4.2 Production of Organic Acids from Sorghum Carbohydrates

Abstract

Lignocellulosic biomass is one of the most extensively researched and promising renewable feedstocks for bio-based fuels and the replacement of chemicals and specialty products traditionally sourced from nonrenewable sources. With over 150 billion tons of lignocellulosic biomass available globally per year, this biomass is considered the most feasible long-term source of renewable carbons and energy. Lignocellulosic biomass is primarily sourced from agricultural wastes like corn stover and wheat straw, but is also available from industrial wastes like paper sludge. The main components of lignocellulosic biomass are cellulose, hemicellulose, and lignin.

The cellulose and hemicellulose in forage sorghum biomass is composed of polymeric hexoses and pentoses of glucose and xylose. The recovery and utilization of these carbohydrates from biomass is a well-documented process, with most of the recent literature focus being placed on

optimization of conditions for carbohydrate extraction and the application of the developed recovery techniques to unique biomass sources. Carbohydrates extracted from lignocellulosic biomass are primarily used in biological applications, like fermentation to ethanol or lactic acid. The economics of these biological processes are challenging, especially when compared to starch and sucrose biorefineries. One major barrier associated with these biomass processes is the formation of compounds which inhibit biological activity. This makes non-biological applications attractive for utilization of lignocellulosic sourced carbohydrates.

The study presented herein examined the decomposition of carbohydrates over Sn-Beta catalysts to form building block acids, with the goal to maximize conversion to lactic acid. Catalyst doping, the decomposition of model carbohydrates and the decomposition of carbohydrates recovered from forage sorghum were examined in this work.

It was found that the use of either Sn 2+ or Sn 4+ salts as dopants for beta zeolite catalyst can be effectively used in the conversion of carbohydrate sugars to form organic acids. There is no statistical significance between the performance of the two tin dopants when using the same Si-Al zeolite scaffold. Both dopants replace Al atoms in the Si-Al zeolite matrix which increases the ratio of Lewis to Brønsted acid sites in the catalyst. Brønsted acid sites facilitate the reaction pathway to the formation of levulinic acid while Lewis acid sites facilitate the reaction pathway to lactic acid.

The silica-to-alumina ratio of the catalyst scaffold is a significant factor in how the catalytic decomposition reactions perform. Decreasing the silica-to-alumina ratio increases the fraction of alumina in the catalyst. This increases the number of Brønsted acid sites that are not replaced by Lewis (Sn) sites in the final catalyst mixture and thus promotes levulinic acid formation pathways at the expense of lactic acid pathways.

In examining the decomposition of model carbohydrate compounds, the catalytic decomposition of xylose leads to increased lactic acid with minimal levulinic acid, when compared to the comparable decomposition of glucose. This is attributed to differences between the most likely reaction pathways for xylose and glucose. While the keto-form of glucose is available for lactic acid formation, both the keto- and aldo- forms of xylose are available for lactic acid formation. Additionally, xylose does not participate in the HMF-to-levulinic acid pathway.

Overall recovery of glucans and xylans from forage sorghum biomass in the form of sugars (i.e. glucose and xylose) were found to be 80 to 90% of the initial glucan and xylans in the biomass. When using these recovered sugar mixtures in Sn-Beta catalytic decompositions, it was found that the yield of lactic acid was lower than the yield obtained from model compounds. This may be due to catalyst deactivation by contaminants in the sugars mixture. It was determined that the catalyst to carbohydrate loading has significant impacts on lactic acid formation. The maximum lactic acid formation found in this work was using forage sorghum sourced carbohydrates with a sugar concentration of 8 g/L providing 65% of the carbon fed as carbohydrates being recovered as lactic acid.

4.2.1 Introduction

This research expands upon previous work performed at the University of North Dakota by Clancy Kadrmas.[73] In this previous work, glucose was catalytically converted into building block acids over a tin-doped beta zeolite (Sn-beta), with a focus on lactic acid formation. Starting from this previous work, the current research had the following objectives:

1. Recreate previous work to verify catalyst functionality and dopant impact on reaction products.
2. Perform preliminary catalytic decomposition reactions using pure xylose feedstocks, to provide insight on potential hemicellulose sourced carbohydrate decomposition reactions.
3. Apply optimum reaction conditions to model monomeric carbohydrate mixtures which simulate projected compositions of forage sorghum-sourced carbohydrates.
4. Perform catalytic decomposition reactions with actual sugar mixtures derived from forage sorghum biomass.

The majority of forage sorghum biomass is composed of polymeric hexoses and pentoses of glucose and xylose. The recovery and utilization of these carbohydrates from biomass is a well-documented process, with most of the recent literature focus being placed on optimization of conditions for carbohydrate extraction and the application of the developed recovery techniques to unique biomass sources. [27, 28]. One of the most successful methods is the NREL method.[74, 75] This method consists of two steps. First, acid hydrolysis of the biomass is performed with sulfuric acid at elevated temperatures (100 - 250°C) to liberate the hemicellulose as xylose monomers and to make the cellulose more readily available for the next processing step.[27] In the second step, the residual biomass undergoes enzymatic saccharification with a cellulase enzyme, to recover the cellulose as glucose monomers.[76]

Forage sorghum is composed of approximately 34 wt% cellulose, 22 wt% hemicellulose, 15 wt% lignin, 25 wt% extractives, and 4 wt% ash.[28] This provides approximately 56 wt% of the biomass in the form of carbohydrates that are the focus of this research. In literature, acid hydrolysis for the recovery of xylose from forage sorghum was optimized with 1 wt% sulfuric acid at a solids

loading of 10 wt% processed at 150°C for 20 minutes. This resulted in a xylose recovery of 95 wt% from the forage sorghum biomass. [28] The enzymatic saccharification step was optimized using 10 wt% cellulose with 1 wt% enzyme loading at 48°C for 72 hours. This resulted in 90 wt% cellulose recovery.[28]

Carbohydrates extracted from lignocellulosic biomass are primarily used as feedstock for biological transformations, such as fermentation to ethanol or lactic acid.[29] The economics of these biological processes are challenging, especially when compared to starch and sucrose biorefineries.[23] One major barrier associated with these biomass processes is the formation of compounds which inhibit biological activity.[25, 28] This makes non-biological applications attractive for utilization of lignocellulosic sourced carbohydrates.

Although the lignocellulosic feedstock is considered to be low cost, the additional processing steps required to recover the carbohydrates at least partially offsets this advantage. Another major barrier associated with these biomass processes is the formation of inhibitors. In performing the acid hydrolysis step, some sugars decompose into components, like acetic acid and hydroxymethylfurfural, which inhibit biological activity.[25, 28] This suggests that non-biological transformations may be more attractive to convert lignocellulosic-sourced carbohydrates. Lactic acid stands out as a chemical which holds the potential to be produced renewably through non-biological means.

Lactic acid has a wide range of applications within pharmaceuticals, cosmetics, foods, and polymers.[77, 78] The most common use for lactic acid is in the production of the biodegradable plastic polylactic acid. The current market for lactic acid is expected to grow by 18.7% annually, providing motivation for the development of more efficient and cost effective production methods.[79] Currently, more than 90% of all lactic acid is produced through fermentation.[80] There

are several issues associated with fermentation for lactic acid production, including: low production rates (<10%), long processing times (up to 6 days), and difficulty in separation of lactic acid from fermentation broth.[73] The most challenging of these is the separation of lactic acid after fermentation, accounting for approximately 50% of lactic acid production costs.[80] This is attributed to the low concentration of lactic acid and presence of impurities added as growth media for the bacteria within the fermentation broth.

Chemical synthesis of lactic acid from carbohydrate feedstocks is most commonly performed with the use of metal doped catalysts. A screening study of commercially available catalysts was performed previously at the University of North Dakota.[73] That study examined tin, zinc, boron, silver, zirconium, titanium, palladium, and nickel dopants on beta zeolites to decompose glucose. It was found that tin doped-beta zeolite provided the highest conversion to lactic acid, which agreed with literature results.[20, 81] The reaction was optimized at a temperature of 160 °C and 20 hour residence time, resulting in 43% conversion of glucose to lactic acid derivatives. The previous catalyst screening study was primarily performed in a methanol solvent with more limited results using water as the solvent. Reaction in methanol leads to the formation of the lactic acid derivative methyl lactate.

The use of an aqueous solvent is preferred to directly form lactic acid. Kadrmas optimized conditions for aqueous facilitated reactions and found that glucose conversion to lactic acid in an aqueous solvent was near optimum at 200 °C and 20 hour residence time, resulting in 27% lactic acid formation.[73] These conditions were later updated by Andrew Kohler at the University of North Dakota to 200 °C and 5 hour residence time, after it was determined extended reaction times were not required.[82]

When comparing reactions in methanol and aqueous solvents, it should be noted that the optimum operating temperatures are higher for aqueous solutions. This is caused due to lower energy requirements in the reaction pathway to methyl lactate.[81] However the costs associated with extracting the sugars out of their original water-based mixture from the hydrolysis step into methanol outweigh the costs of the higher reaction temperature required to leave the sugar solution in water. Therefore in the present work, only aqueous-based reactions were considered.

The chemical conversion of glucose to lactic acid using Sn-beta catalysts relies on the ratio of Lewis and Bronsted acid sites within the catalyst. The formation of lactic acid is facilitated by Lewis acid sites within the catalyst, provided by the metal dopant. Side reactions which form hydroxymethylfurfural (HMF), levulinic acid, and formic acid are facilitated by Bronsted acid sites within the catalyst.[83] The most likely reaction pathway for catalytic decomposition of glucose with Sn-beta catalyst can be seen in Figure 4.2.1-1.[20, 82] This pathway requires the hexoses be in their keto-form, which is facilitated by Sn-beta catalysts at temperatures as low as 100°C.[82] These ketohexoses can then either undergo retro-aldo condensation to form two trioses, at temperatures greater than 150 °C, or undergo triple dehydration to form HMF.[84] The trioses can then hydrate and isomerize to lactic acid, while the HMF can go through double rehydration to levulinic acid and formic acid. The side reaction involving HMF can have large impacts on overall lactic acid conversion, if there are high concentrations of Bronsted acid sites within the catalyst causing the levulinic acid pathway to dominate the reaction.

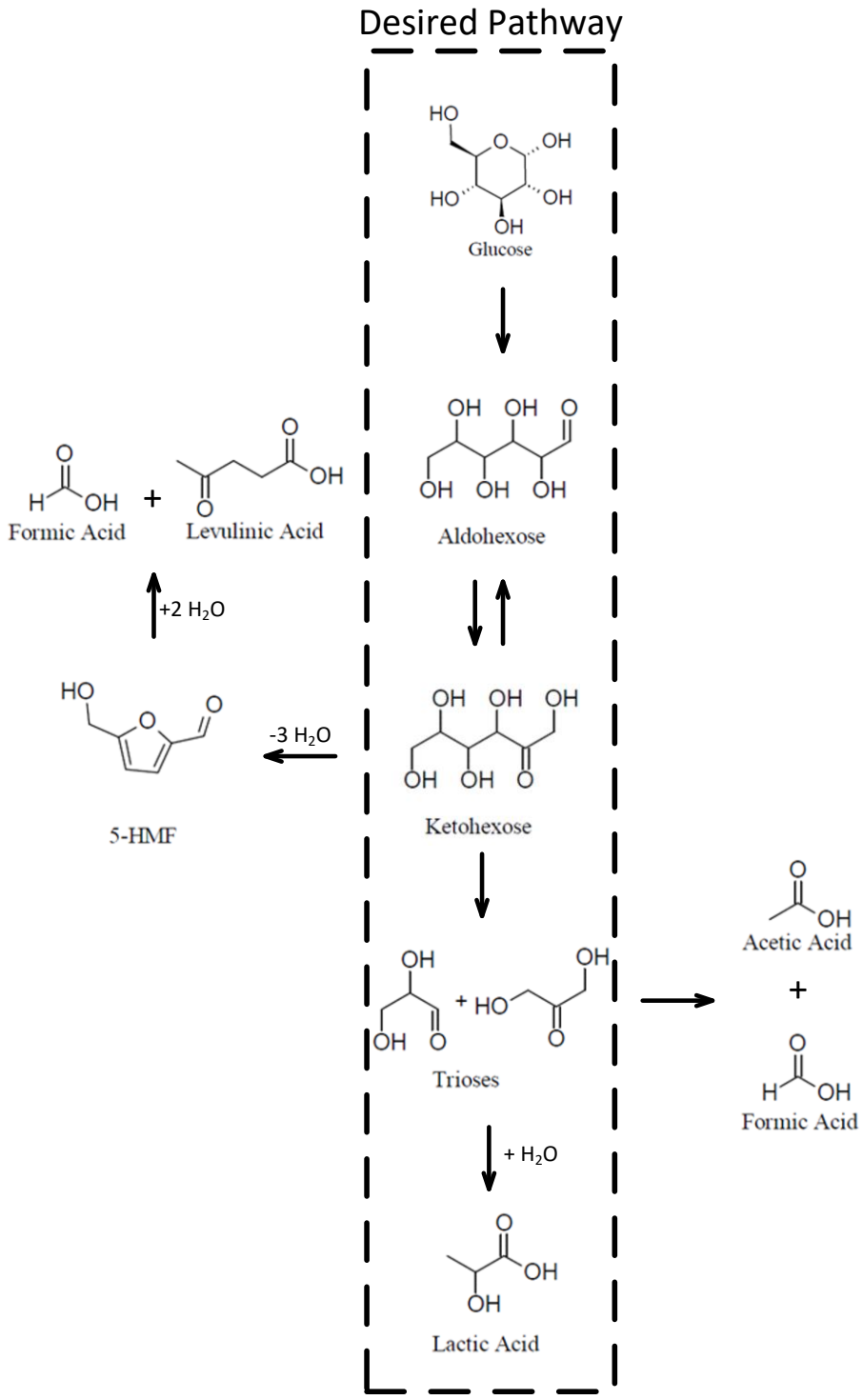

Figure 4.2.1- 1: Proposed reaction pathway for hexose decomposition over Sn-Beta catalysts[82]

One of the main side products that can occur during this reaction pathway is levulinic acid. This acid product is of interest as a platform chemical, i.e., one that must be transformed into other chemicals, for use in biofuels and biofuel additives.[27] Additionally, levulinic acid shows potential for use as a platform chemical for pharmaceuticals, pesticides, and plastics.[21] Generally, levulinic acid can be formed directly from hexoses through acid catalyzed dehydration reactions in aqueous solutions, at temperatures above 140°C. [83, 85]

Reactions of xylose using Sn-Beta to form lactic acid have not been as extensively studied as glucose in the literature. Studies of the conversion of pentose sugars showed a decrease in conversion to lactic acid from 50% to 40%, when compared to lactic acid conversion of hexose sugars.[86] The proposed reaction pathway for xylose to lactic acid can be seen in figure 4.2.1-2.[82] The pentose sugars are capable of undergoing retro-aldo condensations from either their keto- or aldopentose forms. However, it is noted that each pentose will form one triose and one C2 fragment, unlike hexoses which form two trioses after retro-aldo condensations. Considering the trioses are isomerized to lactic acid, this leads to lower maximum theoretical lactic acid production from pentoses. A side reaction forming furfural is also present and catalyzed by Bronsted acid sites within the Sn-Beta.

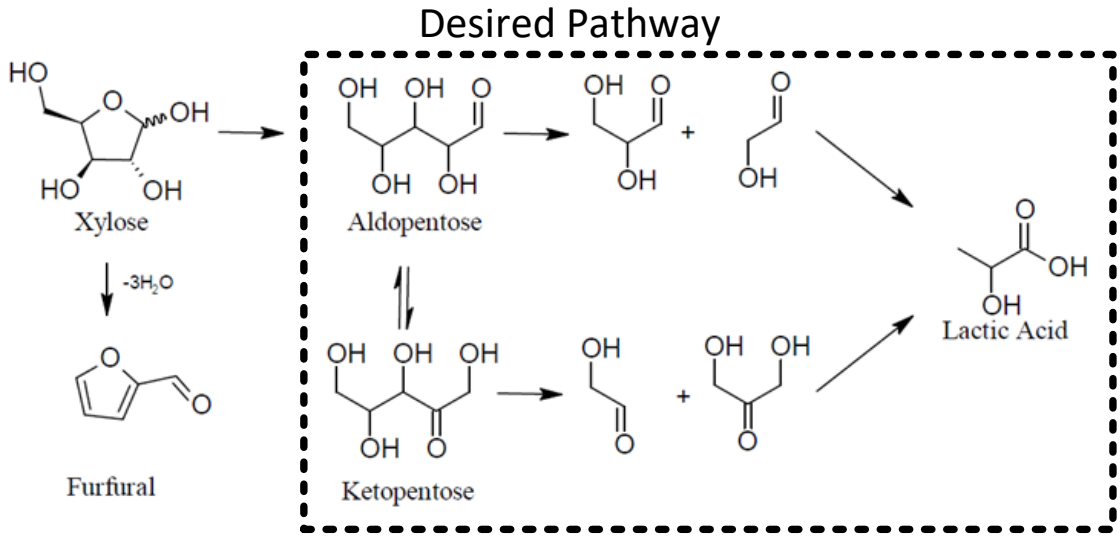

Figure 4.2.1- 2: Proposed reaction pathway for pentoses over Sn-Beta catalysts.[82]

4.2.2 Methods and Materials

This research has several distinct tasks: catalyst preparation, model carbohydrate decomposition reactions, forage sorghum sourced carbohydrate recovery, and forage sorghum sourced carbohydrate catalytic decomposition reactions. Figure 4.2.2-1 shows a flowchart of the steps required to perform Sn-Beta Decomposition reactions on biomass sourced carbohydrates.

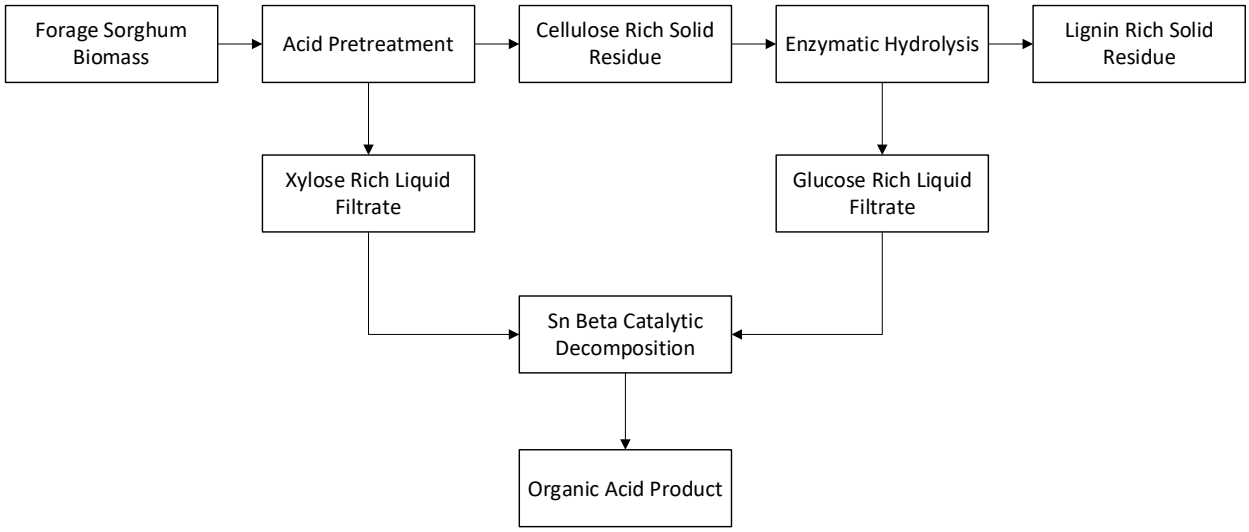

Figure 4.2.2- 1: Steps required to perform Sn-Beta decomposition reactions on biomass sourced carbohydrates

4.2.2.1 Chemicals and Catalysts

The chemicals and catalysts required for catalyst preparation are purchased from several different suppliers. The base beta zeolite scaffold was purchased from Zeolyst International (Kansas City, KS, USA) as either a SiO2/Al2O3 ratio of 300 (CP811C-300) or a SiO2/Al2O3 ratio of 25 (CP814E*). The hydrochloric acid (technical grade, A142212) used for dealumination was purchased from Fisher Scientific (Waltham, MA, USA). The tin (II) chloride (98%, 208256-100G) and tin (IV) chloride (99%, 208930-250G) catalyst dopants were purchased from Sigma Aldrich (St. Louis, MO, USA).

The model carbohydrates used for catalytic decomposition and High Performance Liquid Chromatography (HPLC) standards were purchased from Sigma Aldrich (St. Louis, MO, USA). These carbohydrates are glucose (99.5%) and xylose (99%). Additional chemicals used for HPLC analysis and standards include levulinic acid, lactic acid, formic acid, acetic acid, glycolic acid, and sulfuric acid purchased from Sigma Aldrich (St. Louis, MO, USA) .

Sulfuric acid (technical grade, A298-212), sodium citrate, and calcium carbonate were purchased from Fisher Scientific (Waltham, MA, USA). Initial Accellerase 1500 were obtained from Genencor (Rochester, NY, USA), with additional Cellulase 2XL enzymes being obtained from Bio-Cat (Troy, VA, USA). These chemicals were used for the acid and enzymatic hydrolysis of the forage sorghum biomass.

Additional materials used include compressed nitrogen gas supplied via cylinders purchased from Praxair (Grand Forks, ND, USA) and ultrapure water from an Ultra milli-Q filter system (MilliporeSigma, Burlington, MA, USA).

4.2.2.2 Catalyst Preparation

This catalyst doping method is based on a method described by Kadrmas .[73] Catalyst was prepared using a simple impregnation method. The beta zeolite scaffold was first calcined at 600°C for 8 hours. This is done to remove any water and to activate the zeolite.[87] Ten grams of the calcined catalyst was then mixed with 1 gram of tin dopant and 100 ml of 1 M HCl and placed in an ultrasonic bath for 12 hours. This was done to dealuminate the zeolite catalyst and dope the tin onto the catalyst in a single step process.[87, 88] The catalyst was then separated from the doping liquid and allowed to dry. Finally, the doped catalyst was calcined again at 400°C for 8 hours. More detailed doping instructions can be found in Appendix 3.1.1 Catalyst Doping. A discussion of the advantages and disadvantages of this method can be found in Kohler et al 2020.[82]

4.2.2.3 Sugar Recovery from biomass

Carbohydrates were recovered from forage sorghum biomass following the scheme shown in figure 4.2.2-1. The acid pretreatment was performed to decompose the biomass hemi-cellulose into individual xylan monomers and to ensure that the biomass cellulose was more readily available for the enzymatic hydrolysis step. This acid pretreatment step primarily recovers xylose and some glucose. The acid pretreatment was performed in a 5 liter Parr Series 4580 High Temperature/High Pressure Reactor (Serial number #4580-0908-12536) purchased from Parr Instrument company (Moline, IL, USA). A generalized schematic of the reactor system can be seen in figure 4.2.2.3-1.

The acid pretreatment step was based on previous work at the University of North Dakota performed by Kamireddy.[28] This pretreatment was performed by mixing forage sorghum biomass with 1 wt% sulfuric acid at a solids loading of 10 wt% (10g liquids per 1g solid biomass). The acid/biomass mixture was then placed in the Parr reactor and heated to 150°C under an inert nitrogen atmosphere. The mixture was held at temperature for 20 minutes. Once the processing time had finished, the heating was turned off and the internal cooling coil was used to quickly cool the reactor. The reaction products were then filtered. The solid residues were dried and saved for further treatment with enzymatic hydrolysis. The liquid xylose-rich filtrate was neutralized with calcium carbonate and stored for future use in the catalytic decomposition step. More detailed instructions on this acid hydrolysis procedure can be found in Appendix 3.1.2 Acid Hydrolysis.

The enzymatic pretreatment was performed to break the cellulose portion of the biomass into its monomeric glucose units. This was performed using a cellulase enzyme. The enzymatic hydrolysis was based on previous work at the University of North Dakota performed by

Kamireddy.[28] This process started by making a slurry with a solids loading of 10 wt% using washed and dried cellulose-rich acid pretreatment solids and ultrapure water. The pH of the slurry was buffered to 5 by adding sodium citrate. The cellulase enzymes were added with a loading of 1 gram of enzyme per 100 grams of dry cellulose. The samples were incubated in a MAXQ 4000 shaker table (Fisher Scientific, Waltham, MA, USA) for 72 hours at a temperature of 48°C and an agitation of 250 RPM. After the incubation period, the glucose rich hydrolysate was filtered and store for future use in the catalytic decomposition step. The lignin-rich biomass solid residue was dried and saved for use in the lignin decomposition experiments discussed in section 4.3. A more detailed description of the enzymatic hydrolysis procedure can be found in Appendix 3.1.3 Enzymatic Hydrolysis.

Biomass solids were analyzed for cellulose, hemicellulose, and lignin based on the NREL lab analytical procedures NREL/TP-510-42618 and NREL/TP-510-42623.[74, 75]

4.2.2.4 Catalyst Decomposition Reactor Set-Up and Operation

The catalytic decomposition reactions were performed in a 500 ml bench top Parr Series 4575 High Temperature/High Pressure Reactor (Serial number #4570-0803-6955) purchased from Parr Instrument company (Moline, IL, USA). A generalized schematic of the reactor system can be seen in figure 4.2.2.3-1. This apparatus was used for all Sn-Beta catalytic decomposition reaction experiments.

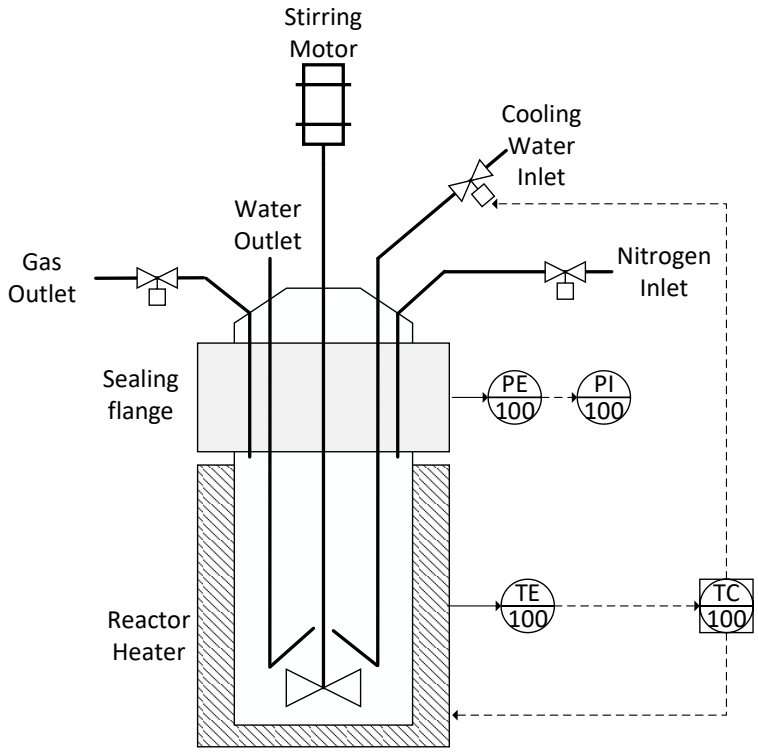

Figure 4.2.2.3- 1: Batch Reactor Schematic

A detailed description of the catalyst decomposition reactor procedure can be found in Appendix 3.1.4 Catalytic Decomposition Reactor Operation. In general, the reactor feedstock consisted of 5 grams of carbohydrate sugars dissolved in 300 milliliters of water with 10 grams of Sn-Beta powdered catalyst. This feedstock was placed into the reactor vessel, which was then sealed to the reactor head using the 8-bolt sealing flange. The reactor vessel was purged with nitrogen 5 times to remove oxygen and avoid unwanted side oxidation reactions. The normal operating conditions for the decomposition reactions were:

1) an initial charge of 2.06 MPa nitrogen,

2) 200 °C reaction temperature with 5°C per minute heating rate and 30 minute cool down, and

3) 400 rpm stirring rate. Depending on the experimental parameters, these reactions were allowed to run for 20 hours. After the reaction time was complete, the reactor contents were filtered and saved for analysis.

4.2.2.5 Analytical Methods

For this research two forms of analysis were employed: HPLC and TCA. The HPLC allowed for direct analysis of organic acids and carbohydrates in aqueous samples without the need for drying or derivatization. TCA was used to evaluate the total carbon pyrolyzed from a sample as it is exposed to a series of increasingly aggressive temperature steps.[71] The temperature fraction at which carbon is evolved gives an indication of the complexity/stability of the original sample and its constituents.

HPLC analysis was performed on an Agilent 1200 series system (Agilent Technologies Inc, Santa Clara, CA, USA). The Agilent 1200 series consisted of five modular pieces: vacuum degasser (G1322A), Isocratic pump (G1310A), temperature controlled autosampler/injector (G1329A, G1330B), column oven (G1316A) , and Refractive Index detector (G1326A). Separation was performed on an Agilent Hi-Plex H column (Agilent Technologies Inc, Santa Clara, CA, USA) with a mobile phase of 5 mM H2SO4, flowrate of 0.6 ml/min, temperature of 40 °C and stop time of 45 minutes. A more detailed description of HPLC analysis can be found in Appendix 3.1.5 HPLC Analysis.

The TCA analysis was performed using a thermal optical analyzer from Sunset Laboratory Inc. (Portland, OR, USA). Aqueous samples were placed on a 2500QAT-UP tissue quartz filter pad (Pall Corp. East Hills, NY) and dried for 7 minutes at 55 °C. The filter pad was placed in the

TCA oven and analysis was run. Results were calculated as a carbon percentage of total carbon evolved from the sample. A more detailed description of the TCA analysis can be found in Appendix 3.1.6 TCA Analysis.

4.2.3 Results and Discussion

This research had several different goals. The first was to replicate and extend the catalytic decomposition work previously performed by Kadrmas.[73] In doing this, it was desired to examine the behavior of tin 2+ and tin 4+ dopants with glucose as previous attempts by other student researchers had failed to recreate the initial results. It was also desired to update the derivatized GC/MS analytical methods used by Kadrmas to allow quantification of formic acid which could not be analyzed by the method used by Kadrmas, and to provide results in terms of fraction of inlet carbon present in the reactor outlet stream as the target compound. Another goal was to use Kadrmas' optimum conditions for glucose decomposition to decompose model xylose and xylose/glucose blends to determine the conversion efficiency for xylose and xylose/glucose mixtures under these conditions. Yet another goal was to perform catalytic decomposition reactions with actual sugar solutions derived from forage sorghum biomass following the 2-step hydrolysis/extraction procedure described in section 4.2.2.

4.2.3.1 Pure and model carbohydrate Sn-Beta decomposition reactions

The first goal of this research was to replicate and extend catalytic decomposition work on pure carbohydrate feedstocks previously performed by Kadrmas.[73] Table 4.2.3.1-1 shows the catalytic decomposition results from Kadrmas' triplicated optimized conditions using glucose and pure

water. This data has been modified from its original reported format of mol fraction in the outlet solution to mass fraction of inlet carbon converted into the target compound. It was observed that a significant difference between the ratio of lactic and levulinic acid was produced by Sn 2+ and Sn 4+. At the time, this was attributed to the metal dopant being used and which reaction pathway was favored. Further, data for more volatile organic acids were not available due to the use of GC-MS as the analytical method. This method required that the sample be dried to completion before performing derivatization. In doing this, the more volatile compounds, most notably formic acid and acetic acid are expected to evaporate.

Table 4.2.3.1- 1: Optimized conditions from Kadrmas for glucose in pure water, modified from mol fraction in the outlet solution to mass fraction of inlet carbon percent converted into the target compound [73]

Sugar		**Glucose**	
Catalyst Dopant		Tin II	Tin IV
Analyte (C%)	Formic Acid	Unavailable	Unavailable
	Lactic Acid	4.4% ± 0.2%	27% ± 2%
	Levulinic Acid	68% ± 4%	48% ± 2%
	Acetic Acid	Unavailable	Unavailable
Total		72.5% ± 3.5%	75% ± 3%

The attempt to recreate these results can be seen in table 4.2.3.1-2. These data represent glucose decomposition in pure water, reported as mass fraction of inlet carbon percent converted into the target compound, analyzed using HPLC. It can be seen that there is no statistical difference between the two dopants. This agrees with previous work to recreate the data. This result

indicates that the number of available Lewis (lactic acid pathway) and Brønsted (levulinic acid pathway) acid sites on the two catalysts are approximately equal and the charge of the tin salt being used does not appear to impact this availability of acid sites. In order to recreate the tin 2+ dopant data seen in table 4.2.3.1-1, this catalyst will need to have significantly more Brønsted acid sites on the catalyst than Lewis acid sites, which is believed to not be happening. It can also be noted that the updated HPLC analysis is capable of qualifying formic and acetic acid.

Table 4.2.3.1- 2: Catalytic decomposition of glucose in pure water at optimized condition, reported as mass fraction of inlet carbon percent converted into the target compound with 95% confidence intervals

Sugar		**Glucose**	
Catalyst Dopant		Tin II	Tin IV
Analyte (C%)	Formic Acid	3.4% ± 0.8%	3.8% ± 1.0%
	Lactic Acid	18% ± 4%	15% ± 2%
	Levulinic Acid	25% ± 5%	25% ± 3%
	Acetic Acid	1.9% ± 0.2%	1.3% ± 0.3%
Total		48%	45%

The simplest way to increase the Brønsted acid sites on the doped catalyst, is to change the beta catalyst scaffold used for doping. In this case, decreasing the SiO2/Al2O3 ratio will increase the amount of alumina present, which acts as the Brønsted acid sites on the catalyst. The results of changing from a SiO2/Al2O3 of 300 to 25 with Sn 2+ dopant can be seen in table 4.2.3.1-3. As shown, increasing the number of Brønsted acid sites has made the levulinic acid pathway the dominant mechanism and overwhelmed the lactic acid pathway. This agrees with what was seen in the work by Kadrmas. It was determined, through use of previous lab notebooks, that when

Kadrmas performed his optimum conditions, the Sn 2+ was doped on catalyst with a SiO2/Al2O3 of 25 and the Sn 4+ was doped onto a catalyst with a SiO2/Al2O3 of 300. This leads to the conclusion that both Sn 2+ and Sn 4+ are capable of acting as Lewis acid sites in Sn-beta catalysts, but neither performs more efficiently than the other in terms of lactic acid production. The ratio of the production of lactic and levulinic acid is more easily influenced by changing the SiO2/Al2O3 ratio of the beta catalyst, by changing the Brønsted acid sites.

Table 4.2.3.1-3: Effect of SiO2/Al2O3 ratio of catalyst scaffold on Sn 2+ doped catalytic decomposition, reported as mass fraction of inlet carbon percent converted into the target compound with 95% confidence interval.

Sugar		**Glucose**	
Si-Al Ratio		300	25
Analyte (C%)	Formic Acid	3.4% ± 0.8%	5.8% ± 0.8%
	Lactic Acid	18% ± 5%	2.2% ± 0.2%
	Levulinic Acid	25% ± 5%	28% ± 1%
	Acetic Acid	1.9% ± 0.2%	1.8% ± 0.1%
Total		48%	38%

When comparing the results in Table 4.2.3.1-1 to those in tables 4.2.3.1-2 and 4.2.3.1-3, it can be seen that the previous work reported higher carbon conversions than the current work. The residual carbohydrate(s) after decomposition are generally below the limit of quantification on the HPLC, which means their conversion is very high, but selectivity to target analytes is lower than previous work. This is likely attributed to side reactions which form compounds that do not elude from the HPLC column or foul/deactivate/attach to the catalyst surface. The TCA can be used to help verify this theory.

TCA analysis was performed by analyzing the carbon content in the original reactor feed, the unfiltered reactor product, and the filtered reactor product. The results from the unfiltered product and the filtered product were then subtracted from each other to provide the carbon content of the sample product solids. These results can be seen in Figure 4.2.3.1-1. This figure shows the results of a 20 hour glucose decomposition run using Sn 2+ dopant. The first thing to note in this figure is that the total amount of carbon in the sample is essentially the same before and after decomposition. The 2% increase in the unfiltered product is attributed to sampling variability. This leads to the conclusion that few to no gaseous products are formed during this decomposition and the unquantified carbon from the feed is still in the reactor products.

Next, approximately 57% of the original carbon is found in the aqueous phase of the reactor product. On average, it is possible to account for approximately 48% of the original carbon as HPLC elutable analytes. This leads to the conclusion that there is roughly 9% of the inlet carbon unaccounted for by the HPLC. When comparing the filtered product to product solids, the aqueous product has more carbon in the 200-, 300-, and 400-degree fractions, while the solid product has more carbon in the 500- and 890-degree fractions. This indicates the solid products are made of larger, more complex oligomeric molecules. It is also important that there are insignificant amounts of char being formed, this means the unaccounted-for carbon is not coke.

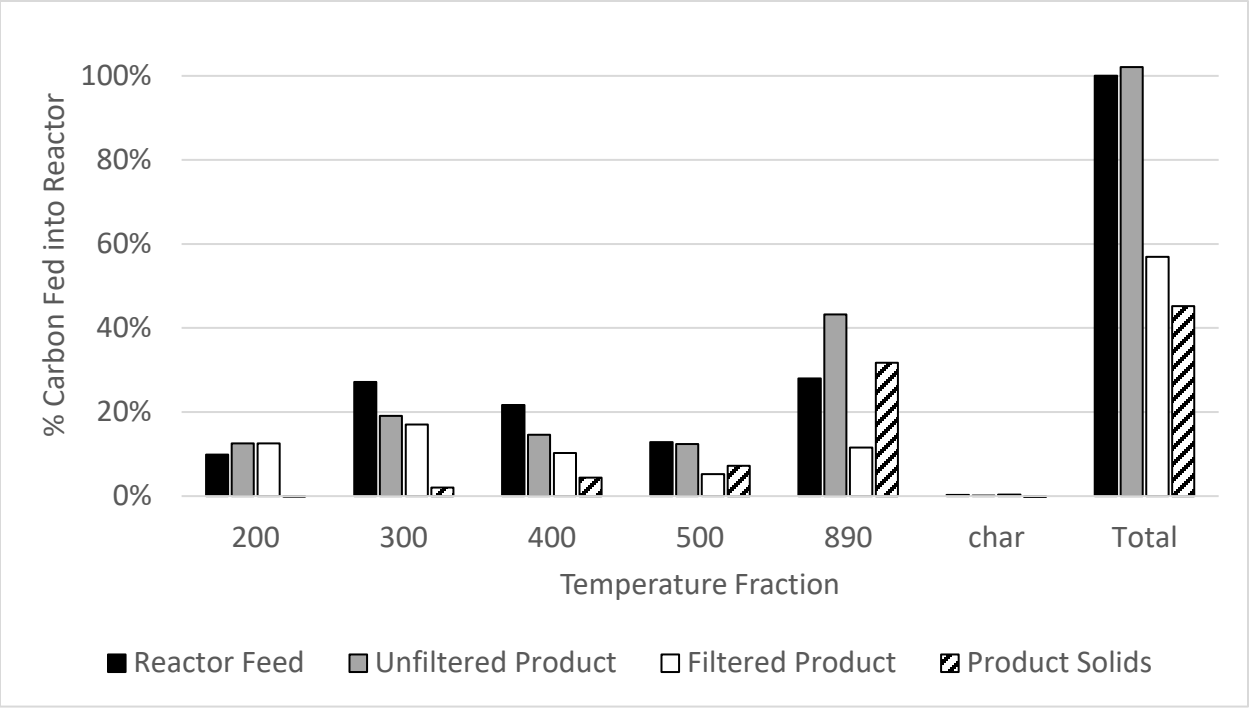

Figure 4.2.3.1- 1: TCA data showing the carbon fractions from a 20 hr glucose decomposition run with Sn 2+ dopant.

The next goal of this research was to extend the results to the decomposition of xylose via Sn-Beta decomposition reactions. Table 4.2.3.1-4 is an updated version of Table 4.2.3.1-2 to include xylose. As before, there is no significant difference between the tin 2+ and tin 4+ doped SiO2/Al2O3 300 catalyst. This is still attributed to the availability of Lewis acid sites on the catalyst. The xylose also has significantly less levulinic acid production than glucose. This is an effect of the pentose sugar xylose not being able to follow the HMF to levulinic acid reaction pathway normally followed by the glucose.[82] This reaction pathway can be seen in figure 4.2.1-1. When comparing figure 4.2.1-1 with figure 4.2.1-2, it can be seen the keto-form of glucose is available for lactic acid formation, while both the keto- and aldo- forms of xylose are available for lactic acid formation. This explains the increased lactic acid production. With fewer dominating side reactions, the selectivity to lactic acid increases.

Table 4.2.3.1- 4: Sn-Beta Catalytic decomposition products from Glucose and Xylose, reported as mass fraction of inlet carbon percent converted into the target compound with 95% confidence

Sugar		**Glucose**		**Xylose**	
Catalyst Dopant		Tin II	Tin IV	Tin II	Tin IV
Analyte (C%)	Formic Acid	3.4% ± 0.8%	3.8% ± 1.0%	3.4% ± 1.6%	4.3% ± 1.1%
	Lactic Acid	18% ± 5%	15% ± 2%	36% ± 2%	37% ± 2%
	Levulinic Acid	25% ± 5%	25% ± 3%	1.4% ± 0.2%	2.0% ± 1.1%
	Acetic Acid	1.9% ± 0.2%	1.3% ± 0.3%	2.0% ± 0.2%	2.0% ± 0.3%
Total		48%	45%	43%	45%

The overall goal of applying this decomposition reaction to biomass-sourced carbohydrates requires an understanding of if/how these two carbohydrates interact with each other during the decomposition reaction. Once the Sn-Beta decomposition behavior of these two carbohydrates was understood separately, it was possible to perform experiments using model mixtures of expected glucose and xylose mixtures from forage sorghum biomass. This was considered the best-case-scenario when examining reaction products.

Table 4.2.3.1-5 shows the results of catalytic decomposition of a model mixture with a 2:1 ratio of xylose and glucose. This ratio was based on initial carbohydrate recovery data. The expected ratios for recovered glucose and xylose from forage sorghum were later updated to 57% glucose and 43% xylose, due to increased efficiencies in the enzymatic pretreatment step. These updated recoveries can be seen in table 4.2.3.2-1. The model catalytic decomposition runs were not repeated with the updated sugar ratios values. This decision was made because literature data examining Sn-beta catalyzed decomposition of model mixtures of glucose and xylose showed

similar results with a feed of 65wt% glucose and 35 wt% xylose, forming 15% levulinic and 12% lactic acid.[82] The model mixture appears to provide more levulinic acid than xylose and less than glucose. This is attributed to the glucose portion of the model mixture. The production of lactic acid is decreased from either of the two pure carbohydrates. This may be attributed to differences in reaction kinetics between the two carbohydrates leading to competition for Lewis acid active sites or deactivation of the catalyst.

Table 4.2.3.1- 5: Model carbohydrate mixture decomposition results of Sn 2+ doped catalyst, reported as mass fraction of inlet carbon percent converted into the target compound with 95% confidence

Sugar		Glucose	Xylose	2 Xylose: 1 Glucose
Analyte (C%)	Formic Acid	3.4% ± 0.8%	3.4% ± 1.6%	8% ± 1%
	Lactic Acid	18% ± 4%	36% ± 2%	14% ± 3%
	Levulinic Acid	25% ± 5%	1.4% ± 0.2%	9.3% ± 0.8%
	Acetic Acid	1.9% ± 0.2%	2.0% ± 0.2%	3.6% ± 0.6%
Total (carbon %)		48%	43%	34%

4.2.3.2 Forage Sorghum Biomass Carbohydrate Recovery

In this research, two variants of forage sorghum were used: Brown Mid Ridge (BMR) and Non-Brown Mid Ridge (NBMR). An analysis of the glucan, xylan, and lignin content of each variant is shown in figure 4.2.3.2-1. As shown, the two variants have similar xylan content while the NBMR sorghum has a higher glucan content and the BMR sorghum has a higher lignin content. Both the glucan and lignin content values have statistically different averages despite the relatively high variability in the results obtained.

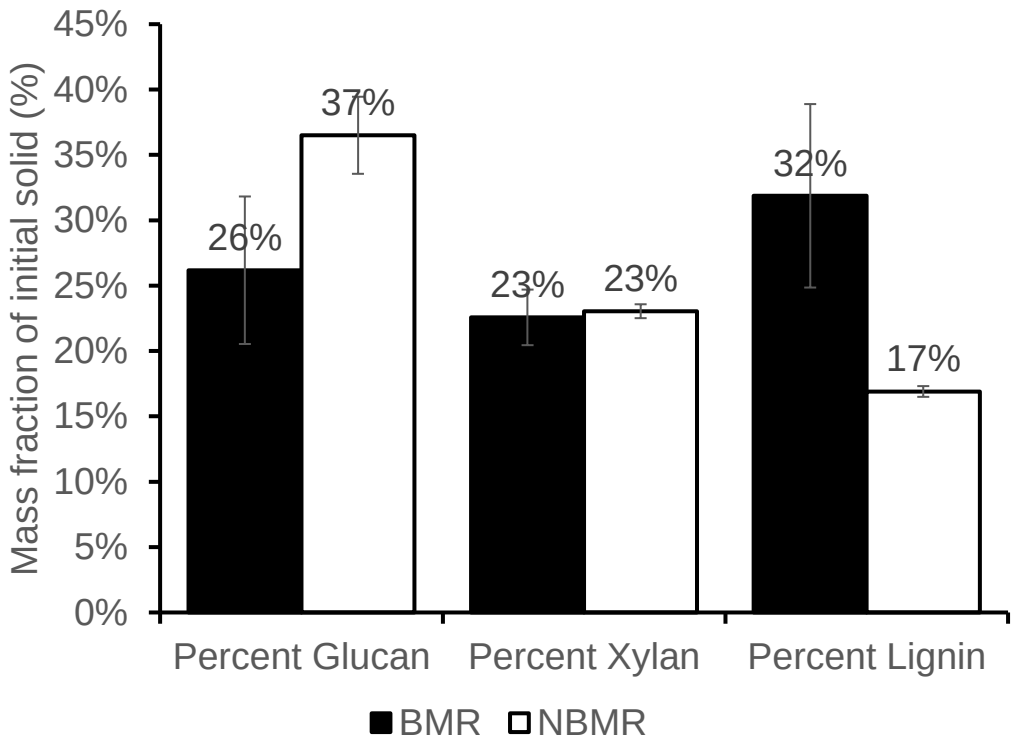

Figure 4.2.3.2-1: Glucan, xylan, and lignin content of the experimental samples of both BMR and NBMR forage sorghum (mass fraction of initial solid as %, 90% confidence interval)

The total glucan and xylan content values can be used to measure the effectiveness of the acid hydrolysis step as shown in figure 4.2.3.2-2. This figure shows that similar amounts of xylan were recovered from both BMR and NBMR sorghum. In the literature, recovery of xylans from acid hydrolysis are generally between 65 and 95 wt% of initial biomass content.[28] Results in current work are lower than optimized literature conditions, but still within acceptable literature values for use in enzymatic hydrolysis. The BMR sorghum shows higher glucan recoveries than the NBMR sorghum, but also had a lower starting glucan concentration. Generally, glucan recoveries from acid hydrolysis are found to be between 40 and 50 wt% of initial biomass content. The BMR sorghum has higher glucan recoveries than predicted in literature, while the NBMR sorghum has lower recoveries than expected. Considering the acid hydrolysis does not target glucan recovery, this is considered acceptable.

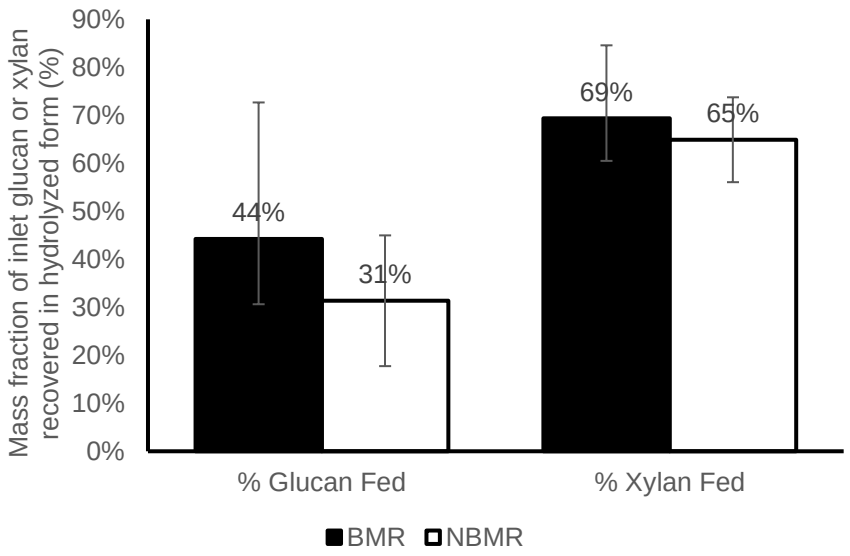

Figure 4.2.3.2- 2: Glucan and Xylan recovery from acid hydrolysis (mass fraction of initial solid as %, 90% confidence interval)

The recoveries of glucan (as glucose) and xylan (as xylose) after the enzymatic hydrolysis step are shown in figure 4.2.3.2-3. As shown, the enzymatic hydrolysis provided fairly low recoveries of both the glucan and the remaining xylan in the biomass. Although the enzymatic hydrolysis is meant to recover glucans as glucose, additional xylose was recovered. This is likely due to residual xylans being freed as cellulose is decomposed. Recoveries of glucose from enzymatic decomposition usually fall within 60 to 90% recover of biomass fed.[28] The current work is below this expected value. However, it was decided that the overall recoveries were sufficient to proceed with the sorghum-based sugar decomposition reactions, since enzymatic hydrolysis has been well studied and developed by others and thus was not the primary focus of the current research. These data experienced large variations which results in the large relative error values seen in the total carbohydrate analysis used to calculate the recovery of these sugars.

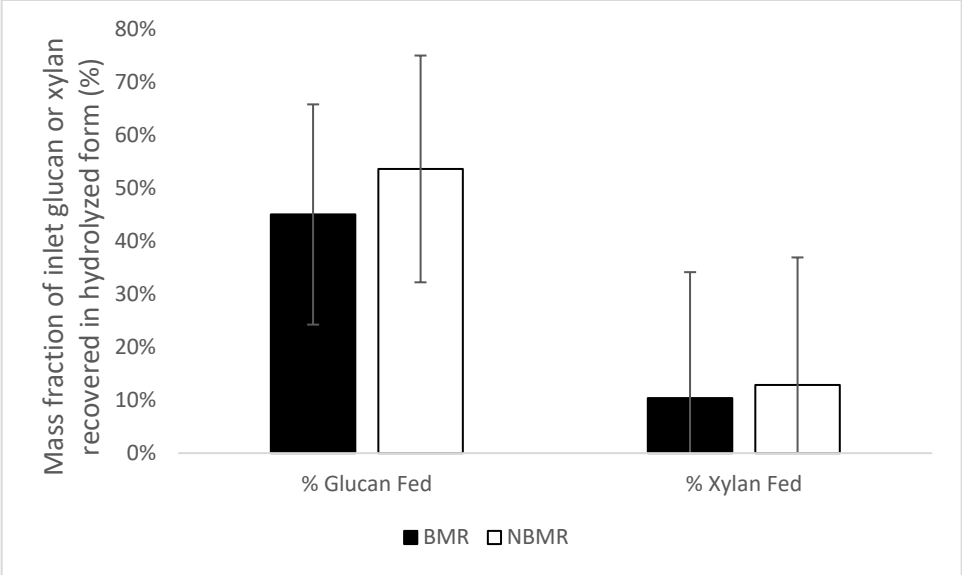

Figure 4.2.3.2-3: Glucan and xylan recoveries from enzymatic hydrolysis (mass fraction of initial solid as %, 90% confidence interval)

The combined recoveries from both the acid and enzymatic hydrolysis steps are shown in figure 4.2.3.2-4. Xylan recovery was similar from both the BMR and NBMR sorghum and are consistent with those seen in literature.[28] The glucan recoveries are also similar to values expected based on literature. Overall, the expected ratios for recovered glucose and xylose from forage sorghum are 57% glucose and 43% xylose. The carbohydrate recoveries discussed in this section are summarized in table 4.2.3.2-1.

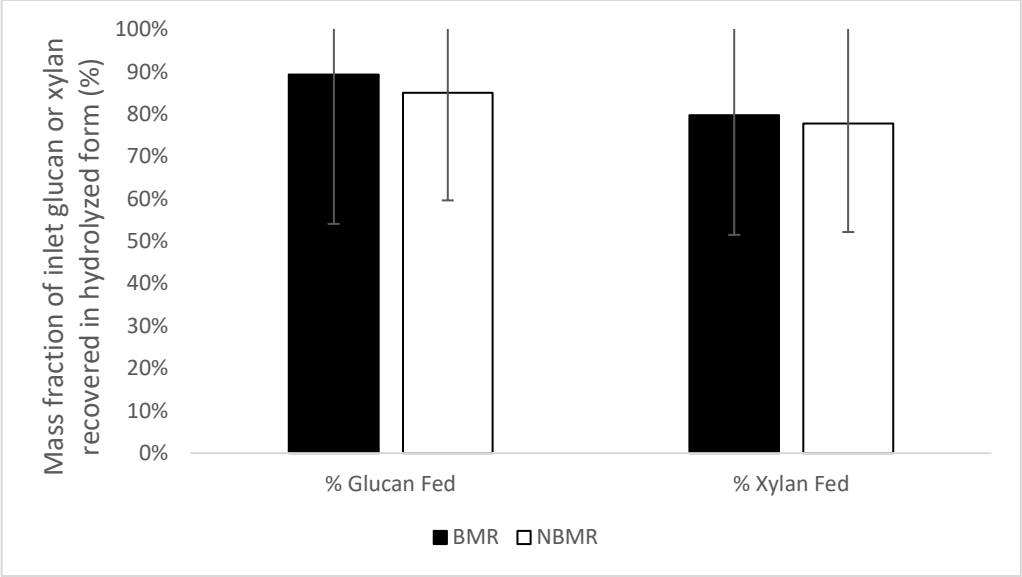

Figure 4.2.3.2- 4: Overall glucan (as glucose) and xylan (as xylose) recoveries from sequential acid and enzymatic hydrolysis (mass fraction of initial solid as %, 90% confidence interval)

Table 4.2.3.2- 1: Mass fraction of inlet glucan or xylan recovered in hydrolyzed form (%)

	BMR			NBMR		
Recovery	Acid Hydrolysis	Enzymatic Hydrolysis	Overall Recovery	Acid Hydrolysis	Enzymatic Hydrolysis	Overall Recovery
% Glucan Fed	44%	45%	89%	31%	54%	85%
% Xylan Fed	69%	10%	80%	65%	13%	78%

4.2.3.3 Forage Sorghum Sourced Carbohydrate Decomposition

The sugars recovered from the acid and enzymatic hydrolysis of forage sorghum, detailed in section 4.2.3.2, were used as feedstock in catalytic decomposition reactions with a tin (2+) doped beta zeolite with a SiO_2/Al_2O_3 ratio of 300. The results from these trials, along with results from the model decomposition experiments are provided in Table 4.2.3.3-1. The results reveal several

differences between the model decomposition products and the sorghum decomposition products. On average, model mixed decomposition products have higher formic acid and levulinic acid concentrations. This is caused by a glucose decomposition pathway, which forms formic and levulinic acid simultaneously. The sorghum decomposition products have higher concentrations of lactic and acetic acid. Acetic acid, although formed through the decomposition of trioses, as seen in figure 4.2.1-1, is also an inhibitor formed from the decomposition of carbohydrates during acid hydrolysis and can exist as residual in the decomposition product, used in the catalytic decomposition feed.[25] This leads to higher errors associated with its measurement.

Acetic acid can also be an indication of additional side decomposition reactions. The lactic acid formation is an indication that the catalytic sugar decomposition reaction experiences higher interactions with the Lewis acid sites than the model mixtures. This is most likely due to the acid hydrolysis neutralization step. In this, the sulfuric acid is neutralized with calcium carbonate to form calcium sulfate. The inclusion of calcium sulfate acts as an inhibitor to the Brønsted acid sites on the catalyst, as well as providing additional Lewis acidity. This facilitates increased lactic acid formation and inhibits levulinic acid production. The effect of calcium sulfate was further explored by Kohler.[82] The decomposition results using biomass sourced carbohydrates are comparable to those seen in literature. The decomposition of corn stover yielded similar results with slightly increased lactic acid formation.[82] Other catalyzed decomposition reaction of biomass to form lactic acid saw values between 20 and 30 wt%.[27]

Table 4.2.3.3- 1: The conversion of model sugars, a model mixture, and actual forage sorghum-derived sugars into four product acids (Mass fraction of inlet carbon recovered, % with a 95% Confidence Interval)

Source		Model			Sorghum	
Sugar		Glucose	Xylose	2 Xylose: 1 Glucose	BMR	NBMR
Analyte	Formic Acid	3.4% ± 0.8%	3.4% ± 1.6%	7.6% ± 1.2%	2.5% ± 1.0%	1.5% ± 0.9%
	Lactic Acid	18% ± 4%	36% ± 2%	13.5% ± 3%	29% ± 2%	23% ± 6%
	Levulinic Acid	25% ± 5%	1.4% ± 0.2%	9.3% ± 0.8%	1.3% ± 1.1%	1.2% ± 1.0%
	Acetic Acid	1.9% ± 0.2%	2.0% ± 0.2%	3.6% ± 0.6%	16% ± 5.5%	10% ± 10%
Total Recovery		48%	43%	34%	49%	36%

An additional explanation for reduced catalytic decomposition products from forage sorghum is catalyst deactivation. It has been observed by several researchers that the use of Sn-beta catalysts in aqueous solvents for the decomposition of carbohydrates leads to catalyst deactivation.[20, 82, 89] This concept was explored by adjusting the concentration of carbohydrates used for catalytic decomposition reactions. This effectively increases the catalyst to sugar ratio in the reactor. These reactions were performed at optimum reactions conditions of 200 °C and 5 hours, as determined by Kohler.[82] Initial results from these experiments can be seen in table 4.2.3.3-2. It can be seen that decreasing the sugar concentration leads to significant increases in lactic acid recoveries, with values greater that 60% possible. This agrees with values seen in literature and matches high end conversions of carbohydrates to lactic acid.[82, 84] It was theorized by Kohler that the neutralization step used for acid hydrolysis modifies the Sn-beta catalysts to increase yields and may be contributing to the lactic acid increase seen.[82] It can be seen that the optimum for lactic acid conversion has not been bounded in regards to sugar concentration.

Table 4.2.3.3- 2: Sugar concentrations and lactic acid formation from Sn-Beta catalyst decomposition

Sugar Concentration (g/L)	8	17	21
Lactic Acid Recovery (C%)	64	34	18

4.2.4 Conclusions and Recommendations

1. Both Sn 2+ and Sn 4+ salts can be used as dopants for beta zeolite catalyst to effectively convert carbohydrate sugars to form organic acids, namely lactic and levulinic acid. There is no statistical significance between the performance of the two tin dopants. Both dopants replace Al atoms in the Si-Al zeolite matrix which increases the ratio of Lewis to Brønsted acid sites in the catalyst. Brønsted acid sites facilitate the reaction pathway to the formation of levulinic acid while Lewis acid sites facilitate the reaction pathway to lactic acid.

2. The silica-to-alumina ratio of the catalyst scaffold is a significant factor in how the catalytic decomposition reactions perform. Decreasing the silica-to-alumina ratio increases the amount of alumina in the catalyst. This increases the number of Brønsted acid sites that are not replaced by Lewis (Sn) sites in the final catalyst mixture and thus promotes levulinic acid formation pathways at the expense of lactic acid pathways.

3. The Sn-Beta catalytic decomposition of xylose leads to increased lactic acid and decreased levulinic acid, when compared to glucose. This is attributed to differences between the

proposed reaction pathways for xylose and glucose. While the keto-form of glucose is available for lactic acid formation, both the keto- and aldo- forms of xylose are available for lactic acid formation. Additionally, xylose does not participate in the HMF-to-levulinic acid pathway.

4. An HPLC with RI detector is capable of quantifying formic, acetic , lactic, and levulinic acids in aqueous Sn-beta decomposition products. Unaccounted for carbon in the catalytic decomposition reaction products is likely contained in complex oligomers, but not coke. Additional analysis of these complex molecules through Pyrolysis GC/MS is recommended. This would provide an understanding of what these complex molecules are and if the catalyst is experiencing deactivation.

5. Carbohydrates recovered from biomass are capable of being used in Sn-Beta decomposition reactions. The neutralization step for acid hydrolysis modifies the Sn-Beta catalyst to provide increased lactic acid formation and decreased levulinic acid formation.

6. The sugar concentration used in Sn-beta catalytic decomposition reaction appears to be a significant factor in lactic acid formation from biomass sourced carbohydrates. It is recommended this be investigated further in an attempt to optimize lactic acid formation.

4.3 Base Facilitated Decomposition of Forage Sorghum Lignin

Abstract

Lignin is one of the most abundant natural polymers, behind cellulose and hemicellulose. Found within lignocellulosic biomass, lignin is a complex, stable polymer responsible for giving a plant structure and rigidity. This functionality is common amongst all plants, including herbaceous species. Structurally, lignin consists of mainly phenyl and hydroxyl functional groups, like p-coumaryl alcohol, p-hydroxyphenal alcohol, coniferyl alcohol, and sinapyl alcohol. Unique amongst renewable biomass, lignin is considered the most promising non-petroleum source of renewable aromatic compounds. The chemical composition of lignin varies widely, depending on the original source where it was formed.

The largest source of commercial lignin is the pulp and paper industry, with annual production of 50 million tons. Currently, lignin is considered a waste product, with most of its production being burnt for heat and electricity. In order to better exploit the unique phenolic content of lignin, it is necessary to liberate these desirable monomer compounds from the polymer. Given the complex nature of lignin, an efficient method to decompose it into chemical intermediates does not currently exist. While extensive research has been performed around the concept of lignin decomposition, few significant discoveries have been made.

The research presented herein utilizes a novel, continuous flow reactor designed to decompose the portion of lignin that dissolves in a pH 10 base solution. This lignin is commonly referred to as reactive lignin. The reactor utilized uses non-catalytic thermal decomposition to depolymerize reactive lignin. It was desired to compare the decomposition of both Kraft lignin and forage sorghum sourced lignin.

The effect of reactor temperature, specifically 335, 340, and 350 °C, was investigated for both lignin sources. It was found that the temperature used for lignin decomposition is a significant factor, with 340 °C showing the best lignin depolymerization. Reactive Kraft lignin was found to maintain a high level of complexity even after the decomposition reactions, with the majority of its carbon profile being contained in the char fraction. By contrast, reactive sorghum-derived lignin shows significantly reduced char fraction carbon, suggesting a less recalcitrant nature. Sorghum-derived lignin also shows significantly higher oligomer and monomer carbon fractions. In all cases, the design of the reactor prevented coke formation within the reaction chamber and all char left the reactor entrained within the product liquid.

This project demonstrated a continuous decomposition reaction system that can at least partially decompose reactive lignin into more tractable fragments. The depolymerization reactions were more effective on alkali grass lignin than softwood kraft lignin.

4.3.1 Introduction

This research expands upon previous work performed at the University of North Dakota by Sara Pourjafar.[90] In this previous work, the thermal degradation of kraft lignin was investigated through two pathways. First, batch decomposition reactions over metal doped catalysts were investigated. Second, a novel reactor was designed to enable non-catalytic, short residence time decomposition reactions in a bench-scale continuous flow reaction system. The most promising of these two methods was found to be the non-catalytic continuous flow reaction system. Similar to work by others, it was discovered that dissolving the lignin into a strong aqueous base solution with a pH of around 10 facilitated the decomposition reactions. The portion of the lignin that dissolved is often referred to as reactive lignin.

Starting from this previous work, the current research had the following objectives:

1. Recreate previous work using the continuous flow reactor system to verify kraft lignin decomposition results.
2. Extract reactive lignin from forage sorghum biomass and perform decomposition reactions using the continuous flow reactor system.

Lignin is one of the most abundant natural polymers, behind cellulose and hemicellulose. Found within lignocellulosic biomass, lignin is a complex, stable polymer responsible for giving a plant structure and rigidity. This functionality is common amongst all plants, including herbaceous species. Structurally, lignin consists of mainly phenyl and hydroxyl functional groups, like p-coumaryl alcohol, p-hydroxyphenal alcohol, coniferyl alcohol, and sinapyl alcohol.[26, 30] Unique amongst renewable biomass, lignin is considered the most promising non-petroleum source of renewable aromatic compounds.[31] The chemical composition of lignin varies widely, depending on the original source where it was formed.

In general, lignin can be split into three broad categories. These are softwood, hardwood, and grass lignins. Table 4.3.1-1 shows the common concentrations of three main constituents within lignin.[91] It can be seen that softwoods are almost exclusively coniferyl alcohol, while hardwoods are generally divided between coniferyl alcohol and sinapyl alcohol. Grass lignins can have appreciable content within each of these three categories and is the only group likely to have significant p-coumaryl alcohol content. This table highlights the variety seen within different lignin groups. It also shows the wide range of potential lignin compositions when dealing with grasses, the subgroup that includes forage sorghum. There is currently no accepted model for the structure of lignin from grasses, given the large diversity seen within these plants.[92]

Table 4.3.1- 1: The common concentrations of three main constituents within various types of lignin. [91]

Lignin Source	p-Coumaryl Alcohol (%)	Coniferyl Alcohol (%)	Sinapyl Alcohol (%)
Softwood	<5	>95	0
Hardwood	0-8	25-50	45-75
Grasses	5-35	35-80	20-55

The largest source of commercial lignin is the pulp and paper industry, with an annual production of 50 million tons.[32] Currently, lignin is considered a waste product, with most of its lignin being burnt for heat and electricity. In order to better exploit the unique phenolic content of lignin, it is necessary to liberate these desirable monomer compounds from the polymer.

Chemical depolymerization of lignin is considered the most direct method to recover valuable chemicals from lignin. Unfortunately, the products from chemical depolymerization are difficult to predict and to date, have resulted in low yields. Depolymerization can be accomplished through several different approaches: acid, base, ionic liquid, and supercritical fluid depolymerization. Acid depolymerization is performed with acids at elevated temperatures. One study used temperatures >350°C , with an ethanol/formic acid solvent.[93] Recovery of lignin decomposition products was less than 7 wt%.[94] The use of ionic liquids and supercritical fluids hold potential for targeted extraction of lignin materials, but are not currently considered an economic option to implement industrially.[92]

Base facilitated decomposition is a fairly common technique within the literature. One study used 300 °C with NaOH, KOH, LiOH, or $Ca(OH)_2$. Recovery of lignin products was between 5 and 20%, with NaOH providing the highest product formation.[95] An additional study used NaOH at 315°C with a lignin decomposition product recovery of 14%.[96] Overall recovery of lignin decomposition products is highly dependent on the starting lignin source but decomposition to useful products, while typically greater than from acid facilitated depolymerization, were still low.

By contrast to these methods, the research presented herein focused on a general non-catalytic thermal decomposition method to depolymerize the lignin. First the lignin is treated with a strong aqueous base solution, to break primarily aryl-aryl bonds, with the β-O-4 bonds being most common.[92] This allows the lignin to dissolve into the liquid phase and makes the remaining structure more amenable to decomposition. The high pH aqueous lignin-rich mixture is then heated rapidly to a target temperature where decomposition occurs. This method can be classified as a base facilitated non-catalytic thermal decomposition method.

Currently, forage sorghum sourced lignin decomposition does not appear to be well studied, with most research focused on lignin removal from sweet sorghum to improve recovery of carbohydrates from the biomass.[23, 97, 98] A focus of the present study was to determine if base facilitated non-catalytic thermal decomposition is an appropriate method for the decomposition of forage sorghum lignin a grass lignin. Grass lignins generally contain a high content of free phenolic groups, making half of total grass lignin easily soluble at room temperature in alkali solutions.[99] This is unique to grass lignin.

4.3.2 Methods and Materials

4.3.2.1 Materials and chemicals

The experiments performed in this work use lignin from two different sources. Wood-derived chemically processed Kraft lignin was provided by MeadWestvaco (Indulin AT, Richmond, VA, USA). Biomass sourced reactive lignin was extracted from forage sorghum biomass provided by Marisol Berti, Professor and Forage Agronomist at North Dakota State University (Fargo, ND, USA). Sodium hydroxide used for reactor feed preparation and neutralization before analysis was purchased as anhydrous pellets from Sigma-Aldrich (≥98%, S5881-1KG, St. Louis, MO, USA). Compressed nitrogen gas cylinders at 99.998% purity were purchased from Praxair (Grand Forks, ND, USA). Ultrapure water (18 MOhm) was obtained from an Ultra milli-Q filter system (MilliporeSigma, Burlington, MA, USA).

4.3.2.2 Lignin Preparation Procedure

For experiments using Kraft lignin, the reactor feedstock was prepared using powdered lignin. The lignin was dissolved in a sodium hydroxide solution. The ratio used for this feedstock was 2 wt% kraft lignin and 1 wt% sodium hydroxide pellets with the balance water. A total of 3.8 liters of solution was required for each experimental run performed using the continuous lignin decomposition reactor.

For experiments using forage sorghum sourced reactive lignin, the reactor feedstock was prepared using lignin rich residual solids obtained after the enzymatic pretreatment described in section 4.2.2.3. It was necessary to solubilize the reactive lignin from the solid biomass through a heated alkaline soak. Any residual biomass was removed via centrifugation followed by 90 mm

filtration through a sintered stainless steel filter. A more detailed description of this procedure can be found in Appendix 3.2.1 Production of Sorghum-derived Lignin.

4.3.2.3 Continuous Lignin Decomposition Reactor Description and Procedure

All continuous lignin decomposition reactor experiments were performed using a reactor apparatus designed and built by former UND ChE PhD student Sara Pourjafar.[90] A simplified schematic is shown in figure 4.3.2.3-1. This system uses a modified 5 liter Parr Series 4580 High Temperature Reactor (Serial number #4580-0908-12536) purchased from Parr Instrument company (Moline, IL, USA) as a feed preheater and high pressure storage vessel. The Parr reactor was modified through the addition of an outlet on the bottom of the reactor vessel. This outlet fitting was attached to a heat-traced transfer line containing on/off and metering manual control valves. This transfer line was connected to the bottom inlet of a coiled reactor vessel. This reactor vessel was installed in a large ceramic heater clamshell. The reactor was made from 4 m of coiled 316 stainless steel with diameter of 0.95 cm and wall thickness of 0.16 cm. The reactor outlet was connected to a cooling heat exchanger, which consisted of coiled stainless steel tubing submerged in room temperature cooling water. The heat exchanger outlet tube was connected to a particulate filter with a mesh of 100 mm. From the filter, the cooled fluid was routed through a backpressure regulator to control the reactor flowrate and pressure. Pressure in the form of regulated nitrogen gas was provided to the feed preheater through a 3-cylinder manifold.

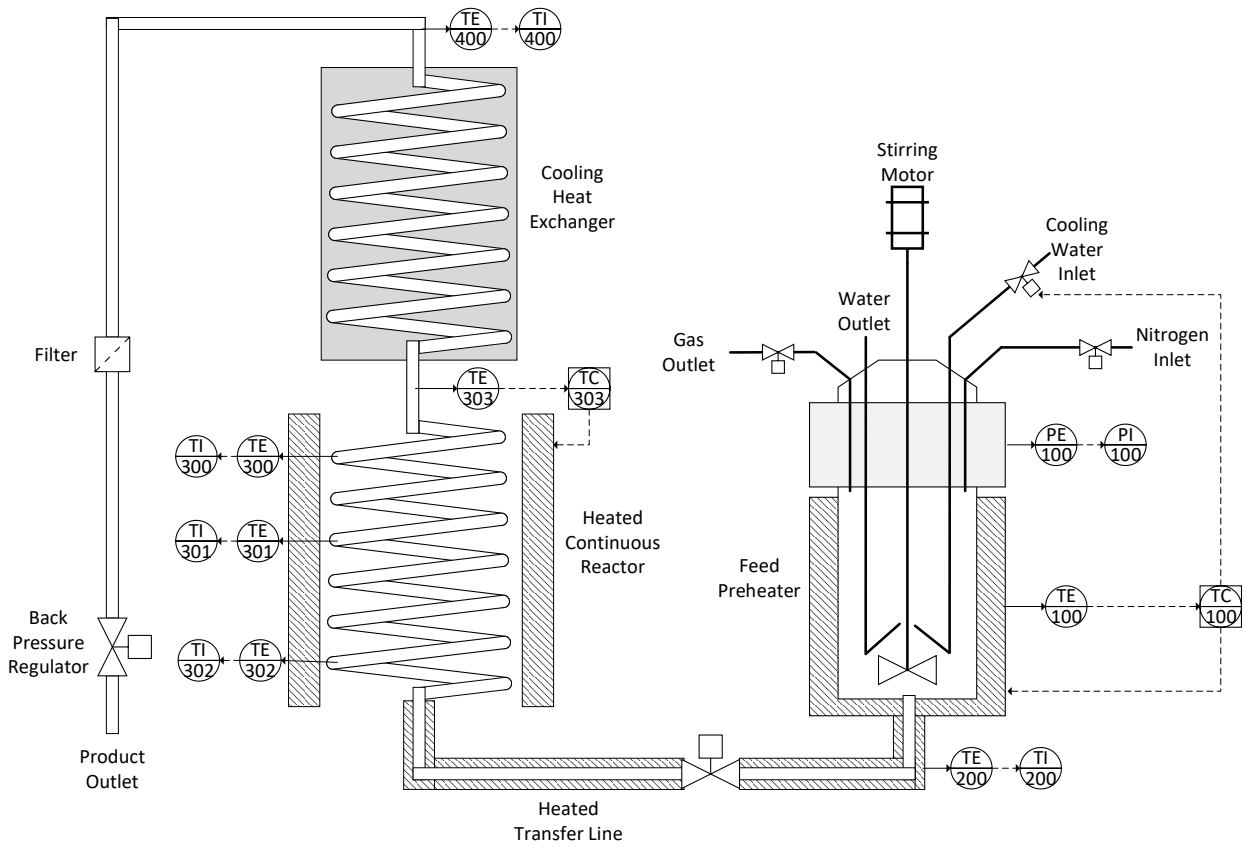

Figure 4.3.2.3- 1: Schematic of the continuous lignin decomposition reactor (based on the original by S. Pourjafar[90])

The reactor was operated by first filling the reaction vessel with ultra-pure water. A prepared lignin feedstock of 2 wt% lignin and 1 wt% NaOH in ultrapure water solution was then placed into the feed preheater where the controls were set to a temperature of 250°C and stir rate of 400 rpm. The heating to the coiled reaction vessel was set to the desired operating temperature and the transfer line heating and heat exchanger cooling water were turned on to reach operating conditions. Once all portions of the reactor system were at reaction conditions, the regulator on the nitrogen tanks was adjusted to reach the desired operating pressure, as determined by the desired operating temperature. The preheated lignin feed could then be continuously flowed through the reaction apparatus. More detailed instructions on running the continuous lignin

decomposition reactor can be found in Appendix 3.2.2 Continuous Lignin Decomposition Reactor Operation.

4.3.2.4 Experimental Design

The goal of this research was to utilize and evaluate a novel continuous flow reactor system for the base facilitated non-catalytic thermal decomposition reactions of both kraft and forage sorghum-based lignin. First, experiments were performed with kraft lignin to identify near optimum decomposition conditions within the reactor system. Next, these optimum conditions were applied to forage sorghum sourced lignin. These experiments are defined in table 4.3.2.4-1. The conditions were selected based on previous work with the same reaction system by S. Pourjafar.[90] Temperature was the only parameter adjusted within the reaction system. It should be noted that the residence time experienced fluctuations of ±10 seconds, due to normal reactor stability.

Table 4.3.2.4- 2: Summary of experimental conditions used in lignin decomposition reactions

Lignin Source	Temperature (°C)	Residence time (s)	Lignin Concentration	NaOH Concentration
Kraft	335	90	2 wt%	1 wt%
Kraft	340	90	2 wt%	1 wt%
Kraft	350	90	2 wt%	1 wt%
Sorghum	340	90	2 wt%	1 wt%

4.3.2.5 Analytical Methods

Samples generated from the continuous lignin decomposition reactor were analyzed using Thermal Carbon Analysis (TCA). TCA is used to evaluate the total carbon pyrolyzed from a

sample as it is exposed to a series of increasingly aggressive temperature steps.[71] The temperature fraction at which carbon evolves gives an indication of the complexity/stability of the original sample and its constituents. The TCA analysis was performed using a thermal optical analyzer from Sunset Laboratory Inc. (Portland, OR). Samples were prepared by neutralizing an aliquot of the reactor outlet to a pH of 4 with hydrochloric acid. The neutralized sample was placed on a 2500QAT-UP tissue quartz filter pad (Pall Corp. East Hills, NY) and dried. The filter pad was placed in the TCA oven and analysis was run. Results were calculated as the mass fraction of total carbon evolved from the sample at each temperature (wt%). A more detailed description of the TCA analysis can be found in Appendix 2.3 TCA Analysis.

4.3.3 Results and Discussion

The goal of this research was to evaluate the potential use of a non-catalytic continuous flow reactor system for the decomposition of reactive lignin where reactive is defined as that fraction of the original lignin that dissolves in a pH 10 NaOH solution. For forage sorghum-derived lignin, approximately 60% is assumed to be reactive. The kraft lignin, having already been dissolved in alkali and precipitated by the manufacturer, experienced 100% reactivity. Both chemical kraft lignin and forage sorghum sourced reactive lignin were evaluated. The decomposition was defined using TCA analysis, providing insight into the extent of decomposition and the complexity of both the feedstock and the resulting decomposition products. The kraft lignin was used to screen for favorable operating conditions, which were then also applied to the decomposition of reactive forage sorghum lignin.

The TCA results from the Kraft lignin decomposition experiments can be seen in Figure 4.3.3-1. This figure shows the thermal carbon profile for sub-critical decomposition at experimental

reaction temperatures of 335, 340, and 350 °C. The TCA temperature profile is split into the following functional categories: 200 and 300 °C are classified as monomers, 400 and 500 °C are classified as oligomers, and 890 °C and Char are designated as char. In respect to the char region of the TCA profile, the instrument operates under inert atmosphere through 890 °C, followed by a rapid heating ramp profile of 550, 625, 700, 775, and 890 °C under an oxidizing atmosphere to combust any residual chars. The Inert 890 °C section has been included in the Char fraction, because lignin is oxygen rich and will self-oxidize at extremely elevated temperatures, even under inert atmospheres.[100] This is supported by the near zero char profile fraction.

In interpreting the TCA data, the monomer fraction is the most desirable portion of the lignin decomposition products. This is where the targeted aromatic products would be found. The oligomer fraction is the next most desirable fraction, containing partial decomposition products. Lastly, the char fraction contains large, complex molecules and coke.

The combined char fraction represents the majority of the carbon contained within the kraft lignin samples, for both feed and decomposition products. This indicates the lignin begins as a very complex molecule and maintains the majority of this complexity after decomposition. This effect may be attributed to the recalcitrant nature of the starting kraft lignin or due to repolymerization reactions upon cooling of the reaction solution.[101] When looking at the effect of reaction temperature, it can be seen the char fraction reaches a minimum at 340 °C, with the mass fraction of char increasing at both lower and higher temperatures. These results coincide with an increase in carbon at lower temperatures in the oligomer and monomer fractions, with the highest occurring at 340 °C. Further increasing temperature to 350 °C, causes the content of monomers to decrease. This shift in carbon suggests that more of the original lignin complex molecules are decomposed with increasing temperature up to 340 ^{o}C. After 340 ^{o}C, the monomer

and oligomers may begin repolymerizing into more complex molecules, as indicated by the increase in the char fraction. This agrees with previous work performed by Pourjafar when using this reaction system with Kraft lignin.[90] Given these results, it was determined that 340 °C was the near optimum reaction temperature. Therefore, this reaction temperature was used for the sorghum-derived reactive lignin decomposition experiments.

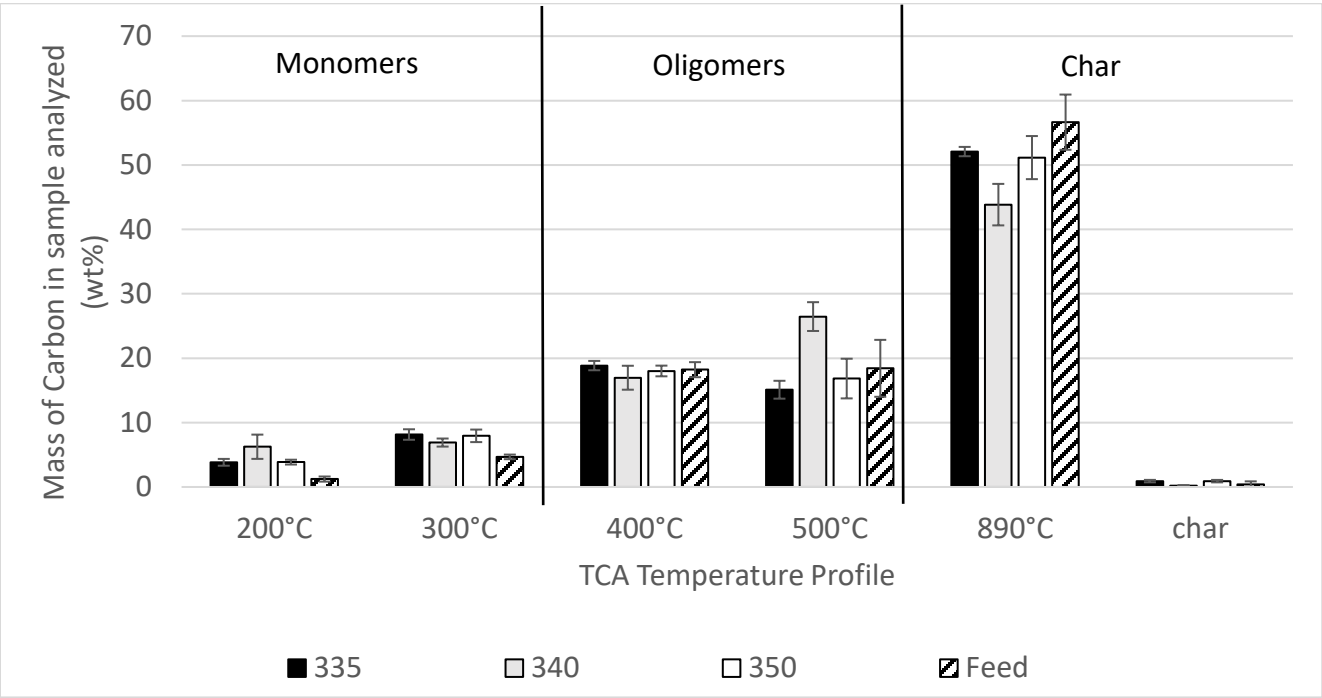

Figure 4.3.3- 1: Results from the thermal carbon analysis for Kraft lignin decomposition at three different reaction temperatures shown in wt% of carbon in sample analyzed, with 90% confidence.

The TCA results for the base facilitated non-catalytic thermal decomposition of both types of reactive lignin can be seen in figure 4.3.3-2. This figure shows the sub-critical decomposition at a reaction temperature of 340 °C for both sorghum-derived lignin and kraft lignin, along with their respective reactor feedstocks. When comparing the kraft to sorghum-derived lignin, several differences in the TCA profiles can be noted. First, the char fraction for kraft lignin is significantly higher than that of the sorghum-derived lignin, in both the feed and decomposition

products. This suggests the carbon contained within the sorghum-derived lignin is less recalcitrant and likely less constrained by its complexity, allowing it to more readily decompose than the Kraft lignin. Further, a higher fraction of the sorghum-derived lignin decomposes into simple monomers which are the most useful compounds generated. A larger fraction of small-sized oligomers was also generated from the sorghum-derived lignin. Consistent with the results shown in Figure 4.3.3-1, a general decrease in char fraction carbon with increasing oligomer and monomer carbon can be observed in the results shown in Figure 4.3.3-2. This suggests that more complex carbon molecules are being decomposed into smaller fractions during the reaction process.

In both cases, roughly half of the original lignin can be decomposed into usable monomer and oligomer fractions with a single pass non-catalytic reaction at 340^{o}C. In previous base facilitated decomposition reactions with similar conditions, 8.4% monomers were generated from kraft lignin, which is lower, but similar to results from the current study (figure 4.3.3-2). [96] The base facilitated decomposition of biomass lignin has been shown to form between 5 and 20% monomers at 300 °C.[101] Results from current work shows approximately 30% monomer content, which is better than the highest conversions found in the literature from these types of reactions.

When comparing the present study results to catalytic literature results, the closest comparison is the decomposition of wheat straw (a grass lignin) with nickel doped catalysts. In that work, approximately 27% of the lignin was converted to products with 65% remaining as lignin residues. In the current work, overall monomer content within forage sorghum sourced lignin decomposition samples was approximately 28% with an oligomer content of 64%. Approximately 73% of the converted lignin was converted to monomers in the current work

(figure 4.3.3-2). Overall oligomer content remains essentially unchanged before and after decomposition reactions of forage sorghum sourced lignin.

Coke formation is commonly reported in literature, with some catalytic reactions forming up 40% coke.[102] Coke formation is undesirable, because it limits the overall possible conversion of lignin into desirable products and deactivates the catalyst, shortening its lifetime. In the current work, coke formation was not observed. The char fraction reported was collected from the reactor in the form of tars, which hold the potential to be further converted into useful products through additional processing, perhaps using the methods described in Chapter II to generate a mesophase pitch for carbon fiber production.

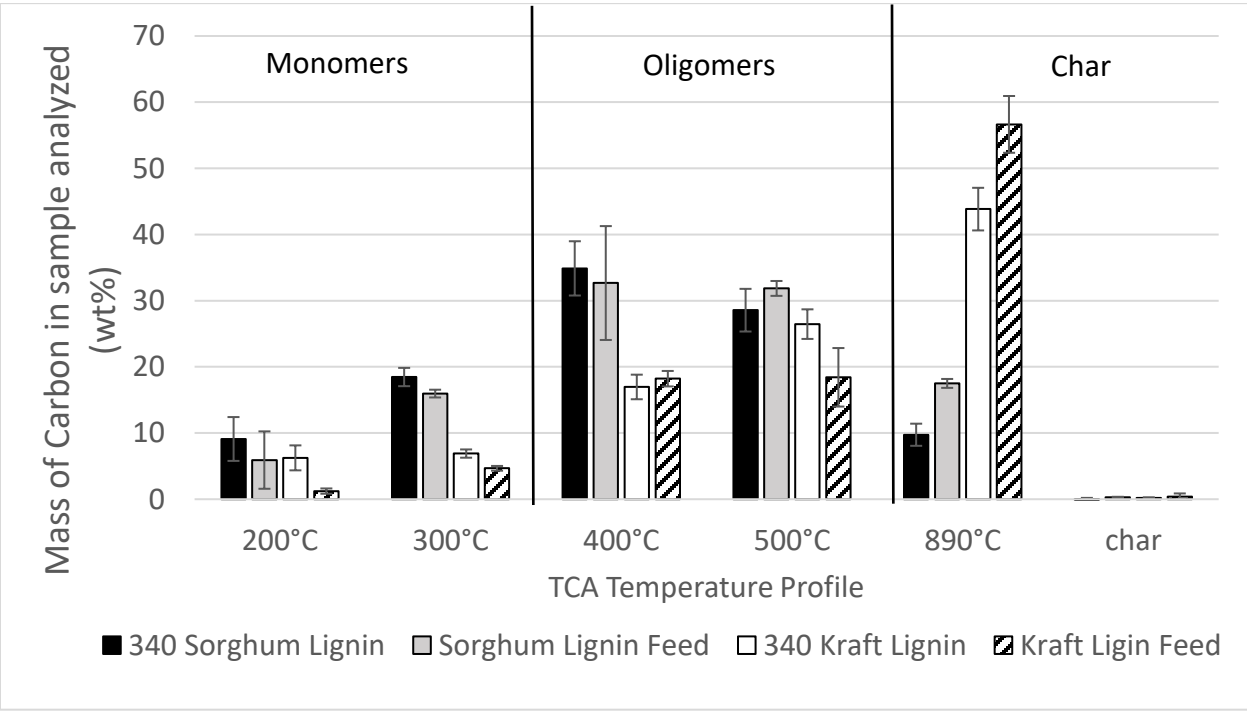

Figure 4.3.3- 2: Results from the thermal carbon analysis for Kraft and sorghum-derived lignin at 340°C decomposition temperature shown in wt% of carbon in sample analyzed, with 90% confidence.

4.3.4 Conclusions/Recommendations

- A novel reactor system for the base facilitated non-catalytic thermal decomposition of reactive lignin was successfully demonstrated.
- The fraction of monomers and oligomers generated in this novel system are higher than those from acid and base facilitated polymerization methods reported in the literature. This demonstrates that this system has the potential to be used for the decomposition of reactive lignin.
- The reaction temperature used for lignin decomposition was found to be a significant factor, with 340 °C showing the best results of the reaction temperatures investigated.
- Kraft lignin maintains a high level of complexity after decomposition reactions, with the majority of its carbon profile being contained in the char fraction.
- Sorghum-derived lignin shows significantly reduced char fraction carbon, suggesting a less recalcitrant nature, when compared to Kraft lignin.
- Sorghum-derived lignin shows significantly higher Oligomer and Monomer carbon fractions, when compared to kraft lignin.
- It is suggested that a more detailed quantitative analysis be performed to determine/compare decomposition products of both kraft and sorghum-derived lignin and to identify the specific compounds generated during decomposition. Use of PY/GC-MS is suggested to avoid the need for organic extraction and to better evaluate the solids and char fraction which would be contained within the samples. To our best knowledge, a comprehensive method for lignin decomposition product identification and quantification does not yet exist, but is under development by analytical chemists at the University of North Dakota.

- It is suggested that the pre-heat temperature be investigated further for sorghum-derived lignin. The 250 °C preheat temperature was chosen to avoid thermal decomposition of kraft lignin. Given the drastic difference between the char fraction of sorghum-derived and kraft lignin, this assumption may not hold true for sorghum-derived lignin, leading to decomposition in the reactor pre-heater.
- It is recommended that experiments be performed to assess the ability to rerun unreacted solids collected from the reactor outlet.
- Not evaluated in this work was the impact of residence time within the reactor. This factor should be investigated via changes to the reactor flow rate.

Chapter V. Conclusions and Recommendations

Status of Research Objectives

Chapter II

1. Design and build a pre-processing and continuous pitch processing system for the production of mesophase pitch. Status: completed
2. Perform initial experiments to evaluate the reactor system functionality. Status: completed

Chapter III

1. Perform a comprehensive survey of candidate solvents to identify the most attractive potential solvent(s) for lipid extraction from microalgae. Status: completed
2. Determine which, if any, of the most commonly proposed pretreatment methods (microwave-assist, sonication-assist, grinding, in-situ transesterification) were worthwhile. Status: completed
3. Identify the near-optimum conditions for lipids extraction from microalgae. Status: completed

Chapter IV

Carbohydrate Decomposition

1. Replicate and extend the catalytic decomposition work previously performed by Kadrmas.[73] Status: completed
2. Update derivatization GC/MS analytical methods to be able to qualify formic acid. Status: completed
3. Use optimum conditions for glucose decomposition to decompose model xylose and xylose/glucose blends. Status: completed

4. Perform catalytic decomposition reactions with actual sugar solutions derived from forage sorghum biomass. Status: completed

Lignin Decomposition

1. Evaluate the potential usage of a non-catalytic continuous flow reactor system for the decomposition of reactive lignin. Status: completed
2. Determine favorable operating conditions for lignin decomposition with kraft lignin. Status: completed
3. Apply favorable conditions to forage sorghum sourced biomass. Status: completed

Conclusions

Chapter II

1. This work successfully demonstrated a pre-processing and continuous pitch processing system for the production of mesophase pitch from the non-volatile organic compounds generated during the non-catalytic cracking of a triglyceride oil (soybean oil).
2. Operating temperatures of 325, 350, 375, and 390 °C were investigated in the pitching reactor. All of these temperatures experienced additional devolatilization of the tar feed stock, with 390 °C experiencing the highest degree of devolatilization at 25 wt% pitch product recovery. The 390 °C operating temperature was the only condition tested which produced a solid pitch product. The softening point of the 390 °C pitch product was 122 °C. This softening point is too low for carbon fiber formation and indicates the molecules within the pitch are too small to be drawn into fibers and stabilized.

Chapter III

1. This study determined methanol was the best performing solvent for lipid extraction from Chlorella Vulgaris microalgae. Methanol consistently outperformed the other solvents examined, namely: Bligh Dyer, ethanol, chloroform, acetonitrile, and hexane. Methanol was the top solvent for use with microwave and sonication assisted extraction, as well as, for in-situ transesterification.
2. In the comparison between microwave and sonication assisted extraction, it was found that both methods improved extraction, but the microwave provided higher extraction efficiency. This is believed to be due to a higher fraction of additional cell wall rupture provided by the microwave heating, which heats internally, compared to sonication, which heats externally. The use of in-situ transesterification was found to increase the extraction of lipids for methanol as a solvent. This is believed attributed to increased cell rupture from the transesterification and the polarity of methanol making it more effective at breaking the cell wall-membrane layer.[68] Additional factors found to have a potential impact on extraction efficiency that warrant further investigation include: pretreatment ball mill grinding speed, extraction temperature, and lipids-to-solvent ratio. These factors were further investigated in subsequent work by Jasmine Oleksik (Kreft) and documented in her thesis.[54]
3. Maximum extraction of lipids from microalgae biomass was achieved with a combination of ultrasonication and insitu-transesterification with methanol solvent.

Chapter IV

Carbohydrate Decomposition

1. The use of Sn 2+ and Sn 4+ salts as dopants for beta zeolite catalyst can be effectively used in the conversion of carbohydrate sugars to form organic acids, namely lactic and levulinic acid. There is no statistical significance between the performance of the two tin dopants. Both dopants replace Al atoms in the Si-Al zeolite matrix which increases the ratio of Lewis to Brønsted acid sites in the catalyst. Brønsted acid sites facilitate the reaction pathway to the formation of levulinic acid while Lewis acid sites facilitate the reaction pathway to lactic acid. The silica-to-alumina ratio of the catalyst scaffold is a significant factor in how the catalytic decomposition reactions perform. Decreasing the silica-to-alumina ratio increases the amount of alumina in the catalyst. This increases the number of Brønsted acid sites that are not replaced by Lewis (Sn) sites in the final catalyst mixture and thus promotes levulinic acid formation pathways at the expense of lactic acid pathways.
2. The use of HPLC with RI detector is capable of qualifying formic and acetic acid in aqueous Sn-beta decomposition products.
3. The Sn-Beta catalytic decomposition of Xylose leads to increased lactic acid and decreased levulinic acid, when compared to glucose. This is attributed to the inability of xylose to participate in the HMF to levulinic acid pathway. Mixtures of glucose/xylose experience reduced performance in formation of lactic and levulinic acid, compared to their pure carbohydrate constituents.
4. Carbohydrates extracted from biomass are capable of being used in Sn-Beta decomposition reactions. The neutralization step for acid hydrolysis modifies the Sn-Beta catalyst to provide increased lactic acid formation and decreased levulinic acid formation.

The sugar concentration used in Sn-beta catalytic decomposition reactions appears to be a significant factor in lactic acid formation from biomass sourced carbohydrates.

Lignin Decomposition

1. The use of a continuous decomposition reaction system shows the potential to be used for the decomposition of reactive lignin.
2. The reaction temperature used for lignin decomposition was found to be a significant factor, with 340 °C showing the best results of the reaction temperatures investigated.
3. Kraft lignin maintains a high level of complexity after decomposition reactions, with the majority of its carbon profile being contained in the char fraction. Sorghum-derived lignin shows significantly reduced char fraction carbon, suggesting a less recalcitrant nature, when compared to Kraft lignin. Sorghum-derived lignin shows significantly higher Oligomer and Monomer carbon fractions, when compared to kraft lignin.

Recommendations

Chapter II

It is recommended the tar feed stock be more heavily devolatilized in the vacuum distillation step, before being used in the pitching reactor to test if longer post-devolatilization in the pitching reactor will improve the softening point. This would either be done through longer dwell times at the 350 °C temperature used previously or by increasing the maximum devolatilization temperature. It is important to avoid coking of the tar feed stock, as the 350 °C operating temperature is the beginning of the coking region for tars. A tar feedstock with reduced volatility should experience increased reactor

efficiency, as seen in initial pitching reactor trials. Other options that could be explored are: 1) increase the length of the pitching reactor to increase the time available for complex component formation and 2) replace the existing spinning brush with a material that can withstand higher temperatures so that the pitching reactor can be operated above 390 ^{o}C.

It is recommended additional analytical steps be performed on the pitch products formed. The components within the tar and pitch product experience boiling points >350 °C, making them difficult to analyze in traditional GC/MS systems. Py-GC/MS can be employed on both tar feedstocks and pitch products to better understand the changes within the tar before and after processing into pitch products, without the likelihood of damaging GC injectors and columns. Additionally, the molecular weight distribution of feed tars and pitch products could be examined using a GPC system, assuming an appropriate solvent was determined for sample preparation. Softening point analysis through the drop formation method was performed on pitch samples by CAEFF and is recommended when measuring the softening point of pitch products. The rheological properties of pitch products should be examined, to determine expected behavior when melt spinning the samples. This would require a rheometer with heating capabilities, like the TA Instruments AR 2000 in the chemical engineering department at UND.

Chapter III

The use of TCA and gravimetric analysis provides a reasonable quantitative analysis of the lipids extracted from microalgae. However, this should be verified using more rigorous analytical methods, like GC/MS, to provide a qualitative lipid analysis. This would help to highlight additional differences seen between the solvents being

investigated and whether they impact the quality of lipids being extracted. Additional analytical techniques to consider are high temp GC/MS and APCI-MSTOF.

Chapter IV

Carbohydrate Decomposition

The sugar concentration used in Sn-beta catalytic decomposition reactions appears to be a significant factor in lactic acid formation from biomass sourced carbohydrates. It is recommended this be investigated further in an attempt to optimize lactic acid formation.

Unaccounted for carbon in the catalytic decomposition reaction products is likely contained in complex oligomers, but not coke. Additional analysis of these complex molecules through Pyrolysis GC/MS is recommended. This would provide an understanding of what these complex molecules are and if the catalyst is experiencing deactivation.

Lignin Decomposition

It is suggested that more qualitative analysis be performed to determine/compare decomposition products of both kraft and sorghum-derived lignin and to identify the specific compounds generated during decomposition. Use of PY/GC-MS is suggested to avoid the need for organic extraction and to better evaluate the solids and char fraction which would be contained within the samples.

It is recommended that experiments be performed to assess the ability to rerun unreacted solids collected from the reactor outlet.

Not evaluated in this work was the impact of residence time within the reactor. It is recommended this factor be investigated via changes to the reactor flow rate.

APPENDIX 1: Production of Mesophase Pitch from Renewable Sources of Tar

Appendix 1.1 Production of Soy Based Tars

The first step in generating bio-tar was the non-catalytic cracking of soybean oil. The reaction apparatus used in this experimentation was a pilot-scale continuous tubular thermal cracking reactor designed and fabricated by the University of North Dakota. Soybean oil was cracked by controlling pressure, temperature, and flowrate inside the reactor. The cracking temperature and pressure was recorded using a Labview data logging system. A schematic of this reaction system can be seen in figure A1.1-1. This system consists of a feedstock holding tank, pump, preheater, heated reactor, cooling heat exchanger, in-line filter, back-pressure regulator, and knock-out drum.

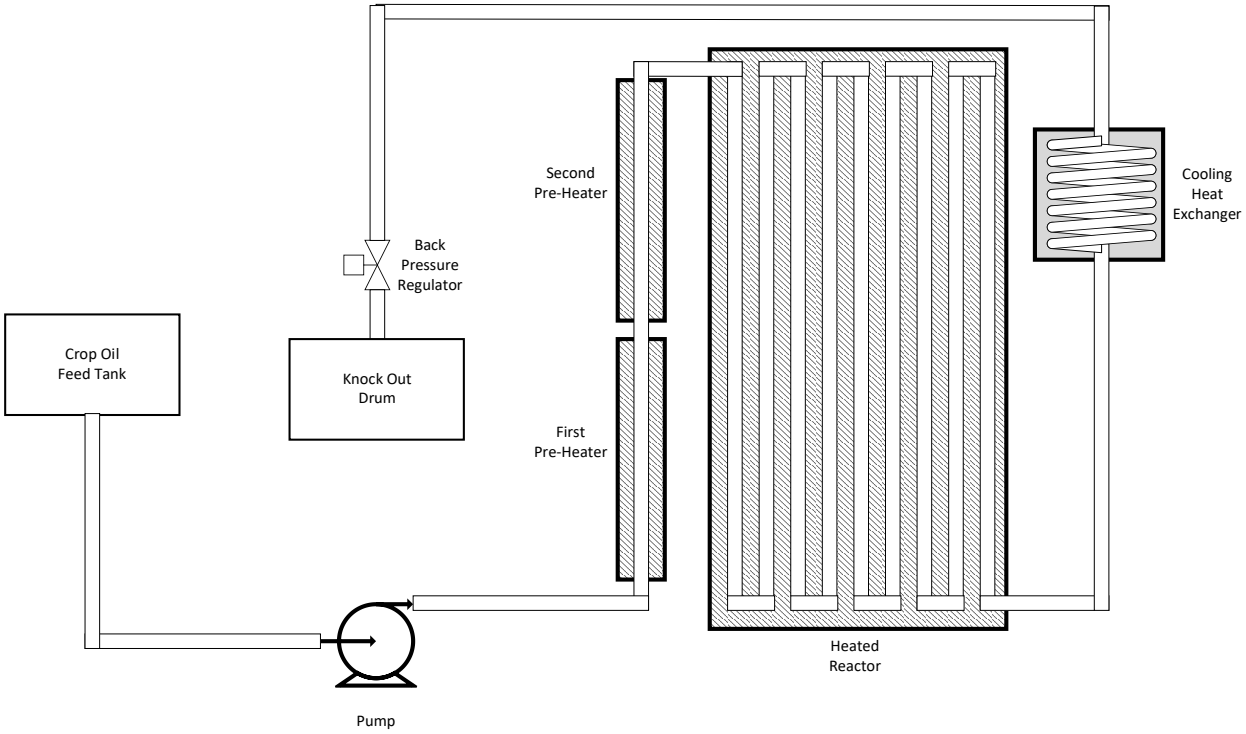

Figure A1.1- 1: A schematic of the crop oil cracking reactor

In running the cracking reactor, it was first necessary to ensure the tubular reactor system was cleaned and purged of any storage media, like toluene. This included performing maintenance on the filters and back-pressure regulator, to ensure proper operation. The system was then purged and filled with soybean oil. Then the power to all PID controllers, pumps, and computers was turned on using the circuit breakers in the electrical panel. The cooling water was turned on for the cooling heat exchanger. This is the state of the reactor system before starting a cracking run.

At the beginning of a crop oil cracking run, several steps are required to bring the reactor up to operating conditions. First, the temperature and pressure data logging were started using the labview computer program. Next, the temperature setpoints on the PID controllers were set to the following: first preheater 340 °C, second preheater 410 °C, reactor top and bottom 420 °C. Next the crop oil flowrate and pressure was set. This is done by priming the reactor feed pump, then adjusting the pump feed control knob until the desired flowrate of 2L/hr was achieved. The flowrate of the pump was measured using a graduated feed container and a stopwatch. Next, the back pressure regulator was adjusted to bring the pressure to operating condition, in this case 420 psig. Finally, the power to the heaters was turned on using the circuit breakers in the electrical panel allowing the system to begin heating. The pressure and crop oil flowrate were verified systematically while heating the reactor system and while performing crop oil cracking runs.

Once the cracking reactor reached operating conditions, the run was started. This required any collected product during the preheating be drained from the product collection vessel and discarded. The cracking reactor system was allowed to run as long as necessary to meet the desired product volumes. While running the reactor, it was important to systematically check and adjust the pressure and crop oil feed rate. It was also necessary to monitor the pressure for indications of the filter clogging, switching the filter cartridge as necessary. Once the run was

finished, the product collection vessel was drained and the crackate saved for further processing. The reactor system was allowed to cool, while still maintaining flow through the system, to avoid coking. Once cooled, all electric power was turned off and cooling water stopped. Additional operating instructions can be found in Linnen's dissertation.[5]

The second step for this process was atmospheric distillation. This was performed through a bulk flashing process. This flash used a modified 5 liter Parr Series 4580 High Temperature Reactor (Serial number #4580-0908-12536) purchased from Parr Instrument Company (Moline, IL, USA) as a boiling pot with condenser coil. A schematic of this apparatus can be seen in figure A1.1-2. The cooling coil was made of coiled ¼ inch stainless steel and was air cooled. Cooled condensate was collected in a large 6-liter Erlenmeyer flask, where gas was vented.

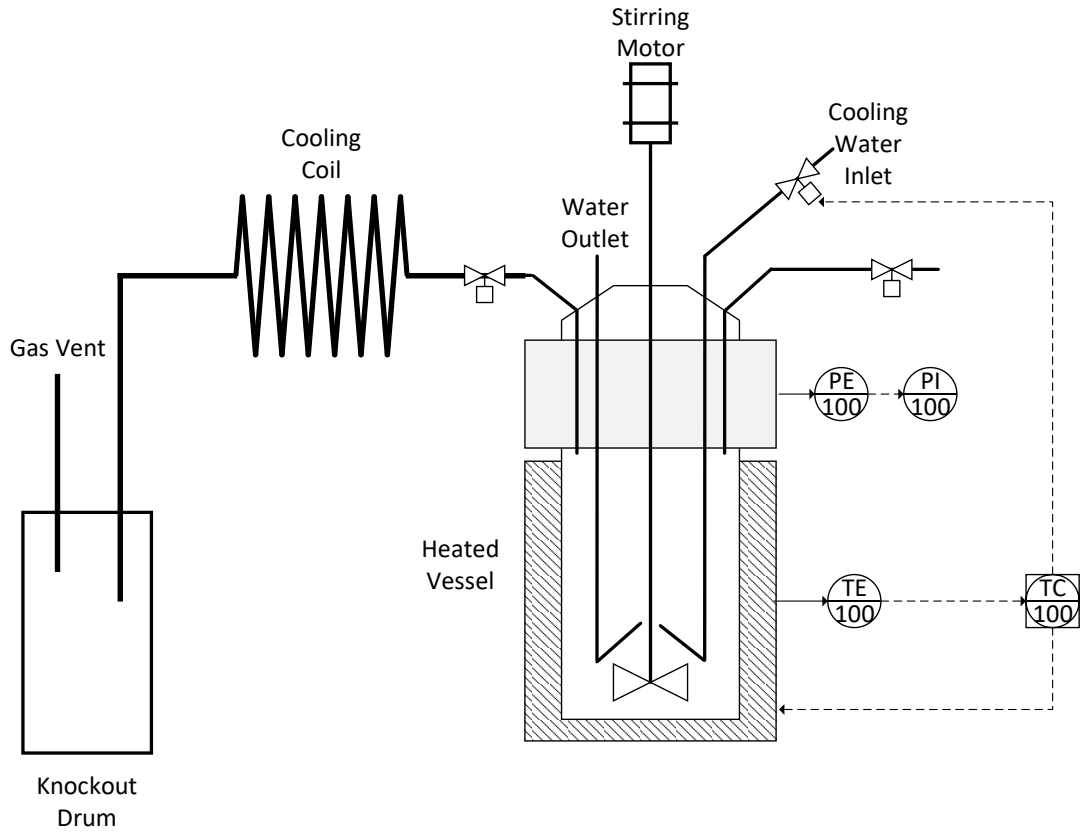

Figure A1.1- 2: A schematic of the modified Parr reactor used for crackate flashing

It was necessary to first clean the reactor vessel, impeller, cooling coil, and reactor head. This was done by scrubbing all of the pieces thoroughly with soapy water, then rinsing with ultrapure water. The gasket contained within the mounted reactor head must be wiped clean to remove any residual vacuum grease or reactor debris. Once clean, the graphite gasket was visually inspected for any apparent signs of damage and replaced if necessary. Finally, the sealing surface on the reactor vessel was cleaned and polished using a fine emery paper, to ensure a secure seal once closed. The reactor vessel was filled with approximately 4 liters of crop oil crackate from the continuous tubular cracking reactor.

To close the reactor vessel and prepare it for operation, first a thin layer of vacuum grease was spread on the reactor vessel sealing surface. This was done to protect and extend the lifespan of the graphite gasket in the reactor head. Next, the reactor vessel was aligned under the reactor head, while situated on the pneumatic lift platform. Using the pneumatic lift lever on the side of the reactor stand housing, the reactor vessel was slowly raised to fit in the reactor head. With the pneumatic lift pressing the reactor vessel into the vessel head, the two halves of the sealing clamp were slid into place and fastened. The bolts on the sealing clamp were sealed using a 16-bolt flange pattern. A torque wrench was used and the sealing force was increased by 5 pound increments, until a force of 35 pounds was achieved. Once sealed, the pneumatic lift platform was lowered and moved out from under the reactor vessel. The heater surround was then positioned under the reactor vessel and raised using the pull knob on the heater support shaft.

Next, the reactor vessel was purged with compressed nitrogen using the gas inlet and vent valves on the reactor head. The vessel was filled and purged five times, to ensure no residual oxygen remained. A pressure check was performed by filling the reactor vessel to 200 psig and allowing it to stand for 5 minutes. The pressure check passed if the pressure remained stable and did not

appear to be leaking. The pressure was then vented and the vent valve left fully open, to allow for devolatilized components to exit the reactor vessel. The PID controller was then given an initial temperature setpoint of 150°C with the heater power control turned to level I and the impeller set to 350 rpm. The temperature was monitored and once reaching the desired setpoint of 150 °C the reactor was allowed to dwell for 5 minutes, before the setpoint was adjusted to 200 °C. This was repeated for 250 °C and finally 300 °C. The final flashing temperature of 300 °C was chosen to provide the most devolatilization, while still remaining below the cracking/coking region of 350 °C. After the processing time was finished, the PID temperature set point was changed to 20°C, the heater controller turned off, and the heater surround lowered to increase the rate of cooling. It was important to monitor the volume of distillate being collected, because removing more than 3 liters of volume from the reactor vessel would expose the thermocouple well inside the vessel. This will lead to incorrect readings and temperature control.

Once the reactor vessel had cooled to room temperature, it could be opened. First, the pneumatic lift platform was positioned under the reactor vessel and raised to firmly press up on the reactor vessel. Next, the torque wrench was used to slowly loosen the sealing clamp bolts, using a 16-bolt flange pattern. The locking clips on the sealing clamp were then opened and the clamp slid completely clear of the reactor vessel. Next the stirring impeller was slowed to 20 rpm. Then, the vessel was then slowly lowered until the pneumatic lift platform was in its lowest position. The impeller was then turned off completely. This was to ensure the increased viscosity of the heavy oils did not cling to the impeller, making removing the vessel more difficult. The reactor vessel was then swung out from under the reactor head, using the pneumatic lift platform. The stainless-steel transfer handles were attached to the reactor vessel and the vessel was moved to the lab bench counter for product collection, being careful to employ proper lifting techniques to avoid

injury while moving the very heavy reactor vessel. Reactor products were transferred from the reactor vessel to a 2L beaker, for ease of handling. The heavy oils were weighed, before being stored for further processing.

The third step in producing bio-tar was vacuum distillation. This was performed using the tar devolatilization apparatus and multi-stage condensation system described in section 2.2.1. Approximately 1.5 liters of heavy oils from the bulk flashing step were loaded into the glass boiling flask of the tar devolatilization apparatus. A magnetic stir bar was added to the boiling flask filled with heavy oils. The flask was attached to the distillation head, a thermocouple was inserted into the boiling flask thermocouple well, the heating wrap was placed around the flask, and vacuum was applied to the system. The spinning band on the distillation head was turned on and a magnetic stir plate was placed under the boiling flask and gentle stirring applied. The boiling water, cooling water, and refrigerant cooling loop heat exchange fluids were turned on and the condensers allowed to come to temp. The boiling flask was then heated from room temperature to 350 °C at a ramp rate of 1.5 °C/min using labview for monitoring and control. Once the desired distillation temperature was reached, the heating was stopped and the flask allowed to cool to room temperature, before removing and storing the residual tars within the distillation flask. It was necessary to maintain vacuum on the distillation flask until fully cooled, to avoid unintended self-combustion of the bio-tars. These residual tars are the bio-tar feedstock used in the pitching reactor. These tars are stored for future use in the pitching reactor. The tars must be warmed, in order to transfer them from the boiling flask.

Appendix 1.2 Pitching Reactor Operation

The first step in running the pitching reactor was filling and preparing the tar feed vessel. This is done through several steps. The tars were first transferred into a 1 L pressure vessel (316L-50DF8-1000, Swagelok, Solon, OH, USA). This was done by placing a glass funnel into the opening of the pressure vessel, while the entire apparatus was placed into a warm oven (ideally under 100 °C, to avoid tar smoking/fuming). The funnel was filled with tar and allowed to drain into the vessel, while inside the oven. This was repeated as necessary, until the desired amount of tar was loaded into the vessel. A dipstick can be used to verify tar levels inside the vessel. Once filled, the vessel was allowed to cool to room temperature.

Next, the feed tars were pressure filtered. This required to cooled vessel filled with bio-tar to be fitted with a 90 micron sintered stainless steel in-line filter (SS-4F-90, Swagelok, Solon, OH, USA) on the bottom of the vessel. The outlet of this filter was attached to the inlet of the tar feed vessel from the pitching reactor. It is important to have a clean dry weight on this feed vessel. Both the filtering vessel and the pitching reactor feed vessel were held vertically with a large ring stand and clamps. A nitrogen line was attached to the top of the filtering vessel and the vessel purged several times with nitrogen. A heating wrap was placed around both the vessels and the filter. The vessels were heated to approximately 100 °C, then the filtering vessel was pressurized using the nitrogen tank. The vessel was allowed to sit for 10 minutes, before cooling and depressurizing. The tar feed reactor can then be installed onto the pitching reactor. This is done by suspending the vessel from the load cell, with heat tracing and nitrogen line attached. This pressure filtering apparatus can be seen in figure A1.2-1.

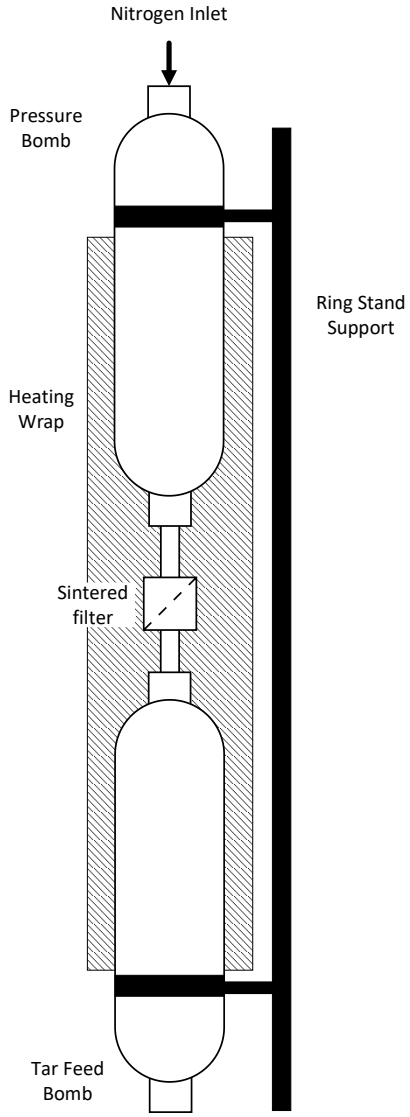

Figure A1.2- 1: A schematic of the tar hot filtering apparatus

To operate the pitching reactor, first the feed preheater was set to 100 °C and an inert atmosphere applied inside the vessel. Next, the vacuum on the reactor and distillation system was applied and a vacuum test performed, generally this was maintaining 200-400 millitorr. The cooling and hot water required for the multi-stage distillation apparatus was turned on and refrigerant cooling loop turned on for the light distillate condenser. The cooling water for the top and bottom of the pitching reactor was turned on and the reactor heating started. Once the reactor had reached the desired operating temperature, the internal spinning brush was turned on to 900 RPM. Next, the

on/off control valve on the tar feed line was opened and the metering valve opened and adjusted. Tar flowrate was confirmed by observing an increase in system pressure and vapor space temperature. The flowrate through the pitching reactor was often less than 5 g/min. The flowrate out of the pitching reactor was often controlled by counting the number of drops leaving the drip cone. On average, a flowrate of 5-10 drops per minute was used. The pitching reactor was allowed to run until a desired amount of product was formed and collected. Then, the tar feed was stopped and the reactor system allowed to cool. The brush and vacuum were kept running until the system had cooled below 150 °C, to avoid combustion of the tar and sticking of the brush.

APPENDIX 2: The Extraction of Fatty Acids from Algae Biomass

Appendix 2.1 Microwave Assisted Extraction

Microwave assisted solvent extraction was performed to determine the impact of microwave heating on solvent extraction efficiency. Microwave conditions were chosen to best approximate the conditions of the ultrasonic bath, which was also being investigated at the time. Unless different conditions were specifically being investigated, the microwave assisted extraction experiments were run with the following conditions: cracked microalgae at 250 rpm for 5 minutes, algae mass-to-solvent loading of 1:10 (g/ml), experimental temperature of 50 °C, and processing time of 10 minutes at temperature.

First, Algae was weighed using a differential approach, in order to most accurately determine the mass of algae being used in the extraction experiments. This was performed by taring a weigh boat on a balance with a resolution of at least 0.1 mg. Then, approximately 1 gram dried microalgae was placed in the weigh boat, and the mass was recorded. The weighed algae was then transferred to a clean, dry 45 ml quartz microwave vessel (compatible with the Q20 Quartz rotor). The empty weigh boat was placed back on the scale and the mass was recorded. The total algae added was calculated by subtracting the empty weigh boat mass from the full weigh boat mass.

Second, approximately 10 ml of the solvent being used in experimentation was measured using a 25 ml graduated cylinder. It was important to have complete wetting of the algae biomass, so the solvent was added as small 2-3 ml aliquots with the sample tube being vortexed between additions, until all solvent was added. The sample vessel was then placed in an unheated

ultrasonic bath for approximately 30 seconds to ensure there were no clumps or large pieces of algae biomass remaining in suspension.

Third, the sample vessel was then placed into its housing and the cap securely tightened, using the manufacturer supplied closure tool. All microwave sample vessels being used were then fitted into the Q20 rotor assembly and the round containing ring placed on top of the sample vessels. It is important to note that multiple samples can be run at one time but must be evenly spaced around the sample rotor and all samples must use the same solvent. This is to avoid improperly measured temperatures within the instrument and provide more balanced rotation of the rotor.

The microwave being used for these experiments was a Start Synth by Milestone with installed Q20 quartz rotor and Terminal 640 controller (Milestone, Sorisole, Italy). The microwave allows for multiple heating and cooling cycles to be programmed into the sample heating profile. For this experimental procedure, a simple 3-part heating profile was used as follows: (1) 5 minutes warm up, (2) 10 minutes isothermal, and (3) 5 minutes cool down. For safety purposes, it is important to avoid standing in front of the microwave while it is running. In the event of a vessel rupture or overheat, the potential for an explosion is increased. To help avoid accidents within the microwave, carefully monitor the heat being supplied to the sample (W) and the sample temperature. If the sample is not increasing in temperature, but the microwave is calling for full power for an extended period of time (30 seconds or more), the infrared thermometer is likely not reading correctly and the run should be terminated.

After the microwave finished its cool down cycle, the sample vessels are removed from the microwave and placed in a fume hood to cool further to room temperature. Once cool, the vessels are slowly opened using the manufacturer supplied closure tool. The sample vessels

should be opened inside of a fume hood with the door mostly closed, in case pressure has built-up while being processed and could depressurize forcefully and unexpectedly.

Once the vessels were opened, the contents were poured into a folded, pre-weighed 12.5 cm double rings 102 filter paper inside of a funnel on a ring stand. The sample was allowed to gravity filter into a pre-weighed 20 ml vial. The microwave vessel and the solid residues collected in the filter paper were rinsed with an additional 10 ml of solvent total, which was collected with the filtrate. Both the solid residues and filtrate were allowed to completely dry inside of a fume hood, before recording their weights. It was then possible to determine how much mass was extracted from the microalgae.

Appendix 2.2 Sonication Assisted Extraction

Sonication assisted solvent extraction was performed to determine the impact of sonication cell rupture on solvent extraction efficiency. A Fisher Scientific 5.7-liter MH Series Ultrasonic Bath (Fisher Scientific, Denver, USA) with non-programmable heating was used for this experimentation. Unless different conditions were specifically being investigated, the sonication assisted extraction experiments were run with the following conditions: cracked microalgae at 250 rpm for 5 minutes, algae mass-to-solvent loading of 1:10 (g/ml), experimental temperature of 50 °C, and processing time of 10 minutes at temperature.

Algae was weighed using a differential approach, in order to most accurately determine the mass of algae being used in the extraction experiments. This was performed by taring a weigh boat on a scale with a resolution of at least 0.1 mg. Then, approximately 1 gram dried microalgae was placed in the weigh boat, and the mass was recorded. The weighed algae was then transferred to a clean, dry 23 ml borosilicate glass test tube. The empty weigh boat was placed back on the scale and the mass was recorded. The total algae added was calculated by subtracting the empty weigh boat mass from the full weigh boat mass.

Next, approximately 10 ml of the solvent being used in experimentation was measured using a 25 ml graduated cylinder. It was important to have complete wetting of the algae biomass, so the solvent was added as small 2-3 ml aliquots until all solvent was added, with the sample tube being vortexed between additions. The test tubes were then capped tightly with aluminum foil and placed into a glass beaker. The beaker was filled with water from the pre-heated ultrasonic bath reservoir and placed into the ultrasonic bath. Lastly, a small, sealed bag of ice was placed on top of the test tubes to reduce pressure build-up and solvent loss in the sample tubes. The

sonication was turned on and the extraction was allowed to run for 10 minutes, before the sonication was turned off and the test tubes were removed.

Once the samples had cooled, the contents were poured into a folded, pre-weighed 12.5 cm double rings 102 filter paper inside of a funnel on a ring stand. The sample was allowed to gravity filter into a pre-weighed 20 ml vial. The borosilicate test tube and the solid residues collected in the filter paper were rinsed with an additional 10 ml of solvent total, which was collected with the filtrate. Both the solid residues and filtrate were allowed to completely dry inside of a fume hood, before recording their weights. It was then possible to determine how much mass was extracted from the microalgae.

Appendix 2.3 TCA Analysis

TCA is used to evaluate the total carbon pyrolyzed from a sample as it is exposed to a series of increasingly aggressive temperature steps.[71] The temperature fraction at which carbon is evolved gives an indication of the complexity/stability of the original sample and its constituents. The TCA analysis was performed using a thermal optical analyzer from Sunset Laboratory Inc. (Portland, OR).

Samples were prepared by dissolving the dried filtrate residues in methanol at a concentration of 25 mg of dried filtrate residue per milliliter of solvent. The solution was then vortexed or sonicated to fully dissolve and suspend the sample. Using a syringe, 10 µL of solubilized sample was placed on a 2500QAT-UP tissue quartz filter pad (Pall Corp. East Hills, NY). The sample filter was placed on a 40°C hotplate for 4 minutes to dry the methanol solvent.

The sample filter pad is placed into the TCA oven and the analysis method "hb_lignin ramp_amb_long_890_170418.par" is selected. This method uses the following steps for analysis: 200°C, 300°C, 400°C, 500°C, 890°C, and char (oxidation). Sample data is automatically saved by the instrument.

The sample data provided by the instrument is in the form of raw FID response signals and is provided as a .TXT text document. An example of this raw data can be seen in figure A2.3-1. The data is processed using an excel spreadsheet provided by the Chemistry department at UND. This spreadsheet converts the FID signal to peak areas for each of the temperature fractions. It then calculates the Carbon content related to each of the FID temperature fraction peaks using internal calibrations. The carbon data is then adjusted to reflect any offset seen by the external sucrose calibration.

	Sample															
	if-08-06-IF423-01-methanolit_dilute															
	Analysis Parameter File Name															
	hb_lignin ramp_amb_long_890_170418.par With Temp Offsets															
	Started:															
	11/21/2019															
	3:27:02 PM															
	ended:															
	11/21/2019															
	4:19:59 PM															
	Atm Pres	mm Hg														
	728.9															
	Analyst															
	Ian															
	Instrument Name															
	Univ. of ND #181-6															
	CalConst															
	19.26108															
	FilterArea															
	1															
	TransitTime															
	8															
	SBasic Version															
	610															
	VBasic Version															
	OCEC828NoPurge_2+2															
	3025															
Row	FID1	FID2	ole_temper	laser	laserlow	essure ps	mode	PD2	PD2Lo	iredTemp	SmpOffse	TimeStamp	lethanatorTem	FrnOvn TC	mputed Offs	
1	2889	122	32.05047	390	39	0.33359	He	4002	38	1	-4	-13779	499.6926	36.05047	-4	
2	2893	122	32.05047	393	34	0.37343	He	4000	41	1	-4	-13907	499.7807	36.05047	-4	
3	2889	122	31.86172	397	33	0.37802	He	4003	38	1	-4	-14035	499.7514	35.86172	-4	
4	2895	125	32.05047	397	30	0.3807	He	4004	40	1	-4	-14163	499.6926	36.05047	-4	
5	2958	139	31.86172	404	27	0.38223	He	4002	41	1	-4	-14291	499.9863	35.86172	-4	
6	3121	178	31.86172	412	25	0.38492	He	4004	41	1	-4	-14419	499.9276	35.86172	-4	
7	3280	219	31.86172	412	26	0.39028	He	3999	44	1	-4	-14547	499.9569	35.86172	-4	
8	3346	232	31.9561	410	30	0.39181	He	4000	43	1	-4	-14675	500.1331	35.9561	-4	
9	3338	231	31.98755	411	30	0.39411	He	3997	44	1	-4	-14803	500.045	35.98755	-4	
10	3293	220	31.83026	404	33	0.39411	He	3995	43	1	-4	-14931	500.1038	35.83026	-4	
11	3243	208	31.9561	395	40	0.39296	He	4000	41	1	-4	-15059	500.1331	35.9561	-4	
12	3200	197	31.92464	396	37	0.39296	He	3998	41	1	-4	-15187	500.1331	35.92464	-4	
13	3168	190	32.01901	394	38	0.39258	He	4002	39	1	-4	-15315	500.1038	36.01901	-4	
14	3136	182	31.9561	392	35	0.39258	He	4003	39	1	-4	-15443	500.045	35.9561	-4	
15	3108	174	32.14484	400	30	0.39219	He	4004	39	1	-4	-15571	500.1919	36.14484	-4	
16	3087	172	32.01901	392	34	0.39181	He	4000	42	1	-4	-15699	500.1038	36.01901	-4	
17	3063	164	31.76735	408	25	0.39066	He	4003	41	1	-4	-15827	500.1038	35.76735	-4	
18	3047	161	31.92464	406	27	0.39181	He	4004	41	1	-4	-15955	500.045	35.92464	-4	
19	3030	155	31.86172	408	28	0.39066	He	4004	42	1	-4	-16083	500.0744	35.86172	-4	
20	3016	154	31.98755	413	29	0.38989	He	3998	44	1	-4	-16211	500.0744	35.98755	-4	
21	3006	149	31.86172	409	32	0.38913	He	3998	43	1	-4	-16339	500.0157	35.86172	-4	
22	2995	147	31.89318	405	34	0.38913	He	3995	43	1	-4	-16467	499.8395	35.89318	-4	
23	2987	144	31.89318	400	37	0.38989	He	3998	42	1	-4	-16595	499.9863	35.89318	-4	
24	2980	144	31.86172	399	37	0.38875	He	3997	41	1	-4	-16723	499.9863	35.86172	-4	
25	2972	141	31.86172	392	38	0.38875	He	3999	41	1	-4	-16851	499.9276	35.86172	-4	
26	2965	142	31.9561	392	40	0.38836	He	4000	39	1	-4	-16979	499.9863	35.9561	-4	
27	2962	141	31.86172	395	35	0.38836	He	4003	38	1	-4	-17107	499.8688	35.86172	-4	
28	2954	138	32.01901	397	32	0.38913	He	4003	40	1	-4	-17235	499.9276	36.01901	-4	
29	2952	137	31.92464	394	34	0.38798	He	4005	38	1	-4	-17363	499.9569	35.92464	-4	
30	2948	135	31.98755	408	25	0.38836	He	4005	40	1	-4	-17491	499.8101	35.98755	-4	
…	…	…	…	…	…	…	…	…	…	…	…	…	…	…	…	
3020	2907	130	143.9909	-6	36	0.35734	CH4+Ox	42	34	1	-22	-6995	499.4283	165.9909	-22	
3021	2906	132	141.6745	-4	37	0.35772	CH4+Ox	40	35	1	-22	-7123	499.3402	163.6745	-22	
3022	2907	132	139.418	-1	34	0.35734	CH4+Ox	42	35	1	-22	-7251	499.6045	161.418	-22	
3023	2906	129	137.1909	3	32	0.35849	CH4+Ox	40	35	1	-22	-7379	499.4283	159.1909	-22	
3024	2905	132	135.1764	5	29	0.35811	CH4+Ox	39	37	1	-22	-7507	499.7514	157.1764	-22	
3025	2906	129	133.0389	4	31	0.35772	CH4+Ox	40	35	1	-22	-7635	499.7807	155.0389	-22	

Figure A2.3- 1: Example of TCA instrument raw data output.

When running a sample on TCA, first two blank runs are completed to clean the filter pad. Then a Sucrose calibration, containing 40.19 µg of carbon, is run as an external calibration. The next run is a solvent blank, to determine a baseline for the solvent used to dissolve the analytical samples. These are followed by the experimental samples, with the sucrose blank completed every 10 sample runs and the blank runs completed once a day. An example of this analytical sample order can be seen in table A2.3-1.

Table A2.3- 1: Example run order for TCA analysis.

Sample Name	Description	Method
IF-08-01	Blank	polymer-calibration.par With Temp Offsets
IF-08-02	Blank	polymer-calibration.par With Temp Offsets
IF-08-03	Sucrose Calibration	polymer-calibration.par With Temp Offsets
IF-08-04	Solvent Blank (Methanol)	hb_lignin ramp_amb_long_890_170418.par With Temp Offsets
IF-08-05	IF423-01	hb_lignin ramp_amb_long_890_170418.par With Temp Offsets
IF-08-06	IF423-02	hb_lignin ramp_amb_long_890_170418.par With Temp Offsets
IF-08-07	IF423-03	hb_lignin ramp_amb_long_890_170418.par With Temp Offsets
IF-08-08	IF423-04	hb_lignin ramp_amb_long_890_170418.par With Temp Offsets
IF-08-09	IF423-05	hb_lignin ramp_amb_long_890_170418.par With Temp Offsets
IF-08-10	IF423-06	hb_lignin ramp_amb_long_890_170418.par With Temp Offsets
IF-08-11	IF423-01	hb_lignin ramp_amb_long_890_170418.par With Temp Offsets
IF-08-12	IF423-02	hb_lignin ramp_amb_long_890_170418.par With Temp Offsets
IF-08-13	IF423-03	hb_lignin ramp_amb_long_890_170418.par With Temp Offsets
IF-08-14	IF423-04	hb_lignin ramp_amb_long_890_170418.par With Temp Offsets
IF-08-15	Sucrose Calibration	polymer-calibration.par With Temp Offsets
IF-08-16	IF423-05	hb_lignin ramp_amb_long_890_170418.par With Temp Offsets
IF-08-17	IF423-06	hb_lignin ramp_amb_long_890_170418.par With Temp Offsets

APPENDIX 3: Decomposition of Forage Sorghum Sourced Carbohydrates and Lignin

Appendix 3.1 Production of Organic Acids from Sorghum Carbohydrates

Appendix 3.1.1 Catalyst Doping

This catalyst doping method is based on a method used by Clancy Kadrmas in his dissertation.[73] Beta Zeolite is doped using a simple impregnation method. This is done by removing the alumina in the beta-zeolite structure using 1M HCl and then replacing the alumina with a tin metal dopant.[88] Two different SiO2/Al2O3 scaffolds were used in this research, 300 and 25. Primarily, the SiO2/Al2O3 of 300 was used in experimentation.

First, catalyst was calcined at 600°C for 8 hours and allowed to cool, this is done to remove any water and to activate the zeolite.[87] The calcined catalyst was then added to a doping solution. The concentration of this doping solution would not change depending on what dopant was desired. For the tin (II) dopant, 10 g of calcined catalyst was added to 100 ml of 1M HCl and 1 gram of tin (II) chloride. If tin (IV) chloride was being used, 10 g catalyst was mixed with 100ml 1M HCl and 1 grams of tin (IV) chloride. The beaker from the doping solution is then placed into an ultrasonic bath and allowed to sonicate overnight (12 hours). These methods were followed regardless of the Sio2/Al2O3 of the initial beta zeolite.

It is important to note how to handle the tin (IV) chloride used for doping. This is a fuming liquid and must be handled in a fume hood. The tin (IV) chloride to be added to the doping solution is measured by volume using a disposable syringe and needle. It is recommended the fume hood sash be lowered to act as a barrier when piercing the septum on the tin (IV) bottle. Also, the

disposable syringe should be left in the fume hood, until it has stopped off-gassing and can be disposed of properly.

Once the sonication was complete, the catalyst and doping solution was placed into centrifuge bottles. An International Equipment Company centrifuge (HN-SII) was used to spin down the catalyst for 20 minutes at 3000 rpm (1500xg). The liquids were decanted, and catalyst cake transferred to a crucible. The catalysts was then calcined again at 400°C for 8 hours. After cooling, the catalyst was crushed in a mortar and pestle and stored in a glass jar.

Appendix 3.1.2 Acid Hydrolysis

This acid pretreatment procedure was based on previous work at the University of North Dakota performed by Kamireddy.[28] The acid pretreatment was performed to decompose hemi-cellulose into individual xylan monomers and ensure cellulose was more readily available for the enzymatic hydrolysis step. This acid pretreatment step primarily recovers xylose and some glucose. The acid pretreatment was performed in a 5 liter Parr Series 4580 High Temperature Reactor (Serial number #4580-0908-12536) purchased from Parr Instrument company (Moline, IL, USA). A generalized schematic of the reactor system can be seen in figure 4.2.2.3-1.

It was necessary to first clean the reactor vessel, impeller, cooling coil, and reactor head. This was done by scrubbing all of the pieces thoroughly with soapy water, then rinsing with ultrapure water. The gasket contained within the mounted reactor head must be wiped clean to remove any residual vacuum grease or reactor debris. Once clean, the graphite gasket was visually inspected for any apparent signs of damage and replaced if necessary. Finally, the sealing surface on the reactor vessel was cleaned and polished using a fine emery paper, to ensure a secure seal once closed.

The reaction conditions for the acid pretreatment require a solids loading of 10 wt%. The reactor vessel is 5 liters but should not be filled more than 2/3 full. Specific calculations are supplied by the manufacturer to determine maximum operating volume, given temperature and reaction materials. For these reactions, a liquid volume of 2 liters was chosen. For each acid pretreatment, 200 grams of forage sorghum biomass was weighed and placed into the reactor vessel. Then, approximately 2000 grams of 1 wt% sulfuric acid was mixed (1980 g water and 20 g H2SO4) and added to the reactor vessel. The reactor contents were mixed thoroughly with a stir rod, to

ensure all of the biomass was wetted. Lastly, the top portion of the reactor vessel was wiped clean, to remove any powder which may have come from the forage sorghum biomass.

To close the reactor vessel and prepare it for operation, first a thin layer of vacuum grease was spread on the reactor vessel sealing surface. This was done to protect and extend the lifespan of the graphite gasket in the reactor head. Next, the reactor vessel was aligned under the reactor head, while situated on the pneumatic lift platform. Using the pneumatic lift lever on the side of the reactor stand housing, the reactor vessel was slowly raised to fit in the reactor head. With the pneumatic lift pressing the reactor vessel into the vessel head, the two halves of the sealing clamp were slid into place and fastened. The bolts on the sealing clamp were sealed using a 16-bolt flange pattern. A torque wrench was used and the sealing force was increased by 5 pound increments, until a force of 35 pounds was achieved. Once sealed, the pneumatic lift platform was lowered and moved out from under the reactor vessel. The heater surround was then positioned under the reactor vessel and raised using the pull knob on the heater support shaft.

Next, the reactor vessel was purged with compressed nitrogen using the gas inlet and vent valves on the reactor head. The vessel was filled and purged five times, to ensure no residual oxygen remained. A pressure check was performed by filling the reactor vessel to 200 psig and allowing it to stand for 5 minutes. The pressure check passed if the pressure remained stable and did not appear to be leaking. The pressure was then vented, because the reaction conditions do not require pressure be added. The PID controller was then given a temperature setpoint of 150°C with the heater power control turned to level II and the impeller set to 60 rpm. The temperature was monitored and a 20 minute timer set once the operating temperature reached the set point. After the processing time was finished, the PID temperature set point was changed to 20°C, the heater controller turned off, and the heater surround lowered to increase the rate of cooling.

Once the reactor vessel had cooled to room temperature, it could be opened. First, any pressure developed during the run was vented and the impeller turned off. Then the pneumatic lift platform was positioned under the reactor vessel and raised to firmly press up on the reactor vessel. Next, the torque wrench was used to slowly loosen the sealing clamp bolts, using a 16-bolt flange pattern. The locking clips on the sealing clamp were then opened and the clamp slid completely clear of the reactor vessel. The vessel was then slowly lowered until the pneumatic lift platform was in its lowest position. The impeller and cooling coil were cleaned of any residual biomass which was collected in the reactor vessel. The reactor vessel was then swung out from under the reactor head, using the pneumatic lift platform. The stainless-steel transfer handles were attached to the reactor vessel and the vessel was moved to the lab bench counter for filtering and cleaning, being careful to employ proper lifting techniques to avoid injury while moving the very heavy reactor vessel.

Reactor products were transferred from the reactor vessel to a 2L beaker, for ease of handling. The solids and liquids were separated using a vacuum filter apparatus. This used a buchner funnel fitted with a coffee filter. Once filtered, the solids were set aside to dry. The liquid filtrate was collected and neutralized using calcium carbonate until a pH of 5.5 to 6 was achieved. The neutralized xylose rich reactor product was stored in glass jars in the refrigerator for future use in Sn-Beta decomposition reactions.

Appendix 3.1.3 Enzymatic Hydrolysis

The enzymatic pretreatment was performed to break the cellulose portion of the biomass into its monomeric glucose units. This was performed using a celluslase enzyme. The enzymatic hydrolysis was based on previous work at the University of North Dakota performed by Kamireddy.[28] This process started by making a slurry with solids loading of 10 wt% using washed and dried cellulose rich acid pretreatment solids and ultrapure water. The pH of the slurry was buffered to 5 by adding sodium citrate. The cellulase enzymes were added with a loading of 1wt% enzyme to dry cellulose. The samples were incubated in a MAXQ 4000 shaker table (Fisher Scientific, Waltham, MA, USA) for 72 hours at a temperature of 48°C and an agitation of 250 RPM. After the incubation period, the glucose rich hydrolysate was filtered and stored for future use with Sn-Beta catalytic decomposition. The lignin rich biomass solid residue was dried and saved for further decomposition, as detailed in section 4.3 of this document.

Appendix 3.1.4 Catalytic Decomposition Reactor Operation

This catalytic decomposition procedure was based on previous work at the University of North Dakota performed by Kadrmas.[73] The Catalytic Decomposition reactions were performed in a 500 mililiter bench top Parr Series 4575 High Temperature Reactor (Serial number #4570-0803-6955) purchased from Parr Instrument company (Moline, IL, USA). A generalized schematic of the reactor system can be seen in figure 4.2.2.3-1.

It was necessary to first clean the reactor vessel, impeller, cooling coil, and reactor head. This was done by scrubbing all of the pieces thoroughly with soapy water, then rinsing with ultrapure water. The gasket contained within the mounted reactor head must be wiped clean to remove any residual vacuum grease or reactor debris. Once clean, the graphite gasket was visually inspected for any apparent signs of damage and replaced if necessary. Finally, the sealing surface on the reactor vessel was cleaned and polished using a fine emery paper, to ensure a secure seal once closed.

The preparation of the reactor feedstock varies depending on the carbohydrate being decomposed. For the case of model carbohydrate decompositions, 5 grams of carbohydrates are dissolved into 300 ml of ultra-pure water. For biomass sourced carbohydrates, neutralized acid pretreatment solution and enzymatic pretreatment solutions, as prepared in appendices 3.1.2 and 3.1.3 respectively, are mixed with ultra-pure water for a final volume of 300 ml and 5 grams of carbohydrates. When mixing the pretreatment liquids, it is important to maintain the glucose to xylose ratios. This is done by calculating the total carbohydrates extracted from the initial biomass and using this to determine the overall glucose to xylose ratio of recovered carbohydrates. Next, 10 grams of doped Sn-Beta catalyst, as prepared in Appendix 3.1.1, was added to the carbohydrate solution. It is important this addition be performed in a fume hood, as

the catalyst is dusty. The reactor feed was then placed into an ultrasonic bath for 5 minutes, to break up any catalyst clumps which may be present. The pH of the feed was measured and recorded before the reactor feed was added to the reactor vessel.

To close the reactor vessel and prepare it for operation, first a thin layer of vacuum grease was spread on the reactor vessel sealing surface. This was done to protect and extend the lifespan of the graphite gasket in the reactor head. Next, the reactor vessel was aligned under the reactor head, while situated on the manual lift platform. Using the reactor lift pull knob on the side of the reactor stand, the reactor vessel was slowly raised until the pull knob locked into place. To fit the reactor into the head, the reactor adjustment knob was twisted until the reactor was in its highest position. The two halves of the sealing clamp were then slid into place and fastened. The bolts on the sealing clamp were sealed using an 8-bolt flange pattern. A torque wrench was used and the sealing force was increased by 5 pounds increments, until a force of 35 pounds was achieved. Once sealed, the reactor lift platform was lowered and moved out from under the reactor vessel. The heater surround was then positioned under the reactor vessel and raised using the pull knob on the heater support shaft.

Next, the reactor vessel was purged with compressed nitrogen using the gas inlet and vent valves on the reactor head. The vessel was filled and purged five times, to ensure no residual oxygen remained. A pressure check was performed by filling the reactor vessel to 300 psig and allowing it to stand for 5 minutes. The pressure check passed if the pressure remained stable and did not appear to be leaking. The PID controller was then given a temperature setpoint of 200 °C with the heater power control turned to level I and the impeller set to 400 rpm. The temperature was monitored and a 20 hour timer set once the operating temperature reached the set point. After the

processing time was finished, the cooling water bypass valve was turned on, the heater controller turned off, and the heater surround lowered to increase the rate of cooling.

Once the reactor vessel had cooled to room temperature, it could be opened. First, any pressure developed during the run was vented and the impeller turned off. Then the manual lift platform was positioned under the reactor vessel and raised to firmly press up on the reactor vessel. Next, the torque wrench was used to slowly loosen the sealing clamp bolts, using an 8-bolt flange pattern. The locking clips on the sealing clamp were then opened and the clamp slid completely clear of the reactor vessel. The vessel was then slowly lowered until the manual lift platform was in its lowest position. The impeller and cooling coil were cleaned of any residual reactor products, which was collected in the reactor vessel.

Reactor products were transferred from the reactor vessel to a 400 ml beaker, for ease of handling. A 5 ml aliquot of the reactor products was collected and filtered through a 0.2 µm syringe filter for analysis. The remaining solids and liquids were separated using a vacuum filter apparatus. This used a buchner funnel fitted with an 11 µm filter paper. Once filtered, the solids were set aside to dry. The liquid filtrate was collected and the pH measured.

Appendix 3.1.5 HPLC Analysis

HPLC analysis was performed on an Agilent 1200 series system (Agilent Technoligies Inc, Santa Clara, CA, USA). The Agilent 1200 series consisted of five modular pieces: vacuum degasser, Isocratic pump, temperature controlled autosampler/injector, column oven, and Refractive Index detector. Separation was performed on an Agilent Hi-Plex H column (Agilent Technoligies Inc, Santa Clara, CA, USA) with a mobile phase of 5 mM H_2SO_4, flowrate of 0.6 ml/min, temperature of 40 °C and stop time of 45 minutes.

Sample analysis began with conditioning of the HPLC system. This is performed by installing the HPLC column, setting the mobile phase flow rate to 0.1 ml/min, and turning on the column heater to operating conditions. This conditioning step is necessary to completely flush the column of its storage solution and avoid unwanted dilution/mixing of the mobile phase. The conditioning should be performed until 10-20 column volumes of mobile phase has been passed through the system. This is often performed overnight and can be left in this state for several days.

Samples for analysis must be diluted and filtered before use on the HPLC system. This was done by mixing 500 µL of sample solution with 500 µL of mobile phase in a 2 ml autosampler vial. Samples are always diluted in the mobile phase, because the change in pH may cause some solid precipitation from the samples. Ensuring this potential precipitation occurs before the sample is filtered and not during injection to the separation column is essential to column life and performance. Once dilute, the samples were drawn into a 1 ml luer lock syringe and passed through a 0.2 µm hydrophilic PTFE syringe filter into a new 2ml autosampler vial. The vial was capped and labeled. All samples were stored in the fridge or the cooled autosampler tray (4 °C) until analyzed.

Analytical standards were created for all analytes of interest in the samples, specifically glucose, xylose, acetic acid, formic acid, glycolic acid, levulinic acid, and lactic acid. First a standard stock solution with concentration of approximately 10 mg/ml was created for each of the individual analytes, using the mobile phase as a solvent. Next 100 µL of each analyte stock solution and enough mobile phase to give a final volume of 1 ml were added to a 2ml autosampler vial. This mixture was syringe filtered into a new 2 ml autosampler vial. This is calibration standard A. Subsequent calibration standards are created by performing a 50% dilution with the calibration standard which comes before the target calibration standard. For example, calibration standard D is made by mixing 500 µL of calibration standard C and 500 µL of mobile phase. At least 5 calibration standards are recommended, but more can be created, if desired. It is recommended that the sample being analyzed has a concentration near the middle of the calibration range.

When performing analysis, the approximate residence time of each analyte through the column at analytical conditions is required. This can be determined experimentally by analyzing standards of individual analytes. It is recommended to verify the analyte retention times if the analytical conditions are modified. For the analysis described in this appendix, the analyte retention times can be found in table A3.1.5-1.

Table A3.1.5- 1: List of analytes and retention times for Agilent Hi-Plex H column with 5 mM H2SO4 mobile phase at 0.6 ml/min and 40C.

Retention Time (min)	Analyte
11.57	Glucose
12.27	Xylose
15.17	Glycolic Acid
15.74	Lactic Acid
16.78	Formic Acid
18.71	Acetic Acid
21.47	Levulinic Acid

When running analysis on HPLC, a programmed needle wash is recommended. For this program before injecting any sample, the autosampler first draws a maximum volume of water into the sample loop and the water is then ejected into a waste vial. Next, the autosampler draws a maximum amount of mobile phase into the sample loop and then ejects it into a waste vial. This autosampler program ensures cross contamination between samples is minimized by rinsing both the sample loop and the surface of the injector needle between samples.

When programming the samples into the autosampler, the following method is recommended. First, two or more blank runs of pure mobile phase are completed. This provides insight into the baseline and stability of the column and detector. Next, the calibration standards are run from least to most concentrated. This helps to ensure the detector is not overloaded with analyte before trying to analyze the calibration standards which require the highest sensitivity from the detector. The calibration standards are followed by another blank. Next, the samples can be run in the program. Up to 10 samples can be analyzed in a row, before rerunning a calibration point near

the center of the calibration range and an additional blank. This is done to verify the column performance and baseline has not shifted due to contaminants or deactivation. An example of this sample order can be seen in Table A3.1.5-2.

Table A3.1.5-2: Example of HPLC Sample Order

Vial Number	Sample Name	Method Name	Sample Amount (uL)	Injection Volume (uL)
1	01_Blank	IF_40C_0.6ml_45min	1000	15
1	02_Blank	IF_40C_0.6ml_45min	1000	15
2	03_IF167-02_Cal A	IF_40C_0.6ml_45min	1000	15
3	04_IF167-03_Cal B	IF_40C_0.6ml_45min	1000	15
4	05_IF167-04_Cal C	IF_40C_0.6ml_45min	1000	15
5	06_IF167-05_Cal D	IF_40C_0.6ml_45min	1000	15
6	07_IF167-06_Cal E	IF_40C_0.6ml_45min	1000	15
1	08_Blank	IF_40C_0.6ml_45min	1000	15
7	09_IF469-01	IF_40C_0.6ml_45min	1000	15
8	10_IF469-02	IF_40C_0.6ml_45min	1000	15
9	11_IF469-03	IF_40C_0.6ml_45min	1000	15
10	12_IF469-04	IF_40C_0.6ml_45min	1000	15
11	13_IF469-05	IF_40C_0.6ml_45min	1000	15
12	14_IF469-06	IF_40C_0.6ml_45min	1000	15
13	15_IF469-07	IF_40C_0.6ml_45min	1000	15
14	16_IF469-08	IF_40C_0.6ml_45min	1000	15
15	17_IF469-09	IF_40C_0.6ml_45min	1000	15
16	18_IF469-10	IF_40C_0.6ml_45min	1000	15
1	19_Blank	IF_40C_0.6ml_45min	1000	15
4	20_IF167-04_Cal C	IF_40C_0.6ml_45min	1000	15
17	21_IF469-11	IF_40C_0.6ml_45min	1000	15
18	22_IF469-12	IF_40C_0.6ml_45min	1000	15
19	23_IF469-13	IF_40C_0.6ml_45min	1000	15
20	24_IF469-14	IF_40C_0.6ml_45min	1000	15
21	25_IF469-15	IF_40C_0.6ml_45min	1000	15
1	26_Blank	IF_40C_0.6ml_45min	1000	15
1	27_Blank	IF_40C_0.6ml_45min	1000	15

Data collected from the HPLC was manually processed in Microsoft Excel. This required that each sample was opened in ChemStation and the area of each analyte peak recorded.

Correlations between standard calibrations and peaks areas were determined and used to calculate sample concentrations. These sample concentrations were then converted into a carbon percentage of initial feed carbon.

Appendix 3.1.6 TCA Analysis

TCA is used to evaluate the total carbon pyrolyzed from a sample as it is exposed to a series of increasingly aggressive temperature steps.[71] The temperature fraction at which carbon is evolved gives an indication of the complexity/stability of the original sample and its constituents. The TCA analysis was performed using a thermal optical analyzer from Sunset Laboratory Inc. (Portland, OR, USA).

For each catalytic decomposition experiment, several different samples are required for data processing. These samples are the reactor feedstock, unfiltered reactor product, and filtered reactor product. These samples allow for the calculation of initial carbon that becomes part of the product phase and to determine if/how the carbon in the solid phase reactor product compares to the liquid phase reactor product.

When running a sample on TCA, first two blank runs are completed to clean the filter pad. Then a Sucrose calibration, containing 40.19 µg of carbon, is run as an external calibration. The next run is a solvent blank, to determine a baseline for the solvent used to dissolve the analytical samples. These are followed by the experimental samples, with the sucrose blank completed every 10 sample runs and the blank runs completed once a day. An example of this analytical sample order can be seen in table A2.3-1.

Samples from the catalytic decomposition reactor did not require any additional dilution or preparation before analysis on the TCA. Each sample was vortexed to fully suspend the solid phase. Using a syringe, 5 µL of sample was placed on a 2500QAT-UP tissue quartz filter pad (Pall Corp. East Hills, NY). The sample filter was placed on a 55°C hotplate for 7 minutes to dry the water solvent.

The sample filter pad is placed into the TCA oven and the analysis method “hb_lignin ramp_amb_long_890_170418.par” is selected. This method uses the following steps for analysis: 200°C, 300°C, 400°C, 500°C, 890°C, and char (oxidation). Sample data is automatically saved by the instrument.

The sample data provided by the instrument is in the form of raw FID response signal and is provided as a .TXT text document. An example of this raw data can be seen in figure A2.3-1. The data is processed using an excel spreadsheet provided by the Chemistry department at UND. This spreadsheet converts the FID signal to peak areas for each of the temperature fractions. It then calculates the Carbon content related to each of the FID temperature fraction peaks using internal calibrations. The carbon data is then adjusted to reflect any offset seen by the external sucrose calibration.

Appendix 3.2 Base Facilitated Decomposition of Forage Sorghum Lignin

Appendix 3.2.1 Production of Sorghum-derived Lignin

For experiments using forage sorghum sourced reactive lignin, the reactor feedstock was prepared using lignin rich residual solids from the enzymatic pretreatment seen in section 4.2.2.3 of this document. To make the reactor feedstock, first a slurry of lignin rich forage sorghum biomass and sodium hydroxide was created. The concentrations for this slurry were 4 wt% lignin and 2 wt% sodium hydroxide. In making this slurry, enough biomass was added to reach the desired lignin loading, given known lignin content in the forage sorghum biomass. The slurry was prepared in 2 L batches to ensure the reactor preheater could be filled to the maximum operating capacity.

To help solubilize the lignin out of the biomass, a heated alkaline soak was performed. This was accomplished by placing the prepared biomass slurry solution into a steam jacketed autoclave. The feedstock was processed at 121 °C for 20 minutes and allowed to cool to room temperature before continuing. Once cooled, it was necessary to remove any residual solids from the feedstock, to avoid fouling and plugging the control valves on the reactor.

Residual solid biomass was removed through a two-step process. First the larger solids were removed and rinsed using an International Equipment Company centrifuge (HN-SII). The heated alkaline slurry solution was placed into centrifuge bottles and spun down at 3000 RPM for 15 minutes. The supernatant was decanted and saved. The bottles were refilled, and the previous step repeated until all alkaline slurry solution was processed. The biomass centrifuge pellets were then rinsed by adding ultra-pure water, agitating the solution to completely suspend the pellet, and following the previous centrifuge/decanting steps to separate the supernatant. This rinse

supernatant was combined with the previous alkaline supernatant. The rinsing step was repeated with a total of 2 L of ultra-pure water.

Second, it was necessary to remove any smaller particles capable of remaining suspended in solution during the centrifuging process. This was performed using a pressure filtration apparatus consisting of a 1 L pressure vessel (316L-50DF8-1000, Swagelok, Solon, OH, USA) and a 90 micron sintered stainless steel in-line filter (SS-4F-90, Swagelok, Solon, OH, USA). A schematic of this apparatus can be seen in figure A3.2.1-1. The pressure filtering step was performed by first loading one liter of the pooled supernatant into the pressure vessel through the top connection of the vessel. Next, a nitrogen line was connected to the top connection of the vessel and pressure was added to the vessel by adjusting the regulator on the cylinder of compressed nitrogen. Filtering pressure was gradually increased from 0 psig to 200 psig to maintain a consistent flow of filtrate from the in-line filter. Once the filtrate had slowed considerably at a pressure of 200 psig, the sintered filter was considered dirty and required disassembly and cleaning. This process was repeated until all pooled supernatant was filtered. The filtrate leaving the in-line filter was collected. Lastly, the pH of the filtrate was measured and adjusted to a pH of 13 using sodium hydroxide, if necessary. This is the reactor feed for sorghum-derived lignin decomposition.

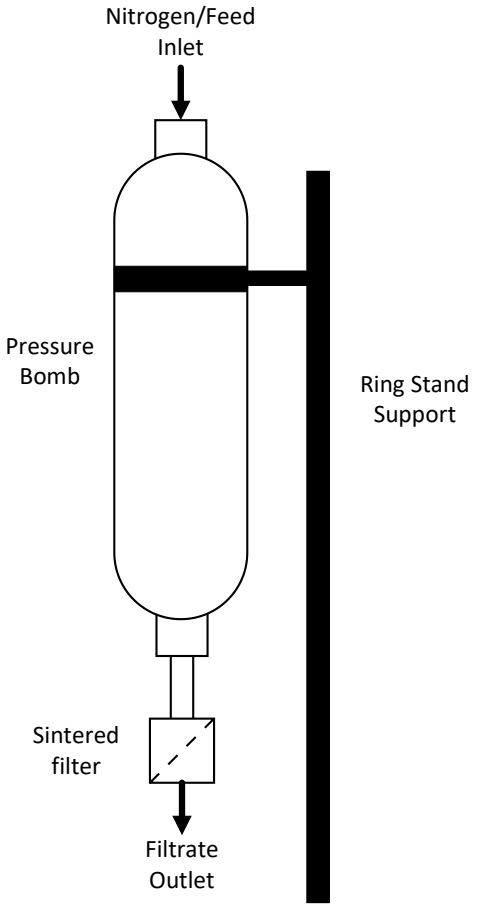

Figure A3.2.1- 1: Pressure filtering apparatus

Appendix 3.2.2 Continuous Lignin Decomposition Reactor Operation

The continuous reactor apparatus was originally designed and built for the dissertation work of Pourjafar.[90] A simplified schematic of this reaction system can be seen in figure 4.3.2.3-1. Before beginning lignin decomposition experiments, it is necessary to verify all pieces of the reactor system are connected properly and pass pressurized leak checks. The flow path of the reactor system utilizes the following order: The outlet fitting on the bottom of the modified Parr reactor was attached to a heat-traced transfer line containing on/off and metering manual control valves. The transfer line connected to the bottom inlet of the coiled reactor vessel. This reactor vessel was placed in a large ceramic heater clamshell. The reactor was made from 4 m of coiled 316 stainless steel with diameter of 0.95 cm and wall thickness of 0.16 cm. The reactor outlet was connected to a cooling heat exchanger, which consisted of coiled stainless steel tubing submerged in cooling tap water. The heat exchanger was connected to a particulate filter. Finally, the reactor flowrate and pressure was controlled with a backpressure regulator on the system outlet. Pressure was provided to the feed preheater through 3 compressed nitrogen gas cylinders connected in series.

The reactor system was prepared for lignin decomposition experiments by first filling the system with ultra-pure water. This was accomplished by filling the external plastic holding tank with ultra-pure water, opening the inlet valve into the Parr reactor head, and either sealing the holding tank and applying a small amount of pressure with nitrogen or raising the holding tank and allowing a gravity fed siphon to form. Once the preheater was filled, it was possible to either flush and clean or fill the system by using the open/close valve on the heated transfer line and the back pressure regulator to control flow or isolate the reactor. In order to operate the reaction system, all portions of the system after and including the heated transfer line were filled with

ultra-pure water and the preheater was emptied. The preheater was then filled with 3.8 L of lignin feedstock, in the same manner as described previously, and purged with nitrogen 5 times. Finally, a pressure check was performed by placing 200 psig of nitrogen on the preheater vessel and waiting 5 minutes.

The first step in operating the reactor system was turning on the labview data logging software. This software provides real-time reactor conditions and logs temperatures associated with the preheater outlet, the bottom, middle, and top of the reactor, and the cooling heat exchanger outlet. Next, the preheater temperature setpoint was set to 250 °C and the stir rate was set to 400 rpm. The time required to preheat the reactor feed was significantly longer than the time required to preheat the reactor system. Because of this, the preheater was allowed to reach a temperature of 175 °C before continuing.

Once the preheater reached 175 °C, the transfer line heat tracing was plugged in and the variable heat controller set to 80%. The PID controller for the ceramic reactor heater clamshell was plugged in and the setpoint chosen to match the desired experimental conditions. Lastly, the cooling water valve for the heat exchanger was opened. It was necessary to have cooling water flowing whenever the reactor heater was running. This prevented heat migration from the reactor to portions of the system which are not intended to be heated. It was necessary to monitor the pressure in the reactor during this preheating step. Given the reactor was isolated and filled with water, heating the reactor can cause large hydraulic pressures to develop. This was mitigated by occasionally draining some water from the reactor to maintain a pressure between 1000 psig and 2500 psig. Once the reactor and the preheater had reached their desired setpoints, the experiment could be started.

After preheating the reactor system, the system had to be brought to operating pressure to begin the experiment. Operation of the continuous flow decomposition reactor is dependent on pressure to reach operating conditions and provide a driving force for flow. This pressure was delivered by compressed nitrogen cylinders. Pressure was added to the system by setting the line side pressure on the nitrogen cylinder regulator to 200 psig more than the pressure inside of the feed preheater. The nitrogen inlet valve on the top of the feed preheater was then opened. This valve was left open for the duration of the experiment to ensure constant feed pressure throughout the experiment. The pressure on the nitrogen regulator was then adjusted to the desired operating pressure, given the desired operating temperature.

Next, the backpressure regulator was opened a minimal amount, to allow for flow out of the system. The control valves on the heated transfer line were then opened and the lignin solution allowed to flow from the preheater, through the reactor, and out of the pressure regulator. The flowrate was controlled by adjusting the backpressure regulator and measuring the grams per second outlet flowrate. The reactor was allowed to stabilize for 10 minutes after the reactor outlet temperature was reached and lignin was observed exiting the back pressure regulator, as evident from the effluent color change. If operating conditions were changed during the course of the experiment, the 10-minute stabilization was again allowed to occur before any sampling was performed.

Once the preheater was empty of lignin feed, the nitrogen inlet valve and the valves on the heated transfer line were closed. The back pressure regulator was opened to slowly vent pressure from the reactor. The preheater set point was set to room temperature, to flow water through the internal cooling coils of the Parr Reactor. The heating on the ceramic reactor heater and the transfer line heat tracing were disconnected from their power source. The entire system was left

overnight to cool to room temperature. Then, the residual pressure was vented from the preheater and the heat exchanger cooling water valve closed. Once the system was fully cooled and all pressure vented, it could be flushed with water to clean.

Cited References

1. Vohra, K.; Vodonos, A.; Schwartz, J.; Marais, E. A.; Sulprizio, M. P.; Mickley, L. J., Global mortality from outdoor fine particle pollution generated by fossil fuel combustion: Results from GEOS-Chem. *Environmental Research* **2021,** *195*, 110754.

2. *Global Warming of 1.5°C.An IPCC Special Report on the impacts of global warming of 1.5°C above pre-industrial levels andrelated global greenhouse gas emission pathways, in the context of strengthening the global response to the threat of climate change,sustainable development, and efforts to eradicate poverty*; IPCC: 2018.

3. Mohiddin, M. N. B.; Tan, Y. H.; Seow, Y. X.; Kansedo, J.; Mubarak, N. M.; Abdullah, M. O.; Chan, Y. S.; Khalid, M., Evaluation on feedstock, technologies, catalyst and reactor for sustainable biodiesel production: A review. *Journal of Industrial and Engineering Chemistry* **2021**.

4. Gebremariam, S. N.; Marchetti, J. M., Economics of biodiesel production: Review. *Energy Conversion and Management* **2018,** *168*, 74-84.

5. Linnen, M. Advanced Reactors and Novel Reactions for the Conversion of Triglyceride Based Oils into High Quality Renewable Transportation Fuels. University of North Dakota, 2014.

6. Baker, D.; Rials, T., Recent advances in low-cost carbon fiber manufacture from lignin. *Journal of Applied Polymer Science* **2013,** *130*.

7. Frank, E.; Hermanutz, F.; Buchmeiser, M., Carbon Fibers: Precursors, Manufacturing, and Properties. *Macromolecular Materials and Engineering* **2012,** *297*.

8. Ogale, A. A.; Zhang, M.; Jin, J., Recent advances in carbon fibers derived from biobased precursors. *Journal of Applied Polymer Science* **2016,** *133* (45).

9. Khayyam, H.; Jazar, R.; Nunna, S.; Golkarnarenji, G.; Badii, K.; Fakhrhoseini, S.; Kumar, S.; Naebe, M., PAN Precursor Fabrication, Applications and Thermal Stabilization Process in Carbon Fiber Production: Experimental and Mathematical Modelling. *Progress in Materials Science* **2019,** *107*, 100575.

10. Wang, S.; Bai, J.; Innocent, M. T.; Wang, Q.; Xiang, H.; Tang, J.; Zhu, M., Lignin-Based Carbon Fibers: Formation, Modification and Potential Applications. *Green Energy & Environment* **2021**.

11. Jacob, A.; Ashok, B.; Alagumalai, A.; Chyuan, O. H.; Le, P. T. K., Critical review on third generation micro algae biodiesel production and its feasibility as future bioenergy for IC engine applications. *Energy Conversion and Management* **2021,** *228*, 113655.

12. Felix, C.; Ubando, A.; Madrazo, C.; Gue, I. H.; Sutanto, S.; Tran-Nguyen, P. L.; Go, A. W.; Ju, Y.-H.; Culaba, A.; Chang, J.-S.; Chen, W.-H., Non-catalytic in-situ (trans) esterification of lipids in wet microalgae Chlorella vulgaris under subcritical conditions for the synthesis of fatty acid methyl esters. *Applied Energy* **2019,** *248*, 526-537.

13. Nagappan, S.; Devendran, S.; Tsai, P.-C.; Dinakaran, S.; Dahms, H.-U.; Ponnusamy, V. K., Passive cell disruption lipid extraction methods of microalgae for biofuel production – A review. *Fuel* **2019,** *252*, 699-709.

14. González-Balderas, R. M.; Velásquez-Orta, S. B.; Valdez-Vazquez, I.; Orta Ledesma, M. T., Intensified recovery of lipids, proteins, and carbohydrates from wastewater-grown microalgae Desmodesmus sp. by using ultrasound or ozone. *Ultrasonics Sonochemistry* **2020,** *62*, 104852.

15. Stirk, W. A.; Bálint, P.; Vambe, M.; Lovász, C.; Molnár, Z.; van Staden, J.; Ördög, V., Effect of cell disruption methods on the extraction of bioactive metabolites from microalgal biomass. *Journal of Biotechnology* **2020,** *307*, 35-43.

16. Kumari, N.; Singh, R. K., Biofuel and co-products from algae solvent extraction. *Journal of Environmental Management* **2019,** *247*, 196-204.

17. Griffiths, M. J.; Harrison, S. T. L., Lipid productivity as a key characteristic for choosing algal species for biodiesel production. *Journal of Applied Phycology* **2009,** *21* (5), 493-507.

18. Heo, Y. M.; Lee, H.; Lee, C.; Kang, J.; Ahn, J.-W.; Lee, Y. M.; Kang, K.-Y.; Choi, Y.-E.; Kim, J.-J., An integrative process for obtaining lipids and glucose from Chlorella vulgaris biomass with a single treatment of cell disruption. *Algal Research* **2017,** *27*, 286-294.

19. Hu, Q.; Sommerfeld, M.; Jarvis, E.; Ghirardi, M.; Posewitz, M.; Seibert, M.; Darzins, A., Microalgal triacylglycerols as feedstocks for biofuel production: perspectives and advances. *Plant Journal* **2008,** *54* (4), 621-639.

20. Hara, M.; Nakajima, K.; Kamata, K., Recent progress in the development of solid catalysts for biomass conversion into high value-added chemicals. *Science and technology of advanced materials* **2015,** *16* (3), 034903-034903.

21. Li, X.; Xu, R.; Yang, J.; Nie, S.; Liu, D.; Liu, Y.; Si, C., Production of 5-hydroxymethylfurfural and levulinic acid from lignocellulosic biomass and catalytic upgradation. *Industrial Crops and Products* **2019,** *130*, 184-197.

22. Ghimire, N.; Bakke, R.; Bergland, W. H., Liquefaction of lignocellulosic biomass for methane production: A review. *Bioresource Technology* **2021**, 125068.

23. Li, M.; Yan, G.; Bhalla, A.; Maldonado-Pereira, L.; Russell, P. R.; Ding, S.-Y.; Mullet, J. E.; Hodge, D. B., Physical fractionation of sweet sorghum and forage/energy sorghum for optimal processing in a biorefinery. *Industrial Crops and Products* **2018,** *124*, 607-616.

24. Kan, T.; Strezov, V.; Evans, T.; He, J.; Kumar, R.; Lu, Q., Catalytic pyrolysis of lignocellulosic biomass: A review of variations in process factors and system structure. *Renewable and Sustainable Energy Reviews* **2020,** *134*, 110305.

25. Deshavath, N. N.; Mohan, M.; Veeranki, V. D.; Goud, V. V.; Pinnamaneni, S. R.; Benarjee, T., Dilute acid pretreatment of sorghum biomass to maximize the hemicellulose hydrolysis with minimized levels of fermentative inhibitors for bioethanol production. *3 Biotech* **2017,** *7* (2), 139-139.

26. Kamireddy, S.; Degenstein, J.; Berti, M.; Ji, Y., Pretreatment and Enzymatic Hydrolysis of Kenaf Biomass as a Potential Source for Lignocellulosic Biofuel and Green Chemicals. *Current Organic Chemistry* **2013,** *17*, 1624-1632.

27. Kang, S.; Fu, J.; Zhang, G., From lignocellulosic biomass to levulinic acid: A review on acid-catalyzed hydrolysis. *Renewable and Sustainable Energy Reviews* **2018,** *94*, 340-362.

28. Kamireddy, S. R.; Li, J.; Abbina, S.; Berti, M.; Tucker, M.; Ji, Y., Converting forage sorghum and sunn hemp into biofuels through dilute acid pretreatment. *Industrial Crops and Products* **2013,** *49*, 598-609.

29. Davila-Gomez, F. J.; Chuck-Hernandez, C.; Perez-Carrillo, E.; Rooney, W. L.; Serna-Saldivar, S. O., Evaluation of bioethanol production from five different varieties of sweet and forage sorghums (Sorghum bicolor (L) Moench). *Industrial Crops and Products* **2011,** *33* (3), 611-616.

30. Toledano, A.; Serrano, L.; Garcia, A.; Mondragon, I.; Labidi, J., Comparative study of lignin fractionation by ultrafiltration and selective precipitation. *Chemical Engineering Journal* **2010,** *157* (1), 93-99.

31. Xiao, Z.; Li, Y.; Wu, X.; Qi, G.; Li, N.; Zhang, K.; Wang, D.; Sun, X. S., Utilization of sorghum lignin to improve adhesion strength of soy protein adhesives on wood veneer. *Industrial Crops and Products* **2013,** *50*, 501-509.

32. Huang, S.; Mahmood, N.; Tymchyshyn, M.; Yuan, Z.; Xu, C., Reductive de-polymerization of kraft lignin for chemicals and fuels using formic acid as an in-situ hydrogen source. *Bioresource Technology* **2014,** *171*, 95-102.

33. Park, S.-J., *Carbon Fibers*. Second ed.; Springer Singapore: p 358.

34. Peebles, L. H., *Carbon Fibers: Formation, Structure, and Properties*. CRC Press, Inc: 1995; p 203.

35. Aldosari, S. M.; Khan, M.; Rahatekar, S., Manufacturing carbon fibres from pitch and polyethylene blend precursors: a review. *Journal of Materials Research and Technology* **2020,** *9* (4), 7786-7806.

36. Huang, X., Fabrication and Properties of Carbon Fibers. *Materials* **2009,** *2* (4), 2369-2403.

37. Kaur, J.; Millington, K.; Smith, S., Producing high-quality precursor polymer and fibers to achieve theoretical strength in carbon fibers: A review: REVIEW. *Journal of Applied Polymer Science* **2016,** *133*.

38. Castro, L., Anisotropy and mesophase formation towards carbon fibre production from coal tar and petroleum pitches - A review. *Journal of The Brazilian Chemical Society - JBCS* **2006,** *17*.

39. Sciti, D.; Zoli, L.; Vinci, A.; Silvestroni, L.; Mungiguerra, S.; Galizia, P., Effect of PAN-based and pitch-based carbon fibres on microstructure and properties of continuous Cf/ZrB2-SiC UHTCMCs. *Journal of the European Ceramic Society* **2021,** *41* (5), 3045-3050.

40. Lou, B.; Liu, D.; Li, M.; Hou, X.; Ma, W.; Lv, R., Modified Effects of Additives to Petroleum Pitch on the Mesophase Development of the Carbonized Solid Products. *Energy & Fuels* **2016,** *30* (2), 796-804.

41. Martín, Y.; García, R.; Solé, R. A.; Moinelo, S. R., Structural Characterization of Coal Tar Pitches Obtained by Heat Treatment under Different Conditions. *Energy & Fuels* **1996,** *10* (2), 436-442.

42. Özel, M., Production of Mesophase Pitch from Coal Tar and Petroleum Pitches using Supercritical Fluid Extraction. *Turkish Journal of Chemistry* **2002,** *26*, 417-424.

43. Brooks, J. D.; Taylor, G. H., The formation of graphitizing carbons from the liquid phase. *Carbon* **1965,** *3* (2), 185-193.

44. Kumar, S.; Srivastava, M., Influence of presence/addition of asphaltenes on semi-coke textures and mesophase development in petroleum feed stocks. *Fuel* **2016,** *173*, 69-78.

45. Piggott, M. R., *Load Bearing Fibre Composites*. Pergamon Press: Great Britain, 1980; p 277.

46. Zhang, X.; Meng, Y.; Fan, B.; Ma, Z.; Song, H., Preparation of mesophase pitch from refined coal tar pitch using naphthalene-based mesophase pitch as nucleating agent. *Fuel* **2019,** *243*, 390-397.

47. Li, P.-P.; Xiong, J.-M.; Ge, M.-L.; Sun, J.-C.; Zhang, W.; Song, Y.-Y., Preparation of pitch-based general purpose carbon fibers from catalytic slurry oil. *Fuel Processing Technology* **2015,** *140*, 231-235.

48. Amsley-Benzie, S. Preliminary Design and Economics of Biorefinery Schemes Based on the Noncatalytic Cracking of Triglyceride Oils. University of North Dakota, 2017.

49. Sajjadi, B.; Chen, W.-Y.; Raman, A. A. A.; Ibrahim, S., Microalgae lipid and biomass for biofuel production: A comprehensive review on lipid enhancement strategies and their effects on fatty acid composition. *Renewable and Sustainable Energy Reviews* **2018,** *97*, 200-232.

50. Doan, Y.; Sivaloganathan, B.; Obbard, J., Screening of marine microalgae for biodiesel feedstock. *Biomass and Bioenergy* **2011,** *35*, 2534-2544.

51. Nascimento, I.; Marques, S.; Teles, I.; Pereira, S.; Druzian, J.; oliveira de souza, C.; Vich, D.; Carvalho, G.; Nascimento, M., Screening Microalgae Strains for Biodiesel Production: Lipid Productivity and Estimation of Fuel Quality Based on Fatty Acids Profiles as Selective Criteria. *BioEnergy Research* **2012,** *6*.

52. Talebi, A. F.; Mohtashami, S. K.; Tabatabaei, M.; Tohidfar, M.; Bagheri, A.; Zeinalabedini, M.; Hadavand Mirzaei, H.; Mirzajanzadeh, M.; Malekzadeh Shafaroudi, S.; Bakhtiari, S., Fatty acids profiling: A selective criterion for screening microalgae strains for biodiesel production. *Algal Research* **2013,** *2* (3), 258-267.

53. Menegazzo, M. L.; Fonseca, G. G., Biomass recovery and lipid extraction processes for microalgae biofuels production: A review. *Renewable and Sustainable Energy Reviews* **2019,** *107*, 87-107.

54. Kreft, J. A Study of the Feasibility of Growth, Extraction, and Industrial Scale Up Processing of Microalgae Lipids. University of North Dakota, 2020.

55. Teo, C. L.; Idris, A., Enhancing the various solvent extraction method via microwave irradiation for extraction of lipids from marine microalgae in biodiesel production. *Bioresource Technology* **2014,** *171*, 477-481.

56. Adamakis, I.-D.; Lazaridis, P. A.; Terzopoulou, E.; Torofias, S.; Valari, M.; Kalaitzi, P.; Rousonikolos, V.; Gkoutzikostas, D.; Zouboulis, A.; Zalidis, G.; Triantafyllidis, K. S., Cultivation, characterization, and properties of Chlorella vulgaris microalgae with different lipid contents and effect on fast pyrolysis oil composition. *Environmental Science and Pollution Research* **2018,** *25* (23), 23018-23032.

57. Ghosh, S.; Banerjee, S.; Das, D., Process intensification of biodiesel production from Chlorella sp. MJ 11/11 by single step transesterification. *Algal Research* **2017,** *27*, 12-20.

58. Kaili, D.; Meng, C.; Yanni, W.; Xueyong, H.; Ahui, X.; Xunan, D.; Liping, L., Effect of Dibutyl Phthalate on the Tolerance and Lipid Accumulation in the Green Microalgae Chlorella vulgaris. *Bulletin of Environmental Contamination and Toxicology* **2018,** *101* (3), 338-43.

59. Liao, Q.; Chang, H.-X.; Fu, Q.; Huang, Y.; Xia, A.; Zhu, X.; Zhong, N., Physiological-phased kinetic characteristics of microalgae Chlorella vulgaris growth and lipid synthesis considering synergistic effects of light, carbon and nutrients. *Bioresource Technology* **2018,** *250*, 583-590.

60. Mardlijah; Ilmayasinta, N.; Irhami, E. A. In *Optimal control for extraction lipid model of microalgae Chlorella Vulgaris using PMP method*, International Conference on Mathematics: Pure, Applied and Computation, 20 Oct. 2018, UK, IOP Publishing: UK, 2019; p 012043 (6 pp.).

61. Nguyen, T. T.; Lam, M. K.; Uemura, Y.; Mansor, N.; Lim, J. W.; Show, P. L.; Tan, I. S.; Lim, S., High biodiesel yield from wet microalgae paste via in-situ transesterification: Effect of reaction parameters towards the selectivity of fatty acid esters. *Fuel* **2020,** *272*, 117718.

62. Šoštarič, M.; Klinar, D.; Bricelj, M.; Golob, J.; Berovič, M.; Likozar, B., Growth, lipid extraction and thermal degradation of the microalga Chlorella vulgaris. *New Biotechnology* **2012,** *29* (3), 325-331.

63. Velasquez-Orta, S. B.; Lee, J. G. M.; Harvey, A., Alkaline in situ transesterification of Chlorella vulgaris. *Fuel* **2012,** *94*, 544-550.

64. Widjaja, A.; Chien, C.-C.; Ju, Y.-H., Study of increasing lipid production from fresh water microalgae Chlorella vulgaris. *Journal of the Taiwan Institute of Chemical Engineers* **2009,** *40* (1), 13-20.

65. Sarayloo, E.; Simsek, S.; Unlu, Y. S.; Cevahir, G.; Erkey, C.; Kavakli, I. H., Enhancement of the lipid productivity and fatty acid methyl ester profile of Chlorella vulgaris by two rounds of mutagenesis. *Bioresource Technology* **2018,** *250*, 764-769.

66. Jazrawi, C.; Biller, P.; He, Y.; Montoya, A.; Ross, A. B.; Maschmeyer, T.; Haynes, B. S., Two-stage hydrothermal liquefaction of a high-protein microalga. *Algal Research* **2015,** *8*, 15-22.

67. Onwudili, J. A.; Lea-Langton, A. R.; Ross, A. B.; Williams, P. T., Catalytic hydrothermal gasification of algae for hydrogen production: Composition of reaction products and potential for nutrient recycling. *Bioresource Technology* **2013,** *127*, 72-80.

68. Garoma, T.; Shackelford, T., Electroporation of Chlorella vulgaris to enhance biomethane production. *Bioresource Technology* **2014,** *169*, 778-783.

69. Khoo, K. S.; Chew, K. W.; Yew, G. Y.; Leong, W. H.; Chai, Y. H.; Show, P. L.; Chen, W.-H., Recent advances in downstream processing of microalgae lipid recovery for biofuel production. *Bioresource Technology* **2020,** *304*, 122996.

70. Hammann, W. Method development and optimization for the recovery of carbohydrates from microalga species of Chlorella Vulgaris by combined physical and chemical pre-treatments. University of North Dakota, 2019.

71. Voeller, K.; Bílek, H.; Kreft, J.; Dostálková, A.; Kozliak, E.; Kubátová, A., Thermal Carbon Analysis Enabling Comprehensive Characterization of Lignin and Its Degradation Products. *ACS Sustainable Chemistry & Engineering* **2017,** *5* (11), 10334-10341.

72. Martínez, N.; Callejas, N.; Morais, E. G.; Vieira Costa, J. A.; Jachmanián, I.; Vieitez, I., Obtaining biodiesel from microalgae oil using ultrasound-assisted in-situ alkaline transesterification. *Fuel* **2017,** *202*, 512-519.

73. Kadrmas, C. Synthesis, Selection, and Optimization of Doped Zeolite Catalyst for the Nonbiological Production of Lactic Acid Derivatives from Biomass Derived Carbohydrates. University of North Dakota, 2014.

74. Sluiter, A.; Ruiz, R.; Scarlata, C.; Sluiter, J.; Templeton, D., Determination of Extractives in Biomass. Golden. *CO: National Renewable Energy Laboratory (NREL)* **2005**, 1-12.

75. Sluiter, A.; Hames, B.; Ruiz, R.; Scarlata, C.; Sluiter, J.; Templeton, D.; Crocker, D., Determination of Structural Carbohydrates and Lignin in Biomass—NREL/TP-510-42618. *Laboratory Analytical Procedure (LAP)* **2008**.

76. Kamireddy, S.; Schaefer, C.; Defrese, M.; Degenstein, J.; Ji, Y.; Pretreatment, Y.; Enzymatic, Pretreatment and enzymatic hydrolysis of sunflower hulls for fermentable sugar production Citation. 2012; Vol. 5.

77. Yang, X.; Zhang, Y.; Zhou, L.; Gao, B.; Lu, T.; Su, Y.; Xu, J., Production of lactic acid derivatives from sugars over post-synthesized Sn-Beta zeolite promoted by WO3. *Food Chemistry* **2019,** *289*, 285-291.

78. Rusu, D.; Boyer, S. A. E.; Lacrampe, M.-F.; Krawczak, P., Bioplastics and Vegetal Fiber Reinforced Bioplastics for Automotive Applications. *Handbook of Bioplastics and Biocomposites Engineering Applications* **2011**, 397-449.

79. Nwamba, M. C.; Sun, F.; Mukasekuru, M. R.; Song, G.; Harindintwali, J. D.; Boyi, S. A.; Sun, H., Trends and hassles in the microbial production of lactic acid from lignocellulosic biomass. *Environmental Technology & Innovation* **2021,** *21*, 101337.

80. Li, C.; Gao, M.; Zhu, W.; Wang, N.; Ma, X.; Wu, C.; Wang, Q., Recent advances in the separation and purification of lactic acid from fermentation broth. *Process Biochemistry* **2021,** *104*, 142-151.

81. Holm, M.; Shunmugavel, S.; Taarning, E., Conversion of Sugars to Lactic Acid Derivatives Using Heterogeneous Zeotype Catalysts. *Science (New York, N.Y.)* **2010,** *328*, 602-5.

82. Kohler, A. The Conversion of Carbohydrates from Microalgae and Corn Stover into Building Block Chemical Acids. University of North Dakota, 2020.

83. Marianou, A. A.; Michailof, C. M.; Pineda, A.; Iliopoulou, E. F.; Triantafyllidis, K. S.; Lappas, A. A., Effect of Lewis and Brønsted acidity on glucose conversion to 5-HMF and lactic acid in aqueous and organic media. *Applied Catalysis A: General* **2018,** *555*, 75-87.

84. Tolborg, S.; Sadaba, I.; Osmundsen, C.; Fristrup, P.; Holm, M.; Taarning, E., Tin-containing Silicates: Alkali Salts Improve Methyl Lactate Yield from Sugars. *ChemSusChem* **2015,** *8*.

85. Bhat, N. S.; Mal, S. S.; Dutta, S., Recent advances in the preparation of levulinic esters from biomass-derived furanic and levulinic chemical platforms using heteropoly acid (HPA) catalysts. *Molecular Catalysis* **2021,** *505*, 111484.

86. Holm, M.; Pagan-Torres, Y.; Shunmugavel, S.; Riisager, A.; Dumesic, J.; Taarning, E., Sn-Beta catalysed conversion of hemicellulosic sugars. *Green Chem.* **2012,** *14*, 702-706.

87. Dijkmans, J.; Demol, J.; Houthoofd, K.; Huang, S.; Pontikes, Y.; Sels, B., Post-synthesis Snβ: An exploration of synthesis parameters and catalysis. *Journal of Catalysis* **2015,** *330*, 545-557.

88. Wang, W.; Zhang, W.; Chen, Y.; Wen, X.; Li, H.; Yuan, D.; Guo, Q.; Ren, S.; Pang, X.; Shen, B., Mild-acid-assisted thermal or hydrothermal dealumination of zeolite beta, its regulation to Al distribution and catalytic cracking performance to hydrocarbons. *Journal of Catalysis* **2018,** *362*, 94-105.

89. Rajabbeigi, N.; Torres, A. I.; Lew, C. M.; Elyassi, B.; Ren, L.; Wang, Z.; Je Cho, H.; Fan, W.; Daoutidis, P.; Tsapatsis, M., On the kinetics of the isomerization of glucose to fructose using Sn-Beta. *Chemical Engineering Science* **2014,** *116*, 235-242.

90. Pourjafar, S. An Investigation of the Thermal Degradation of Lignin. University of North Dakota, 2017.

91. Gellerstedt, G.; Henriksson, G., Chapter 9 - Lignins: Major Sources, Structure and Properties. In *Monomers, Polymers and Composites from Renewable Resources*, Belgacem, M. N.; Gandini, A., Eds. Elsevier: Amsterdam, 2008; pp 201-224.

92. Calvo-Flores, F. G.; Dobado Jiménez, J. A.; Garcia, J. I.; Martín-Martínez, F. J., *Lignin and lignans as renewable raw materials : chemistry, technology and applications*. John Wiley and Sons, Ltd: Chichester, West Sussex, United Kingdom, 2015.

93. Gasson, J. R.; Forchheim, D.; Sutter, T.; Hornung, U.; Kruse, A.; Barth, T., Modeling the Lignin Degradation Kinetics in an Ethanol/Formic Acid Solvolysis Approach. Part 1. Kinetic Model Development. *Industrial & Engineering Chemistry Research* **2012,** *51* (32), 10595-10606.

94. Forchheim, D.; Gasson, J. R.; Hornung, U.; Kruse, A.; Barth, T., Modeling the Lignin Degradation Kinetics in a Ethanol/Formic Acid Solvolysis Approach. Part 2. Validation and Transfer to Variable Conditions. *Industrial & Engineering Chemistry Research* **2012,** *51* (46), 15053-15063.

95. Toledano, A.; Serrano, L.; Labidi, J., Organosolv lignin depolymerization with different base catalysts. *Journal of Chemical Technology & Biotechnology* **2012,** *87* (11), 1593-1599.

96. Beauchet, R.; Monteil-Rivera, F.; Lavoie, J. M., Conversion of lignin to aromatic-based chemicals (L-chems) and biofuels (L-fuels). *Bioresource Technology* **2012,** *121*, 328-334.

97. Yan, Z.; Li, J.; Li, S.; Chang, S.; Cui, T.; Jiang, Y.; Cong, G.; Yu, M.; Zhang, L., Impact of lignin removal on the enzymatic hydrolysis of fermented sweet sorghum bagasse. *Applied Energy* **2015,** *160*, 641-647.

98. She, D.; Xu, F.; Geng, Z.; Sun, R.; Jones, G. L.; Baird, M. S., Physicochemical characterization of extracted lignin from sweet sorghum stem. *Industrial Crops and Products* **2010,** *32* (1), 21-28.

99. Sipponen, M. H.; Lapierre C Fau - Méchin, V.; Méchin V Fau - Baumberger, S.; Baumberger, S., Isolation of structurally distinct lignin-carbohydrate fractions from maize stem by sequential alkaline extractions and endoglucanase treatment. (1873-2976 (Electronic)).

100. Yang, J.; Zhao, L.; Liu, S.; Wang, Y.; Dai, L., High-quality bio-oil from one-pot catalytic hydrocracking of kraft lignin over supported noble metal catalysts in isopropanol system. *Bioresource Technology* **2016,** *212*, 302-310.

101. Toledano, A.; Serrano, L.; Labidi, J., Improving base catalyzed lignin depolymerization by avoiding lignin repolymerization. *Fuel* **2014,** *116*, 617-624.

102. Li, X.; Su, L.; Wang, Y.; Yu, Y.; Wang, C.; Li, X.; Wang, Z., Catalytic fast pyrolysis of Kraft lignin with HZSM-5 zeolite for producing aromatic hydrocarbons. *Frontiers of Environmental Science & Engineering* **2012,** *6* (3), 295-303.